The chiral menthoxy groups was removed in membrane state of the copolymer (Scheme 2). As a result, the resulting copolymer showed CD signals in spite of no chiral sources in chloroform solution (Fig. 3,4).

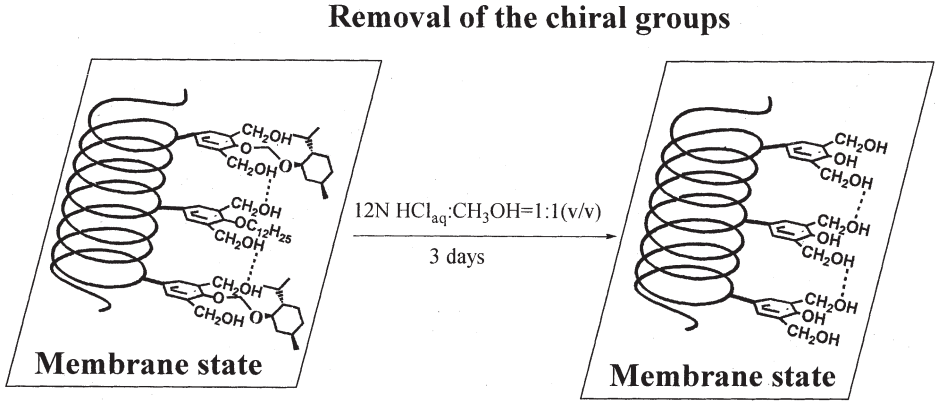

Scheme 2. Removal of the chiral groups in membrane state.

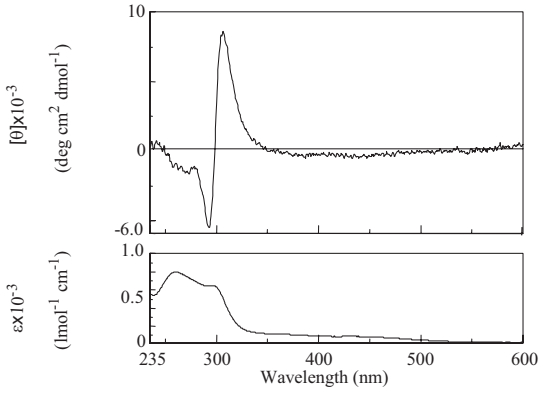

Figure 3. CD and UV-vis spectra of poly(**MDHPA**-*co*-**DoDHPA**) (1 : 9)**;** before removal of the menthoxy groups in chloroform(*c* 0.001mol/l) at room temperature**.**

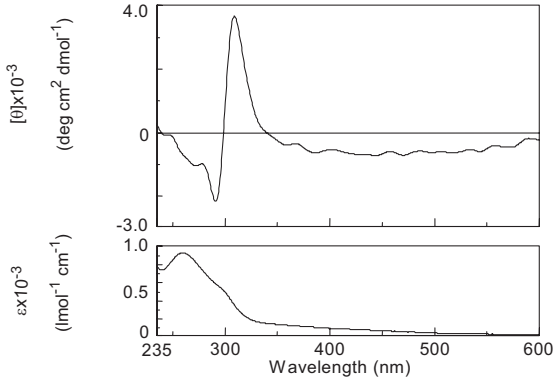

Figure 4. CD and UV-vis spectra of poly(**MDHPA**-*co*-**DoDHPA**) (1 : 9) **;** after removal of the menthoxy groups in chloroform(*c* 0.001 mol/l) at room temperature**.**

Reference

1) Kazuomi Mottate, Sun-young Kim, Masahiro Teraguchi, Shingo Hadano, Toshiki Aoki, and Takashi Kaneko, *Polym. Prepr., Japan,* **54**, 252 (2005).

P066C

SYNTHESIS OF CHIRAL POLYPHNYLACETYLENES BEARING AN ONE-HANDED HELICAL BACKBONE AND PHOTO-RESPONSIVE SIDE CHAINS

Ippei Suzuki[1], Masahiro Teraguchi,[1,2,3] Takeshi Namikoshi,[3,4] Edy Marwanta,[3,4] Takashi Kaneko[2,3], and Toshiki Aoki,[1,2,3,4*]

[1] Graduate School of Science and Technology, [2]Center for Education and Research on Environmental Technology, Materials Engineering, and Nanochemistry, [3]Center for Transdisciplinary Research, [4]Venture Business Laboratory, Niigata University, Ikarashi 2-8050, Nishi-ku, Niigata 950-2181, Japan

We previously reported the polymer having an one-handed helical structure was obtained by the helix-sense-selective polymerization(**HSSP**) of achiral phenylacetylenes bearing two hydroxyl groups using a rhodium catalyst in the presence of chiral 1-phenylethylamine(**PEA**).[1,2,3)] Furthermore, we studied response of the chiral helical backbone upon external stimuli such as change in polarity of solvent[4)] and temperature.[5)]

In this study, we synthesized phenylacetylenes bearing a photo-responsive group, [3,5-bis(5-*tert*-butylsalicylideneamino)phenyl-acetylene(**BSAPA**) and 4-{3-(phenylazo)phenylmethoxy}-3,5-bis(hydroxymethyl)phenylacetylene(**AzoDHPA**)]. **BSAPA** and **AzoDHPA** contains two salicylideneamino groups and an azobenzene group as photo-responsive substituents, respectively. Poly(**BSAPA**) and poly(**AzoDHPA**) were synthesized by polymerization of the corresponding monomer using the chiral rhodium catalyst(Scheme 2, 3). By CD measurement, we found that poly(**AzoDHPA**) had an one-handed helical structure in the backbone, the fact indicating the monomer was suitable for **HSSP**(Figure 1), but poly(**BSAPA**) did not. A chiral helical polymer containing **BSAPA** unit was synthesized by asymmetric-induced copolymerization of **BSAPA** with **PSPA**(Scheme 3).

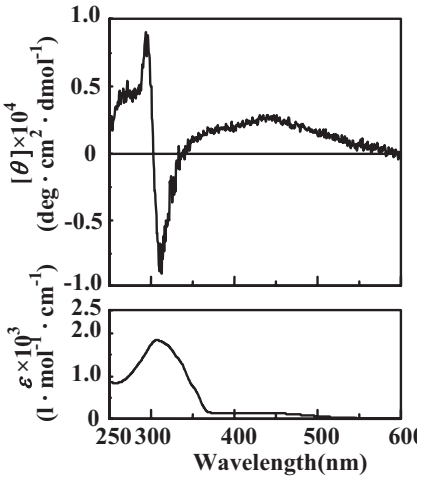

Figure 1. CD and UV-vis spectra of poly(AzoDHPA) in THF at 20 °C

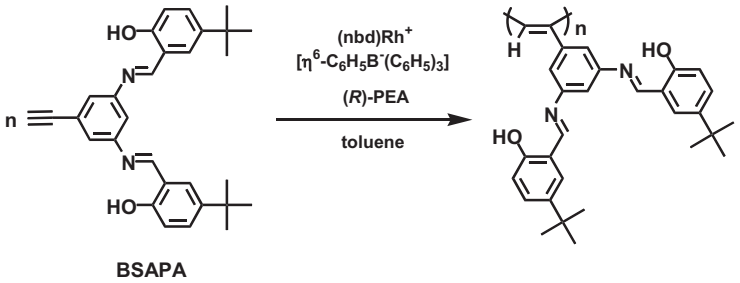

BSAPA

Scheme 1. Polymerization of BSAPA

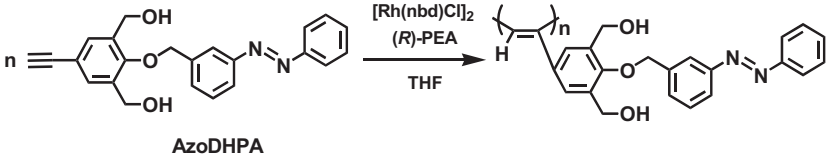

Scheme 2. Helix-sense-selective polymerization(HSSP) of AzoDHPA

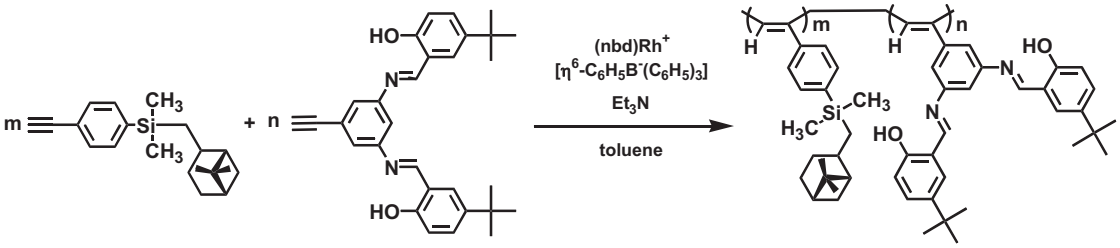

Scheme 3. Asymmetric-induced copolymerization of BSAPA with PSPA

References

1) Toshiki Aoki, Takashi Kaneko and Masahiro Teraguchi, *Polymer*, **47**, 4867(2006).

2) Toshiki Aoki and Takashi Kaneko, Polym.J., **37**, 717(2005).

3) Toshiki Aoki, Takashi Kaneko, Naoki Maruyama, Atsushi Sumi, Masahiko Takahashi, Takashi Sato, and Masahiro Teraguchi, *J. Am. Chem. Soc.*, **125**, 6346(2003).

4) Kazuomi Mottate, Masahiro Teraguchi, Shingo Hadano, Toshiki Aoki and Takashi Kaneko, *Polym. Prepr. Jpn.*, **55**(2), 5018 (2006).

5) Shingo Hadano, Toshiki Aoki, Masahiro Teraguchi and Takashi Kaneko, *Polym. Prepr. Jpn.*, **54**(2), 2855(2005).

P067A

HELIX-SENSE-SELECTIVE POLYMERIZATION OF PHENYLACETYLENE HAVING TWO AMINOALCOHOL RESIDUES

Kazuki Matsumoto,[1] Masahiro Teraguchi,[1,2,3] Takeshi Namikoshi,[3,4] Edy Marwanta,[3,4] Takashi Kaneko,[2,3] and Toshiki Aoki,[1,2,3,4*]

[1] Graduate School of Science and Technology, [2]Center for Education and Research on Environmental Technology, Materials Engineering, and Nanochemistry, [3]Center for Transdisciplinary Research, [4]Venture Business Laboratory, Niigata University, Ikarashi 2-8050, Nishi-ku, Niigata 950-2181, Japan

We achieved synthesis of a chiral helical polymer without the coexistence of any other chiral moieties by helix-sense-selective polymerization.[1)] After that when we tried helix-sense-selective polymerization of a monomer having one aminoalcohol group (-$NHCH_2CH_2OH$), the resulting polymer was insoluble. We also reported asymmetric alkylation of benzaldehyde using a helical copolymer containing the monomer(Scheme 1).[2)] We found the effectiveness of the chiral helical main-chain on the enantioselective addition. However, optical yields and chemical yields in this reaction were relatively low.

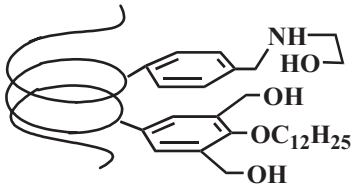

Scheme 1. Structure of helical polymer.

In this presentation, we will report synthesis and helix-sense-selective polymerization of achiral phenylacetylene monomers, **DMIPA** and **DHIPA**(See Scheme 2) having a dodecyl group to increase the solubility of the resulting polymer and two bidentate ligands to enhance optical yields and chemical yields of the enantioselective reaction.

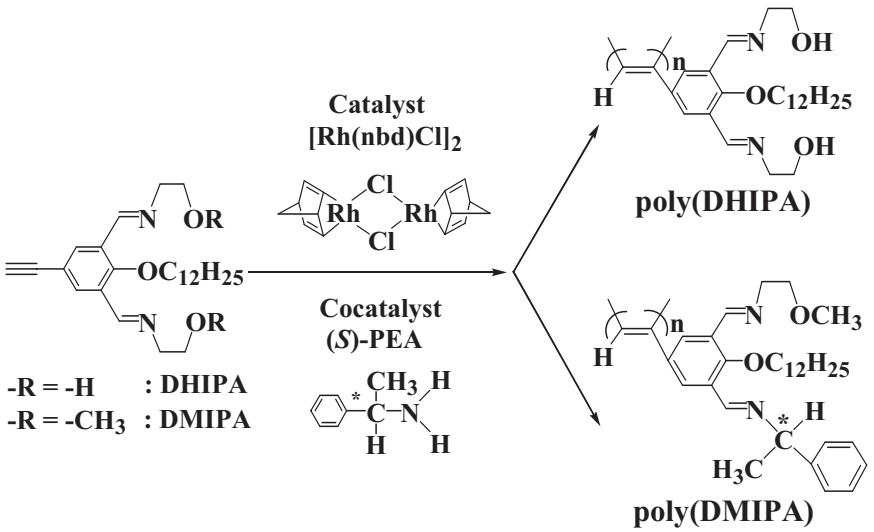

Scheme 2. Polymerization of DHIPA and DMIPA.

Poly(**DMIPA**) and poly**(DHIPA**) showed very strong Cotton effects(Figs.1 and 2). In addition, helical structures of these polymers were very stable when it was heated. While we found that **DHIPA** was suitable for the helix-sense-selective polymerization, **DMIPA** was substituted by chiral amines added as a cocatalyst during polymerization and then occurred asymmetric-induced polymerization(Scheme 2). These are very interesting findings.

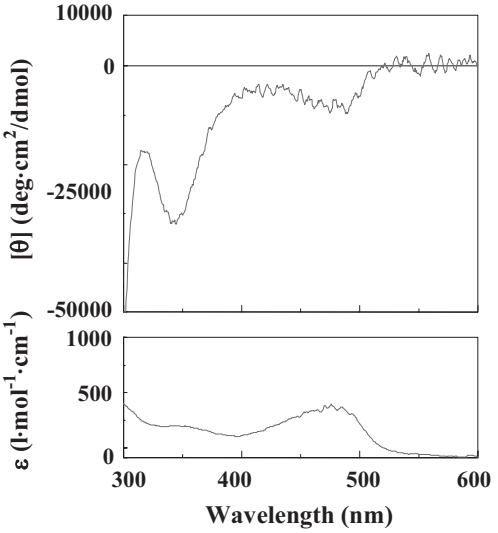

Fig. 1. CD&UV-vis spectra of poly(DHIPA) in THF.

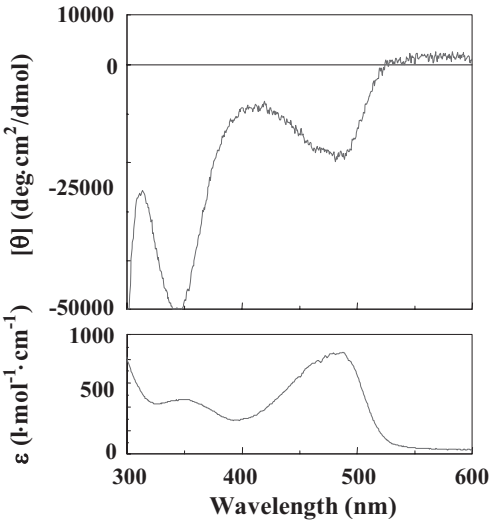

Fig. 2. CD&UV-vis spectra of poly(DMIPA) in THF.

1) T. Aoki, T. Kaneko, N. Maruyama, A. Sumi, M. Takahashi, T. Sato, and M. Teraguchi, *J. Am. Chem. Soc*., **125**, 6346 (2003).

2) T. Hara, M. Teraguchi, T. Kaneko, and T. Aoki, *Polym. Prepr. Jpn*., **53**(2), 2926 (2004).

P068B

HELIX-SENCE-SELECTIVE POLYMERIZATION OF 3,5-BIS(HYDROXYMETHYL)-4-BENZYL-OXYPHENYLACETYLENE BEARING GALVINOXYL, AND CHIROPTICAL AND MAGNETIC PROPERTIES

Hiroo Katagiri,[1] Takashi Kaneko,[2,3*] Takeshi Namikoshi,[3,4] Edy Marwanta,[3,4] Masahiro Teraguchi,[1,2,3] and Toshiki Aoki[1,2,3,4]

[1] Graduate School of Science and Technology, [2]Center for Education and Research on Environmental Technology, Materials Engineering, and Nanochemistry, [3]Center for Transdisciplinary Research, [4]Venture Business Laboratory, Niigata University, Ikarashi 2-8050, Nishi-ku, Niigata 950-2181, Japan

Optically active helical π conjugated polymers bearing stable radicals are expected to display interesting magnetic and chiroptical properties. We have already reported the helix-sense-selective polymerization of achiral phenylacetylenes, using the catalyst $[Rh(nbd)Cl]_2$ in the presence of optically active 1-phenylethylamine(PEA).[1-3] In this study, we synthesized monomer **1a** bearing galvinoxyl residue, and found that the helix-sense-selective polymerization improved in the polymer yield due to addition of CuI to the catalyst system (Scheme 1). The polymer obtained by polymerization at low temperature (0°C) showed larger Cotton effects than the polymers obtained by polymerization at room temperature. These results indicate the improvement of the helix-sense-selectivity on the polymerization. Additionally, it was found that the catalyst $Rh(nbd)[B(C_6H_5)]_2$ was more effective for the helix-sense-selective polymerization of **1a**. The helical conformation of poly**1a** was kinetically stabilized by intramolecular hydrogen bonds among hydroxyl groops in poly**1a**. Therefore, we have succeeded in synthesizing the optically active helical polyradical poly**1b** with high spin concentration via chemical oxidation of poly1a with rigid and one-handed helical conformation in THF solution.

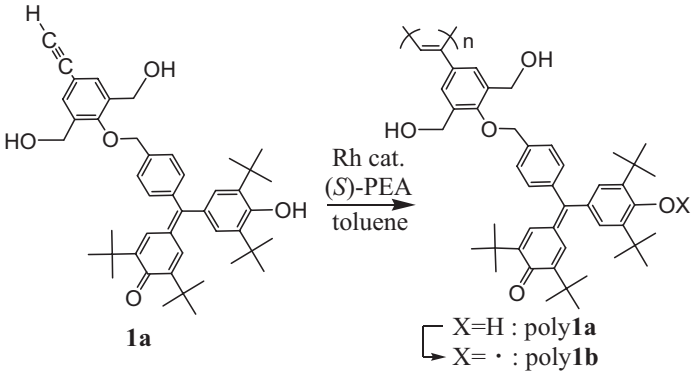

Scheme 1. Polymerization of monomer 1a.

References

1) Toshiki Aoki, Takashi Kaneko et al., *J. Am, Chem. Soc.*, **125**, 6346(2003).

2) Takashi Kaneko et al., *Macromolecules*, **38**, 9429(2005).

3) Umeda Yasuhiro, Takshi Kaneko et al., *Chem. Lett*, **34**, 854(2005).

P069C

ASYMMETRIC-INDUCED POLYMERIZATION OF PHENYLACETYLENE HAVING TWO HYDROXYL GROUPS AND A CHIRAL PINANYLSILYL GROUP

Jia Hongge[1], Kazuomi Mottate[1],Masahiro Teraguchi,[1,2,3] Takeshi Namikoshi,[3,4] Edy Marwanta,[3,4]Takashi Kaneko[2,3], and Toshiki Aoki[1,2,3,4*]

[1] Graduate School of Science and Technology, [2]Center for Education and Research on Environmental Technology, Materials Engineering, and Nanochemistry, [3]Center for Transdisciplinary Research, [4]Venture Business Laboratory, Niigata University, Ikarashi 2-8050, Nishi-ku, Niigata 950-2181, Japan

We synthesized and polymerized a chiral monomer, 4-[Dimethyl(10-pinanyl)silylmethyloxy]-3,5-bis(hydroxylmethyl)phenylacetylene(**PiDHPA**) by a rhodium complex(Scheme 1). Poly(**PiDHPA**) exhibited intense Cotton effects at around 400nm where the polyphenylacetylene backbone absorbs, the fact showing that the polymer took a one-handed helical conformation (Fig.1). When the polymer solution was heated to 50 °C, the CD absorptions did not change (Fig.1). The membrane of poly(**PiDHPA**) made by solvent-casting method also showed Cotton effects at 400nm (Fig.2). It proved that the one-handed helical conformation of the polymer was also maintained in the membrane state.

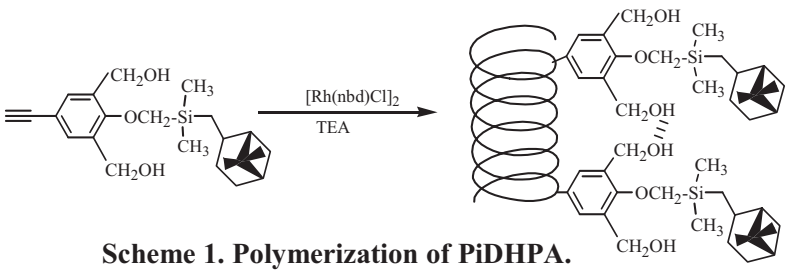

Scheme 1. Polymerization of PiDHPA.

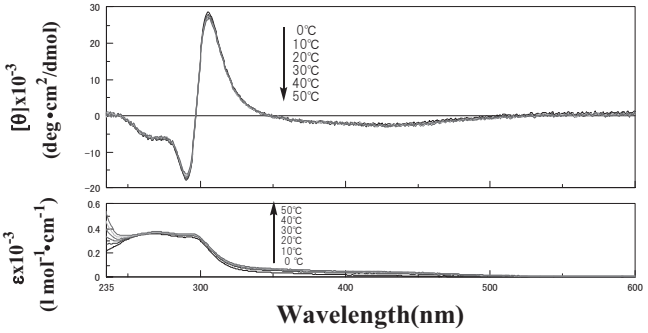

Fig. 1. CD and UV/vis spectra of poly(PiDHPA) at several temperatures in chloroform.

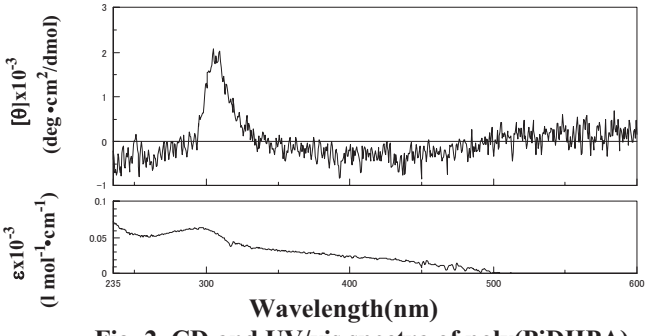

Fig. 2. CD and UV/vis spectra of poly(PiDHPA) in the membrane.

∗) Kazuomi Mottate, Sun-youg Kim, Masahiro Teraguchi, Shingo Hadano, Toshiki Aoki and Takashi Kaneko, *Polym. Prepr., Japan,* **54**, 252 (2005).

P070A

ATTEMPT TO LIVING HELIX-SENSE-SELECTIVE POLYMERIZATION OF ACHIRAL PHENYLACETYLENES BY $MoOCl_4$ OR $WOCl_4$-ALKYLATING AGENT-CHIRAL ALCOHOL

Motohiro Kiuchi,[1] Masahiro Teraguchi,[1,2,3] Takeshi Namikoshi,[3,4] Edy Marwanta,[3,4] Takashi Kaneko,[2,3] and Toshiki Aoki[1,2,3,4*]

[1] *Graduate School of Science and Technology,* [2]*Center for Education and Research on Environmental Technology, Materials Engineering, and Nanochemistry,*
[3]*Center for Transdisciplinary Research,* [4]*Venture Business Laboratory,*
Niigata University, Ikarashi 2-8050, Nishi-ku, Niigata 950-2181, Japan

We reported a novel synthetic method(helix-sense-selective polymerization(**HSSP**)) for obtaining a chiral helicalpolymer from an achiral substituted acetylene monomer only by adding a chiral amine to an achiral rhodium initiator.[1)] However, the control of molecular weight and molecular weight distribution(M_w/M_n) was not attained and monomer structures suitable for the **HSSP** were limitted. On the other hand, Masuda et al. reported that only the addition of an achiral alcohol to a metathesis polymerization catalyst made the M_w/M_n smaller.[2)]

In this study, in order to add **HSSP** to the living metathesis polymerization, we used a chiral alcohol instead of an achiral alcohol. In polymerization of **G_0SPA**(Scheme 1), the obtained polymer had a smaller M_w/M_n (1.20). Since the Cotton effect was observed for poly(**G_0SPA**), the possibility of formation of a chiral structure to the backbone was suggested.

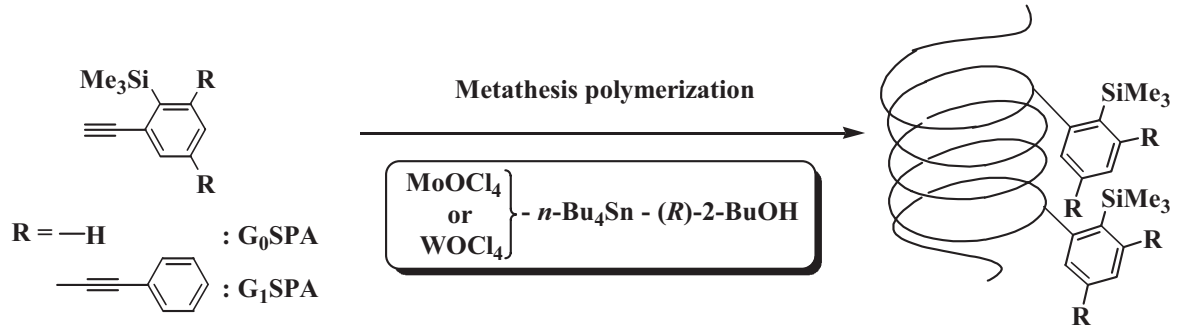

Scheme 1

References

1) Toshiki Aoki, Takashi Kaneko, Naoki Maruyama, Atsushi Sumi, Masahiro Takahashi, Takashi Sato and Masahiro Teraguchi, *J. Am. Chem. Soc*., **125**, 6346(2003).
2) Shigetaka Hayano and Toshio Masuda, *Macromolecules*, **31**, 3170(1998).

P071B

SYNTHESIS OF TEMPO-PENDANT POLY(PHENYLACETYLENE)S, AND THEIR CHIROPTICAL AND MAGNETIC PROPERTIES

Atsuko Kawami,[1] Takashi Kaneko,[2,3*] Takeshi Namikoshi,[3,4] Edy Marwanta,[3,4] Masahiro Teraguchi,[1,2,3] and Toshiki Aoki[1,2,3,4]

[1] Graduate School of Science and Technology, [2]Center for Education and Research on Environmental Technology, Materials Engineering, and Nanochemistry, [3]Center for Transdisciplinary Research, [4]Venture Business Laboratory, Niigata University, Ikarashi 2-8050, Nishi-ku, Niigata 950-2181, Japan

Recently, we have succeeded in the helix-sense-selective polymerization of achiral phenylacetylene monomers bearing galvinoxyl moiety using the catalyst $[Rh(nbd)Cl]_2$ (nbd = 2,5-norbornadiene) in the presence of chiral 1-phenylethylamine.[1),2)] In the present study, we synthesized achiral phenylacetylene monomer(**1**) with TEMPO pendant(**1**). The monomer was polymerized by $Rh(nbd)Cl[B(C_6H_5)_4]$ in the presence of (S)-(−)-1-phenylethylamine (PEA). The high spin concentration of polyradical was confirmed by integration of the ESR signal in comparison with that of the TEMPO solution as a standard. This fact indicates that degradation of the radical didn't occur during the polymerization reaction. The static magnetic susceptibility of the powdered polyradicals was measured with a SQUID magnetometer at 2-300K. The observed negative Weiss temperature indicated antiferromagnetic interaction between unpaired electrons, and this negative θ value was larger than that of the monomer(**1**).

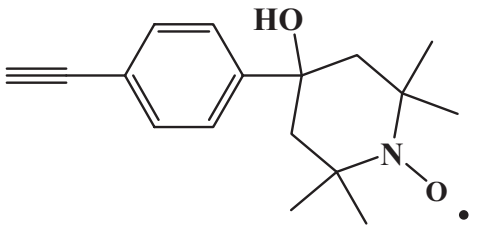

1

References

1) Y. Umeda, T. Kaneko, M. Teraguchi, T. Aoki, *Chem. Lett.* **34**, 854(2005)

2) T. Kaneko, Y. Umeda, T. Yamamoto, M. Teraguchi, T. Aoki, *Macromolecules*. **38**, 9420(2005)

P072C

MAGNETIC PROPERTIES OF TEMPO RADICALS INCLUDED IN A SUPRAMOLECULAR ANTHRACENE DERIVATIVE

Masayuki Sato,[1] Takashi Kaneko,[2,3*] Takeshi Namikoshi,[3,4] Edy Marwanta,[3,4] Masahiro Teraguchi,[1,2,3] and Toshiki Aoki[1,2,3,4]

[1] Graduate School of Science and Technology, [2]Center for Education and Research on Environmental Technology, Materials Engineering, and Nanochemistry, [3]Center for Transdisciplinary Research, [4]Venture Business Laboratory, Niigata University, Ikarashi 2-8050, Nishi-ku, Niigata 950-2181, Japan

It is known that an anthracene derivative, 9,10-Bis(3,5-dihydroxyphenyl)anthracene **1**, forms hydrogen bonded supramolecular architecture, and its cavities possess an ability to include guest molecules[1)]. In this study, we succeeded in modifying the magnetic properties of TEMPO derivatives **2**-**4** by preparing each host-guest adducts (**1**·1.5(**2**), **1**·1.5(**3**) and **1**·1.0(**4**)).

Scheme 1. Host and guest structures

Host : Guest :

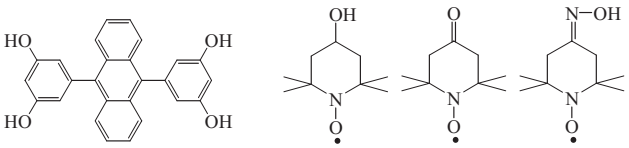

1 **2** **3** **4**

Host-guest adducts were prepared by the solid state guest binding. Solvent-free white apohost crystals were gradually colored upon dipping in a dichloromethane solution of each guest radicals, resulting in colored crystals. Static magnetic susceptibility (2-300 K at 0.5 T) of crystals,neat guest molecules(**2**, **3** and **4**) and host-guest adducts (**1**·1.5(**2**), **1**·1.5(**3**) and **1**·1.0(**4**)),were measured using a SQUID magnetometer. The Weiss constant of all samples are listed in **Table 1**, and the value of neat samples approximately correspond to each data of references[2,3)]. The intermolecular antiferromagnetic interaction of neat **2** is stronger than the intermolecular antiferromagnetic interaction of **2** incorporated in host structure of **1**. On the other hand, the intermolecular antiferromagnetic interaction of neat **3** became strong by incorporating it into host structure, and the intermolecular ferromagnetic interaction of neat **4** changed into the intermolecular antiferromagnetic interaction. These results indicate that incorporating guest radicals into host matrix is effective for restriction of magnetic coupling structure.

Table 1. The Weiss constant θ evaluated from susceptibility measurements.

	Weiss constant θ [K]	Magnetic Property[a)]
2 neat	-7.4	(S) AFM
1·1.5 (**2**)	-0.84	AFM
3 neat	-0.11	(W) AFM
1·1.5 (**3**)	-0.98	AFM
4 neat	0.44	(W) FM
1·1.0 (**4**)	-0.14	(W) AFM

a) (S) : strong, (W) : weak,
AFM : antiferromagnetism, FM : ferromagnetism

References

1) K. Endo et al., *J. Am. Chem. Soc.*, **117**, 8341(1995).

2) Karimov. Yu. S., *Zhurnal Eksperimental'noi I Teoreti cheskoi Fiziki*, 57(**12**), 1962(1969).

3) J. YAMAUCHI, *B. C. S. J.*, **44**, 2301(1971).

P073A

SYNTHESIS OF POLY(BINAPHTHYL-6,6'-DIYLETHYNYLENE-1,3-PHENYLENEETHYNYLENE)-BASED CHIRAL POLYRADICAL BEARING GALVINOXYL, AND ITS CHIROPTICAL AND MAGNETIC PROPERTIES

Hiromasa Abe,[1] Takashi Kaneko,[2,3*] Takeshi Namikoshi,[3,4] Edy Marwanta,[3,4] Masahiro Teraguchi,[1,2,3] and Toshiki Aoki[1,2,3,4]

[1] Graduate School of Science and Technology, [2]Center for Education and Research on Environmental Technology, Materials Engineering, and Nanochemistry, [3]Center for Transdisciplinary Research, [4]Venture Business Laboratory, Niigata University, Ikarashi 2-8050, Nishi-ku, Niigata 950-2181, Japan

In recent years, there has been considerable interest in search for new features of optically polymers. In our laboratory, we have tried to fusion their polymers with magnetic properties, and have synthesized various chiral polyradicals. We have already synthesized a poly(m-phenyleneethynylene)-based chiral polyradical bearing galvinoxyl units, which are known as a stable radical, and optically active pinanylsilyl groups[1)]. In this study, to introduce more rigid asymmetric main chain framework, we synthesized a chiral polyradical using optically active binaphthyl units and m-phenyleneethynylene-based structures bearing galvinoxyl units into the alyleneethynylene main chain, and discussed its optical activity, magneto-optical effect and magnetic property.

The hydrogalvinoxyl precursor polymer (**3a**) was given by polymerization of chiral diethynyl-1,1' -binaphthyl (**(R)-1**) and (1,3-diiodephenyl)hydrogalvinoxyl (**2**) monomers using $Pd(PPh_3)_4$ catalyst (100%, $M_n=1.5\times10^4$, $M_w/M_n=3.0$). In the CD spectrum of **3a** taken in chloroform solution, large Cotton effects were observed in the absorption region of the binaphthyl choromophore, which were incorporated into the poly(alyleneethynylene) backbone. In addition, this intensity hardly changed when measured under various temperature and acetonitrile addition, indicating that the polymer contained stable asymmetric main chain structure. The polymer yielded the corresponding polyradical with high spin concentration by treatment of the polymer solution in benzene with PbO_2. MCD spectra were observed about both **3a** and **3b** with large

intensity. The differential spectrum ([θ]$_M$-[θ]) were in agreement with the MCD spectrum of the racemic **3a**, indicating that the MCD spectra of chiral **3a** and **3b** included the Faraday effects overlapping with Cotton effects in the absorption region of the hydrogalvinoxyl chromophore (420nm) and galvinoxyl-radical chromophore (470nm) respectively. The static magnetic susceptibility of **3b** was measured using a SQUID magnetometer, and showed the weak antiferromagnetic interaction regardless of chiral or racemic one (Weiss const. =-0.7 to -0.5K).

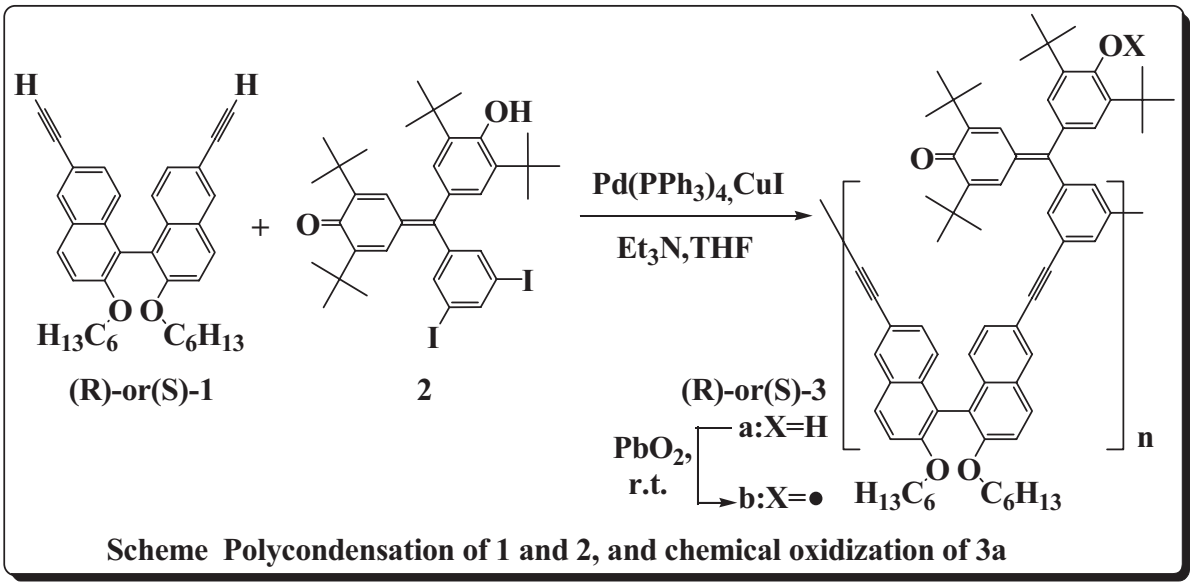

Scheme Polycondensation of 1 and 2, and chemical oxidization of 3a

References

1) Takashi Kaneko, Shota Yoshimoto, Shingo Hadano, Masahiro Teraguchi and Toshiki Aoki, *Polyhedron*, 26, 1825(2007).

P074B

SYNTHESIS OF OLIGO(ANTHRYLENEETHYNYLENE)-BASED FOLDAMERS CONTAINING STABLE RADICALS.

Kensuke Ochiai,[1] Takashi Kaneko,[2,3*] Takeshi Namikoshi,[3,4] Edy Marwanta,[3,4] Masahiro Teraguchi,[1,2,3] and Toshiki Aoki[1,2,3,4]

[1] Graduate School of Science and Technology, [2]Center for Education and Research on Environmental Technology, Materials Engineering, and Nanochemistry, [3]Center for Transdisciplinary Research, [4]Venture Business Laboratory, Niigata University, Ikarashi 2-8050, Nishi-ku, Niigata 950-2181, Japan

We have reported that poly(9,10-anthryleneethynylene)-based polyradical with two pendant stable phenoxyls at 2- and 7-positions in anthracene skelton was synthesized via polymerization of the corresponding bromoethynylanthracene monomer using a Pd(0) catalyst.[1)] The polyradical was prepared from the corresponding hydroxyl precursor polymer and was appropriately stable at room temperature. The ESR spectrum of the corresponding monomeric radical suggested an effectively delocalized spin density distribution on the backbone anthracene. The magnetization and the static magnetic susceptibility of the polyradical were measured using a SQUID magnetometer. The experiment diluted in diamagnetic solvent indicated that the ferromagnetic intrachain spin coupling network of the polyradical had spread throughout the π-conjugated chain. But the neat powder sample exhibited the antiferromagnetic interchain interaction among the π-conjugated polymer chains. In this study, we have designed a new polyradical which has an alkyl spacer between the poly(9,10-anthryleneethynylene)-based polyradical units to form foldamer, and aim to control the aggregation structure of the molecule in the solid state and to construct the ferromagnetic spin coupling network.

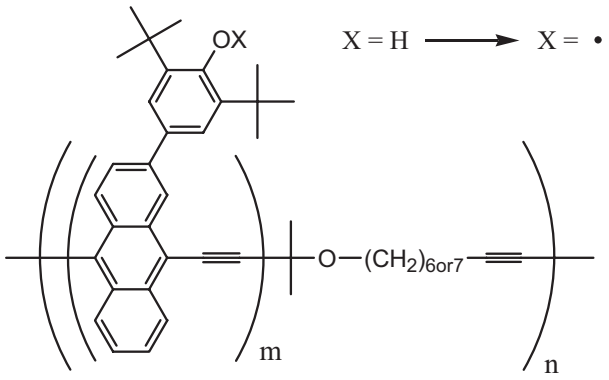

References

1) Takashi Kaneko, Takahisa Makino, Hiroshi Miyaji, Masahiro Teraguchi, Toshiki aoki, Makoto Miyasaka, and Hiroyuki Nishide, *J.Am.Chem.Soc*, **125**, 3554(2003).

P075C

SYNTHESIS OF CHIRAL HELICAL POLY(PHENYLENETHYNYLENE) MEMBRANES BY DESUBSTITUTION OF CHIRAL GROUP

Makoto Inoue,[1] Masahiro Teraguchi,[1,2,3] Takeshi Namikoshi,[3,4] Edy Marwanta,[3,4] Takashi Kaneko,[2,3] and Toshiki Aoki[1,2,3,4*]

[1] Graduate School of Science and Technology, [2]Center for Education and Research on Environmental Technology, Materials Engineering, and Nanochemistry, [3]Center for Transdisciplinary Research, [4]Venture Business Laboratory, Niigata University, Ikarashi 2-8050, Nishi-ku, Niigata 950-2181, Japan

We previously reported that chiral pinanyl groups were completely removed from poly(phenylacetylenes) type with chiral pinanyl groups in membrane state, and the resulting membrane maintained helical structures.[3)]

In this study, we synthesized chiral helical poly(phenyleneethynylene)s having optically active menthyl or pinanyl groups (Scheme 1), and desubstituted the chiral groups in membrane state. **PMtMt** membranes prepared from toluene solution had chiral helical structures in the main chain judging from CD (Figure 1a). In addition, this polymer membrane maintained chiral helical structures after desubstitution of at menthyl groups (Figure 1b).

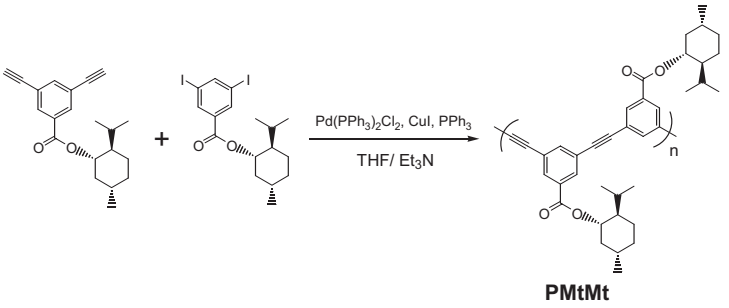

Scheme 1. Synthesis of Poly(phenyleneethynylene) having optical active menthyl groups (**PMtMt**).

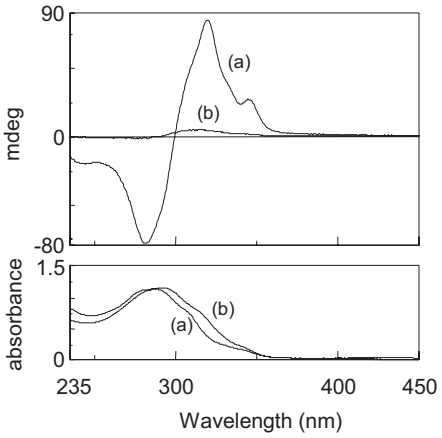

Figure 1. CD and UV-vis spectra of **PMtMt** membrane (a)before (b)after desubstitution of chiral groups prepared from toluen solution.

1) Toshiki Aoki, Takashi Kaneko, and Masahiro Teraguchi, *Polymer*, **47**, 4867(2006).

2) Toshiki Aoki and Takashi Kaneko, *Polym.J.*, **37**, 717(2005).

3) M. Teraguchi, K.Mottate, S-Y. Kim, T. Aoki, T. Kaneko, S. Hadano, and T. Masuda, *Macromolecules*, **38**, 6367 (2005).

P076A

Synthesis of Poly(*p*-benzamide)s Bearing *α*-Branched Chiral Alkyl Side Chain and Investigation of Their Chiral Conformation

Tomoaki SAIKI, Akihiro YOKOYAMA, and Tsutomu YOKOZAWA*

Department of Material and Life Chemistry, Kanagawa University, Rokkakubashi, Kanagawa-ku, Yokohama 221-8686, Japan

Helical structure is often seen in nature such as double helix of DNA and *α*-helix of proteins. We have demonstrated that poly(*p*-benzamide)s **1** bearing a *β*-branched chiral tri(ethylene glycol) (TEG) side chain form a one-handed helical conformation in solution and show temperature-dependent circular dichroism (CD) signals.[1] We now report the synthesis and polycondensation of 4-aminobenzoic acid methyl ester monomer **2** bearing a *α*-branched chiral alkyl side chain on the nitrogen atom, and their chiral conformation by means of CD spectra.

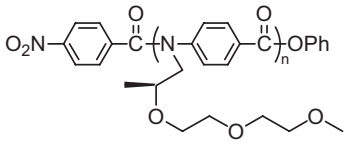

β-chiral TEG polymer **1**

Chiral monomer **2** was prepared by Hartwig's amination method[2] using a Pd catalyst, followed by methyl esterification of the hydrolyzed products (Scheme 1). Polycondensation of **2** was carried out in the presence of an initiator and lithium 1,1,1,3,3,3-hexamethyldisilazide (LiHMDS) at ambient temperature in accordance with chain-growth condensation polymerization method we have developed[3] (Scheme 2). A solution of chiral polymer **3** showed split-type Cotton effect in the CD spectra, suggesting that the polymer **3** forms one-handed helical conformation in solution. When we investigated the effect of temperature on the CD spectrum was investigated, we found that the chloroform ($CHCl_3$) solution showed temperature-dependent CD signals (Figure 1A). On the other hand, the CD spectra of a tetrahydrofuran (THF) solution did not show any temperature dependence (Figure 1B). These results suggest that **3** adopt dynamic helical structure in $CHCl_3$ solution and static one in THF solution, respectively.

Scheme 1

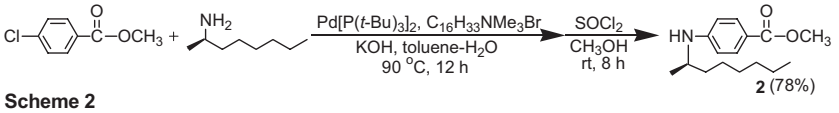

Scheme 2

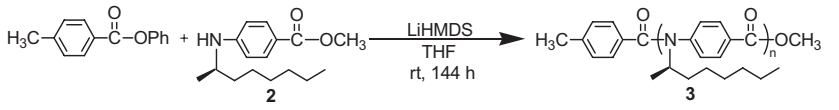

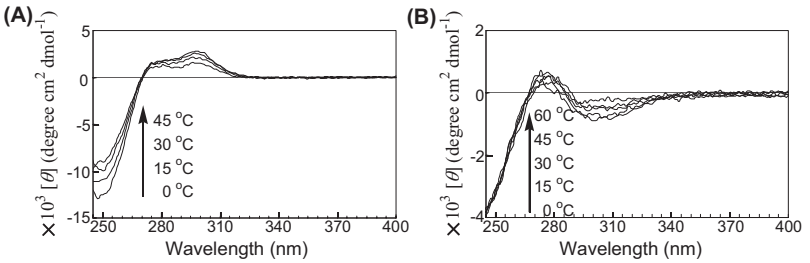

Figure 1. CD spectra of *α*-chiral alkyl polymer **3** in (A) $CHCl_3$ at 0-45 °C and (B) THF at 0-60 °C.

1) A. Tanatani, A. Yokoyama, I. Azumaya, Y. Takakura, C. Mitsui, M. Shiro, M. Uchiyama, A. Muranaka, N. Kobayashi, T. Yokozawa, *J. Am. Chem. Soc*., **2005**, *127*, 8553.

2) R. Kuwano, M. Utsunomiya, J. F. Hartwig, *J. Org. Chem*., **2002**, *67*, 6479.

3) T. Yokozawa, D. Muroya, R. Sugi, A. Yokoyama, *Macromol. Rapid Commun.*, **2005**, *26*, 979.

P077B

Investigation of Catalyst-Transfer Condensation Polymerization for the Synthesis of Well-Defined Polypyridine

Yutaka NANASHIMA, Akihiro YOKOYAMA, and Tsutomu YOKOZAWA

Contribution from the Department of Applied Chemistry, Kanagawa University, Rokkakubashi, Kanagawa-ku, Yokohama 221-8686, Japan

We have already reported that the condensation polymerization of 2-bromo-5-chloromagnesio-3-hexylthiophene with Ni(dppp)Cl_2 proceeds in a chain-growth polymerization manner to yield narrow-molecular-weight distribution poly(3-hexylthiophene), which is a p-type conductive polymer, and that the molecular weight is controlled by the feed ratio of the monomer to the Ni catalyst.[1)] Furthermore, we attempted to synthesize well-defined poly(2-hexylpyridine) and poly(2-dodecylpyridine), which is a n-type conductive polymer, under similar conditions, but were not able to study in detail because of poor solubility of these polypyridines. We now report the polymerization of another pyridine monomer **2** having a methoxy ethoxy propyl (MEP) side chain.

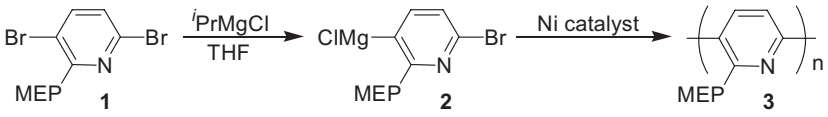

(MEP = $(CH_2)_3O(CH_2)_2OCH_3$)

Scheme 1

Monomer **2** was generated in situ by treatment of 3,6-dibromo-2-[3-(2-methoxyethoxy-propyl)] pyridine (**1**) with 1 equiv of ^{i}PrMgCl in THF at room temperature for 24 h via a magnesium-bromine exchange reaction (88% yield). Polymerization was carried out by addition of 1.8 mol % of a Ni catalyst to the reaction mixture (Scheme 1). Ni(dppp)Cl_2 was first used as a catalyst because it is a suitable Ni catalyst for the synthesis of well-defined poly(3-hexylthiophene). The polymerization proceeded smoothly at room temperature, and the conversion of **2** was 89% in 3 h. The obtained polymer had a very broad polydispersity (Table 1, entry 1), but was highly soluble in $CHCl_3$, CH_2Cl_2, THF, and 5 M HCl. In addition, the regioregularity was highly controlled as head-to-tail (H-T). We next examined the polymerization with the same Ni catalyst at 50 °C (entry 2), in the presence of LiCl (entry 3), and addition of dppp (entry 4), respectively, but the obtained polymer possessed broad

Table 1. Polymerization of **2** with various catalysts in THF[a]

Entry	Cat.	Additive	Temp. (°C)	Time (h)	Conv. of **2** (%)[b]	M_n(M_w/M_n)[c]
1	Ni(dppp)Cl_2	——	rt	3	89	8000 (10.0)
2		——	50	1	95	6650 (10.5)
3		LiCl[d]	rt	6	96	6000 (3.99)
4		dppp[e]	rt	1	78	4200 (12.3)
5	Ni(dppf)Cl_2	——	rt	3	93	8500 (6.75)
6	Ni(dppe)Cl_2	——	rt	3	78	3500 (7.86)
7	Ni(PPh_3)$_2Cl_2$	——	rt	6	73	1500 (4.78)
8	Ni(Bu_3P)$_2Cl_2$	——	rt	3	60	2100 (2.72)
9	Ni(dcpe)Cl_2	——	rt	6	24	510 (1.03)
10	Pd(dppp)Cl_2	——	50	6	85	1300 (2.17)
11	Pd(dppe)Cl_2	——	50	6	98	2400 (1.96)
12	Pd[(^{t}BuP)$_3$]$_2$	——	50	6	20	1850 (6.91)

[a]Polymerization of **2** was carried out by treatment of **1** with 1.0 equiv of ^{i}PrMgCl, followed by addition of 1.8 mol % of catalyst . [b]Detemined by GC. [c]Estimated by GPC based on polystyrene standards (eluent: THF). [d]Polymerization was carried out in the presence of 1 equiv of LiCl to catalyst. [e]Polymerization was carried out in the presence of 1 equiv of dppp to catalyst.

polydispersities. When Ni catalysts with different ligands, Ni(dppf)Cl_2 (entry 5) and Ni(dppe)Cl_2 (entry 6), were used, the products also showed broad polydispersities. When Ni$(PPh_3)_2Cl_2$ (entry 7), Ni$(Bu_3P)_2Cl_2$ (entry 8) and Ni(dcpe)Cl_2 (entry 9) were used, conversion of **2** became low to give polymers with low molecular weights. In addition, the polydispersity was also broad (entries 7, 8). Pd catalysts instead of Ni catalysts were not effective for obtaining polymers with low polydispersity, either (entries 10-12). In conclusion, we conducted polymerization of **2** with a variety of Ni and Pd catalysts, but still have not obtained polypyridine with low polydispersity. However, polymer **3** obtained was found to have high solubility and high H-T regioregularity.

Ligand

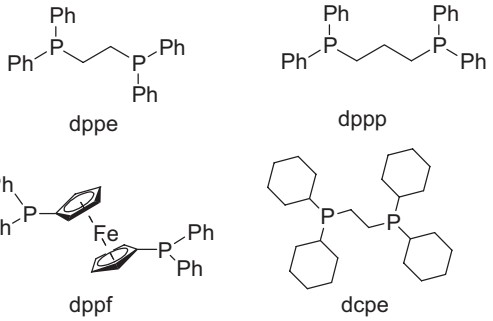

1) R. Miyakoshi, A. Yokoyama, T. Yokozawa, *J. Am. Chem. Soc*., **127**, 17542 (2005).

P078C

Synthesis of a variety of well-defined *N*-alkyl poly(*m*-benzamide)s and their block copolymers by chain-growth condensation polymerization

Tomoyuki OHISHI, Akihiro YOKOYAMA, Tsutomu YOKOZAWA

Department of Material and Life Chemistry, Kanagawa University, Rokkakubashi, Kanagawa-ku, Yokohama 221-8686, Japan

We have succeeded in controlling the molecular weights and polydispersities of *N*-octyl poly(*m*-benzamide)s by chain-growth condensation polymerization of 3-(octylamino)benzoic acid ethyl ester with lithium 1,1,1,3,3,3-hexamethyldisilazide (LiHMDS) through changing the inductive effect,[1] in a manner similar to the case of the *para*-substituted counterparts by virtue of the resonance effect.[2] We now report the polycondensation of 3-aminobenzoic acid esters **1** having various kind of alkyl and oligo(ethylene glycol) side chains on the nitrogen, as well as properties of the polymers (Scheme 1). Furthermore, one-pot two-stage synthesis and the properties of diblock copolymers composed of poly(*m*-benzamide) and/or poly(*p*-benzamide) with various kinds of side chains one also reported.

Scheme 1

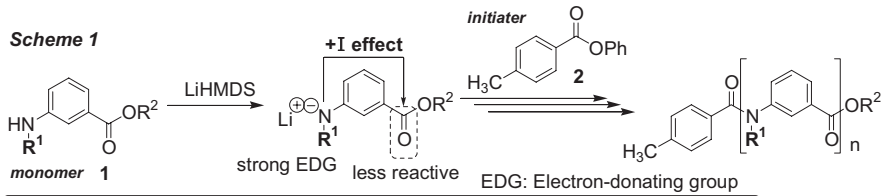

1a: $R^1 = C_8H_{17}$, R^2 = Et **1b**: $R^1 = C_4H_9$, R^2 = Et **1c**: $R^1 = CH_3$, R^2 = Et

1d: $R^1 = CH_2$–C$_6$H$_4$–OC_8H_{17}, R^2 = Me **1e**: $R^1 = CH_2$–C$_6$H$_4$–OMe, R^2 = Et

1f: R^1 = –(CH$_2$CH$_2$O)$_3$CH$_3$, R^2 = Me **1g**: R^1 = –(CH$_2$CH$_2$O)$_4$CH$_3$, R^2 = Me

The polymerization of **1** was carried out in the presence of LiHMDS at 0 °C. In the polymerization of **1b-e** and **1f-g** , LiCl and *N,N,N',N'*-tetrametylethylendiamine (TMEDA) were added, respectively to obtain the polyamides with narrow molecular weight distributions (Table 1). These polyamides showed higher solubility than the poly(*p*-benzamide)s with the corresponding *N*-substituents. Especially, poly(*m*-benzamide)s bearing a tri- or tetra(ethylene glycol) methyl ether unit on the nitrogen were soluble in water. The aqueous solutions showed reversible cloud points by heating, and solubilized hydrophobic azobenzene in water.

Table 1 Polymerization of **1** with **2**[a]

Entry	Monomer	$[\mathbf{1}]_0/[\mathbf{2}]_0$	M_n calcd	M_n[b]	M_w/M_n[b]	Tc (°C)[c]
1	**1b**	20	3670	3930	1.10	—
2[d]		48	8570	7280	1.10	—
3	**1c**	10	1500	1510	1.19	—
4	**1d**	20	6900	5840	1.08	—
5[d]	**1e**	21	5120	4580	1.15	—
6[e]	**1f**	10	2800	3000	1.16	56.5
7[e]	**1g**	10	3240	3640	1.14	74.2

[a] Polymerization of **1** with **2** in the presence of 1.1 equiv of LiHMDS in THF ($[\mathbf{1}]_0$ = 0.33 M) at 0 °C. [b] Determined by GPC based on polystyrene standerds (eluent: THF). [c] Transmittance changes of 0.5 wt% aqueous solution as a function of temperature (rate: 0.5 °C/min; wavelength: 500 nm). [d] In the presence of 5 equiv of LiCl. [e] In the presence of 5 equiv of TMEDA.

We next tried one-pot two-stage synthesis of diblock copolymers composed of poly(*m*-benzamide) and/or poly(*p*-benzamide) with various kinds of side chains (Scheme 2). The block copolymers were synthesized by the chain-growth condensation polymerization of *meta*-substituted monomer **1** (1st

stage monomer) from initiator **2** in the presence of 2.2 equiv of LiHMDS, followed by addition of another kind of **1** or *para*-substituted monomer **3** (2nd stage monomer) into the reaction mixture. The added 2nd stage monomer feed smoothly polymerized. The GPC chromatogram of the product was clearly shifted toward the high molecular weight region, while retaining a narrow molecular weight distribution, indicating successful production of the block copolymers (Table 2).

Scheme 2

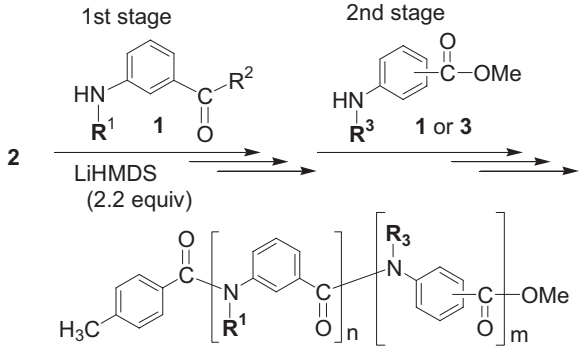

Table 2. Block copolymerization with LiHMDS in THF at 0 °C.

Entry	Block Copolymer	Stage	M_n calcd	M_n NMR	M_w/M_n [a]
1	poly(*meta*-**1a**)-*b*-poly(*meta*-**1d**)	1st	2480	2550	1.09
		2nd	6120	6700	1.06
2	poly(*meta*-**1d**)-*b*-poly(*meta*-**1f**)	1st	3520	3830	1.07
		2nd	6580	6910	1.15
3	poly(*meta*-**1a**)-*b*-poly(*para*-**1d**)	1st	2480	2590	1.09
		2nd	6100	6430	1.11
4	poly(*meta*-**1d**)-*b*-poly(*para*-**1a**)	1st	3520	3730	1.07
		2nd	6230	6480	1.08

[a] Determined by GPC based on PSt in THF.

The 4-octyloxybenzyl group on the amide nitrogen in the block copolymers obtained were removed with trifluoroacetic acid (TFA) in CH_2Cl_2 at ambient temperature for 3 days to give the *N*-H polyamide units. The GPC chromatogram (eluent: DMF) of the block copolymer containing *N*-H poly(*m*-benzamide) unit slightly shifted toward the lower molecular weight region while keeping the polydispersity low. On the other hand, the block copolymer containing *N*-H poly(*p*-benzamide) segment showed a only peak in the high molecular weight region, implying that part of *N*-H poly(*p*-benzamide) unit was aggregated in DMF by virtue of the intermorecular hydrogen bonding between the amide linkages. A solution a the deprotected block copolymer in CH_2Cl_2 or $CHCl_3$ was found to become gel.

1) R. Sugi, A. Yokoyama, T. Furuyama, M. Uchiyama, T. Yokozawa, *J. Am. Chem. Soc.*, **2005**, *127*, 10172.
2) (a) T. Yokozawa, T. Asai, R. Sugi, S. Ishigooka, S. Hiraoka, *J. Am. Chem. Soc.*, **2000**, *122*, 8313. (b) T. Yokozawa, D. Muroya, R. Sugi, A. Yokoyama, *Macromol. Rapid. Commun.*, **2005**, *26*, 979.

P079A

Development of Chain-Growth Condensation Polymerization of Monomer Immobilized on Solid-Support: Model Reaction and Polymerization

Ryota NEGISHI[1], Yoshio KABE[2], Kazuo YAMAGUCHI[2], Akihiro YOKOYAMA[1], and Tsutomu YOKOZAWA[1*]

[1]*Depertment of Material and Life Chemistry, Kanagawa University, 3-27-1 Rokkakubashi, Kanagawa-ku, Yokohama 221-8686, Japan*

[2]*Department of Chemistry, Kanagawa University, 2946 Tuchiya, Hiratsuka 259-1293, Japan*

The polycondensation of monomer, immobilized on solid-support, with an initiator, in which the monomers do not react with each other, would be an approach to chain-growth condensation polymerization. We previously studied the polycondensation of a monomer containing carboxyl group, immobilized with tertiary amine on silica gel, but the polymerization was terminated by the reaction of the propagating benzylic bromide moiety with the tertiary amino group on silica gel. We now report the polycondensation of a monomer immobilized with ammonium-functionalized silica gel (Scheme 1).

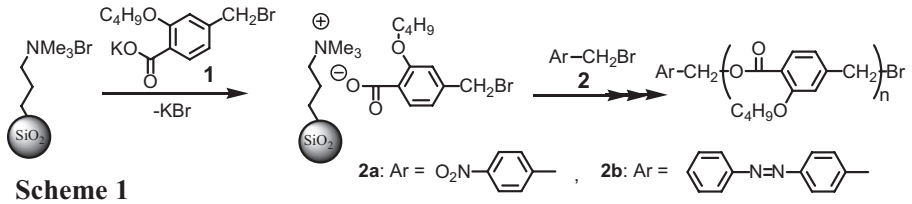

Scheme 1

Monomer, potassium 4-bromomethyl-2-butoxybenzoate **1**, was loaded on the ammonium-functionalized silica gel by salt exchange reaction, and found not to undergo self-condensation and side reaction of the bromomethyl group. Furthermore, the GPC trace of the polymers obtained in the polymerization with an initiator **2b**, possessing an absorption at 330 nm, showed that the immobilized monomer polymerized in a chain polymerization manner from the initiator (Table 1, Figure 1), because self-condensed polymer without the initiator **2b** unit was not absorved in the GPC traces detected by absorption at 254 nm.

Table 1. Elution volume of product in GPC

Polymerization with solid-support at 50 ℃	
Elution volume (mL)	
330 nm[a)]	254 nm[a)]
19.11	19.05
19.34	19.36
19.69	19.64
20.17	20.14

a) Wavelength of UV detector in GPC.

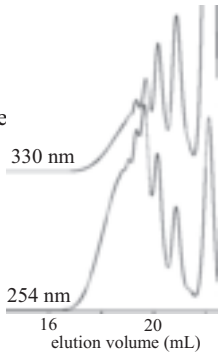

Figure 1. GPC elution curves of product from polymerization of **1** with solid-support.

P080B

Knoevenagel Reactions in Water Catalyzed by Immobilized Organomolecular Catalyst

Hisahiro Hagiwara*[a,c], Kohei Isobe[a], Ayuko Numamae[b], Takashi Hoshi[b,c], Toshio Suzuki[b,c]

[a]Graduate School of Science and Technology; [b]Faculty of Engineering; [c]Center for Education and Research on Environmental Technology, Materials Engineering, and Nanochemistry, Niigata University, 8050, 2-Nocho, Ikarashi, 950-2181, Niigata, Japan

E-mail: hagiwara@gs.niigata-u.ac.jp

In order to afford stability and recyclability to organomolecular catalyst, an amine residue was graft ed on silica and its utility as environmentally benign catalyst was investigated.

<**Knoevenagel reaction in water**>

An environmentally benign and sustainable Knoevenagel reaction of ethyl cyanoacetate **1** (EWG = CO_2Et, EWG' = CN) with aldehyde **2** leading to α-cyano-α,β-unsaturated esters **3** (EWG = CO_2Et, EWG' = CN) has been achieved at ambient temperature in water employing 3-aminopropylated silica (NAP) as a catalyst (Equation 1). Wide applicability of the reaction is illustrated by the results that not only arylaldehydes of both electronic characters but also aliphatic aldehydes afforded the products. The reaction condition was so mild that aldehydes having acid- or base-sensitive substituents provided substituted α-cyano-α,β-unsaturated esters **3**. The catalyst has been efficiently recycled more than five times without any pre-treatment. This protocol was also applicable to the Knoevenagel reaction of malononitrile **1** (EWG and EWG' = CN) in good yields in water. Catalyst loading was successfully reduced to 0.0029 mmol% (TON = up to 9,226).

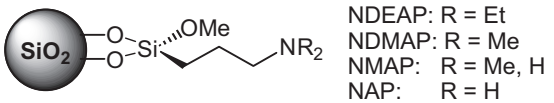

NDEAP: R = Et
NDMAP: R = Me
NMAP: R = Me, H
NAP: R = H

Equation 1

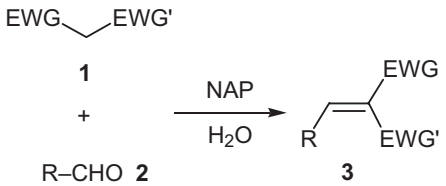

<**Sequential Knoevenagel reaction/ Mislow-Evans Rearrangement in water**>

γ-Hydroxy-α,β-unsaturated nitrile **8** was obtained by the reaction of α-arylsulfinylacetonitrile **4** with aldehyde **2** at ambient temperature in water, which was catalyzed by *N,N*-diethylaminopropylated silica (NDEAP) (Scheme 1). The overall transformation proceeded via five sequential reactions, namely, 1,2-addition of acetonitrile, dehydration (Knoevenagel condensation), isomerization of double bond, rearrangement of sulfinyl group (Mislow-Evans rearrangement) and hydrolysis of sulfinyl ester.

Scheme 1

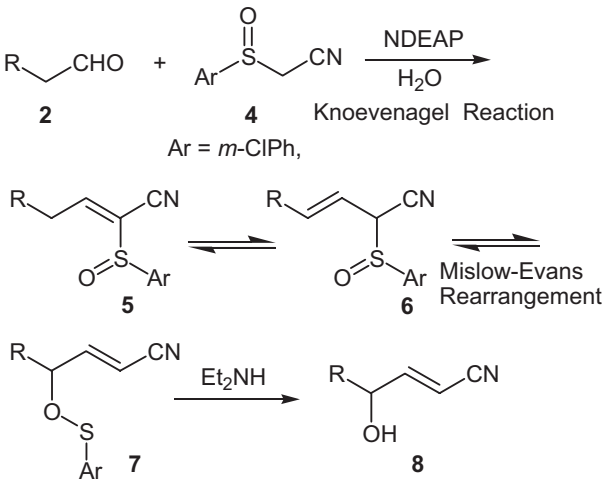

P081C

Biphenylene-Containing Ruthenocenylphosphine Designed as a Novel Phosphine-Arene Ligand: Application to Pd-Catalyzed Suzuki-Miyaura Reaction

Takashi Hoshi,*[,a,c] Ippei Saitoh,[b] Taichi Nakazawa,[b] Toshio Suzuki,[a,c] and Hisahiro Hagiwara*[,b,c]

[a]Faculty of Engineering, [b]Graduate School of Science and Technology, and [c]Center for Education and Research on Environmental Technology, Materials Engineering, and Nanochemistry, Niigata University, Niigata 950-2181, Japan

The use of bulky and electron-rich phosphines as supporting ligands is now a well-recognized strategy for generating highly active palladium catalysts for cross-coupling reactions. Excellent palladium catalysts have also been realized with the use of a biarylphosphine ligand which has the potential to serve as a bidentate phosphine-arene ligand resulting from a □-interaction between the lower arene ring and the phosphine-ligated palladium center.[1] We report herein the development of biphenylene-substituted di-*tert*-butyl ruthenocenylphosphine (R-Phos) designed as a novel phosphine-arene ligand and its unprecedented activating and stabilizing abilities to lead to the excellent palladium catalyst for Suzuki-Miyaura reaction, particularly for the synthesis of extremely hindered tetra-*ortho*-substituted biaryls from aryl chlorides (Table 1). A strong dependence of the activity of our catalytic system on a Pd:R-Phos ratio and the markedly higher activity realized with the use of a 1:3 ratio will be also reported.

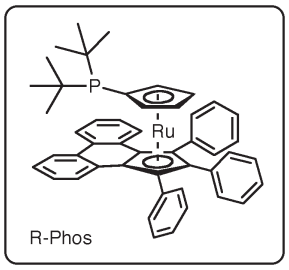

Table 1. Suzuki-Miyaura Reaction Using R-Phos[a]

Entry	Aryl chloride	Boronic acid	Product	Time	Yield [%]
1	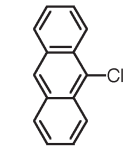	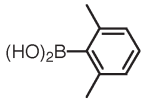	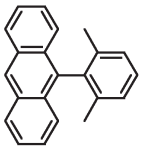	20 min	87
2	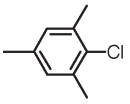	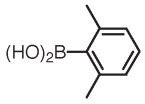	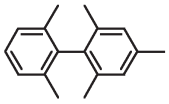	2 h	80
3	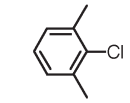	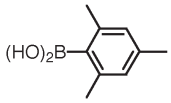	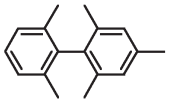	2 h	94

[a] Reaction conditions: 1 mol% $Pd(dba)_2$, 3 mol% R-Phos, 3.0 equiv of boronic acid, 3.0 equiv of K_3PO_4, dioxane, 100 °C.

1) Barder, T. E.; Walker, S. D.; Martinelli, J. R.; Buchwald S. L. *J. Am. Chem. Soc*. **2005**, *127*, 4685 and references therein.

P082A

FRAMEWORK-REARRANGEMENT REACTION OF COMPLETELY-CONDENSED OCTA(ARYL) OCTASILSESQUIOXANE (ARYL-T8)

Ze Li and Yusuke Kawakami*

School of Materials Science, Japan Advanced Institute of Science and Technology, 1-1 Asahidai, Nomi, Ishikawa 923-1292, Japan

In the hydrolysis of octaphenyloctasilsesquioxane (Ph-T8) with water and sodium hydroxide in *iso*-propanol under reflux for 24 hr, a double–deck POSS, DDT8ONa, was obtained (Scheme 1). When the same procedure was repeated at room temperature, the main product was cyclic tetramer tetraol sodium salt, T4ONa (Scheme 2). The main product was T7ONa in the co-hydrolysis of Ph-T8 and *o*-MePh-T8 (Scheme 3). MALDI TOF MS of the T7OTMS indicated statistical distribution of the substituent in the product. Both T7ONa and double-deck DDT8ONa were formed in the co-hydrolysis of non-deuterated and deuterated Ph-T8, in which both hydrogen and deuterium were contained equally in the aromatic ring of the products (Scheme 4). These phenomena provided a clue for the possible mechanism, that is Aryl-T8 decomposed into some fragments such as ring structures like T4ONa and open chains in solution, and these fragments reassembled in solution to form DDT8ONa or T7ONa. In other words, this reaction is a framework-rearrangement reaction.

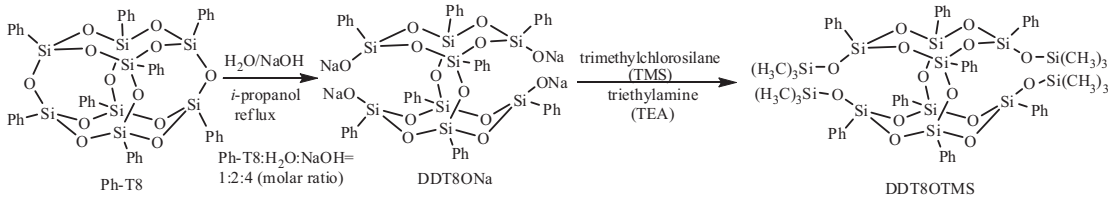

Scheme 1. Hydrolysis of Ph-T8 under reflux.

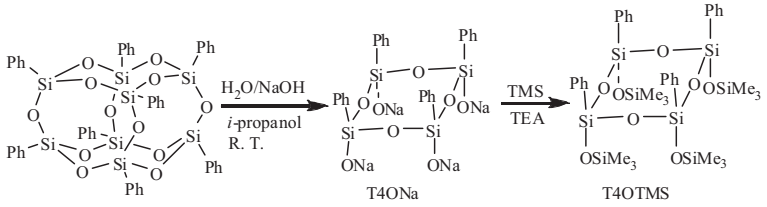

Scheme 2. Hydrolysis of Ph-T8 at R.T.

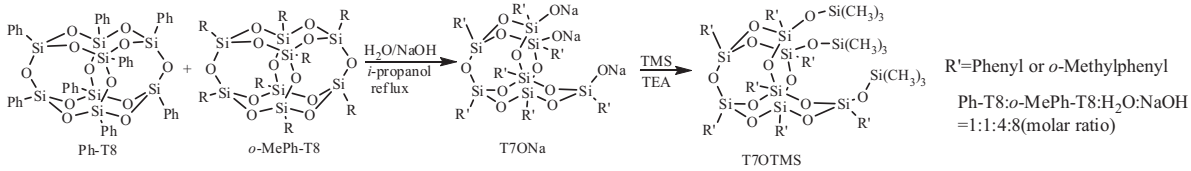

Scheme 3. Co-hydrolysis of Ph-T8 and o-MePh-T8 under reflux.

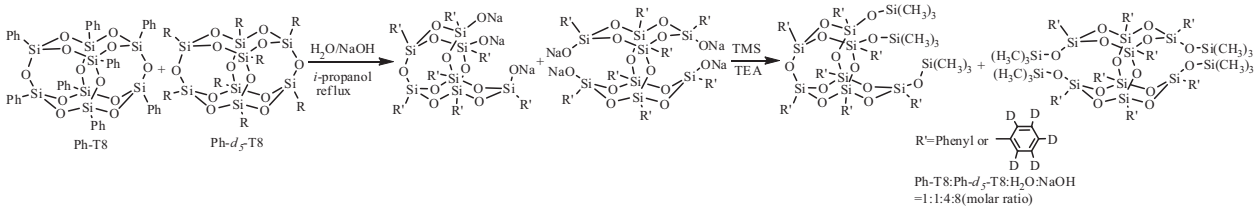

Scheme 4. Co-hydrolysis of Ph-T8 and Ph-d_5-T8 under reflux.

P083B

SYNTHESIS AND CHEMICAL PROPERTIES OF POLYFLUORINATED PORPHYRINS

Yusuke Hoshina[1)], Akihiro Suzuki[2)]*

1) Department of Chemistry, Nagaoka University of Technology, 1603-1 Kamitomioka, Nagaoka, Japan 940-2188

2) Department of Chemistry, Nagaoka National College of Technology, 888 Nishikatakai, Nagaoka, Japan 940-8532

Introduction

Since heme-proteins containg Fe porphyrin play very important role in an organism, such model study is meaningful in scientific interesting. For the research purposed to synthesize and analyze function-structure of novel iron porphyrin complex with fluoride atoms, using ^{19}F-NMR would give us detailed information of electronic structure of the porphyrin, especially for local position of the ring. In order to prepare fluorinated porphyrins such as 2,3,8-trifuluoro-porphyrin (2,3,8-TFP) and 2,3,7,8-tetrafluoroporphyrin (2,3,7,8-TFP), the three or four monofluoro groups were introduced into the porphyrin framework. Coupling reaction of dipyrromethenes having mono-fluoride group were performed (Scheme 1). The properties of the porphyrin were comparable with others such as 2-monofluoroporphyrin and 3,7-difluoroporphyrin by measuring electronic absorption spectra and ^{19}F-NMR spectra of synthesized porphyrins.

Experimental

Difluoropyrrole 1 was used after recrystallization from CH_2Cl_2/pentane solvent. Then, Vilsmeier reaction using $POCl_3$-DMF was carried out in $C_2H_4Cl_2$ solvent at about 80℃ for difluoroformylpyrrole 2. Resultant dipyrromethene derivatives were obtained by coupling of 2 and monofuruoropyrrole 3 for 4. For purification of the coupled 4, diethylether was used to wash resultant dipyrromethene.

Results and discussion

Objective porphyrins having 2,3,8-TFP or 2,3,7,8-TFP were synthesized as follows by using fluorinated pyrrole such as difluoropyrrole 1. Firstly, on the synthesis of 2,3,8-TFP 6 via synthetic route (Scheme 1), cyclization reaction from trifluorodipyrromethene 4 and 5 led to that 1.2% low yield was obtained for 6. It was reasonable that this was caused by low steric repulsion between β-position substitutes of 4, when the coupling was carried out in 5 and 4. Figure 1 shows resultant electronic absorption spectrum measured in $CHCl_3$ for 6.

The data indicated that 6 porphyrin ring was formed and displayed without electron withdrawing effect. Secondly, synthesis of 2,3,8-TFP 9 was taken place as illustrated in Scheme 2. The synthetic route through cyclization of 2 and 7 gave porphyrin 8. In expectation that trimethylacetaldehyde effects on steric hindrance, the cyclization reaction was perfomed. But, obtained 8 was on low yield in 3.4%. Namely, the effect of the trimethylacetaldehyde was unable to be the cyclization. So, electronic absorption spectrum resulted in several evidences of the cycled porphyrin 8 on the meso-position for the presence of alkyl group. A development study is now in progress using ^{19}F-NMR.

Conclusion

Novel fluorinated porphyrins 6 and 8 were synthesized through coupling reaction of fluorinated dipyrromethen or pyrrole. Their reactions were confirmed with electronic absorption spectrum. There were properties shown as follows in porphyrin with monofluoro group; 1) Fluorine hardly displayed electron withdrawing effect by p-π repulsion. 2) Fluorine gave a less deformational conformation of the porphyrin ring.

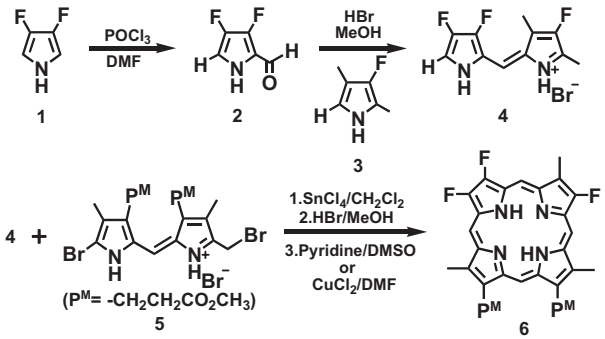

Scheme1. Synthetic routes for 2,3,8-TFP.

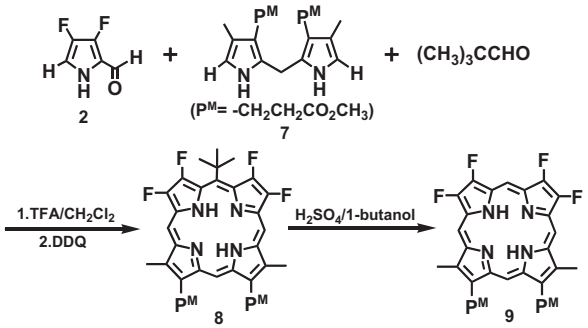

Scheme2. Synthetic routes for 2,3,7,8-TFP.

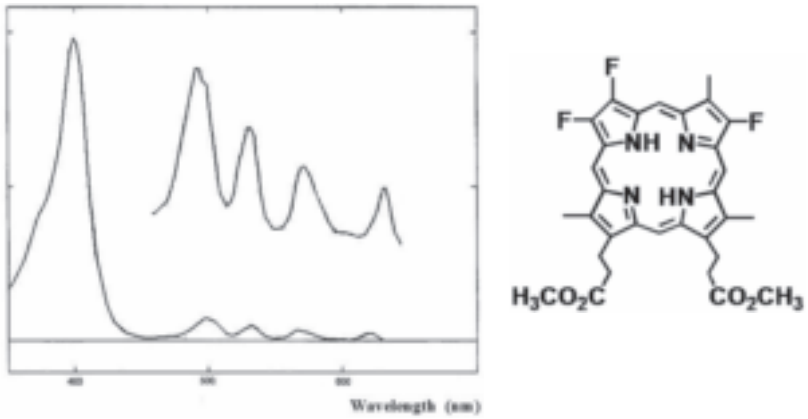

Figure 1. Electronic absorption spectrum of 2,3,8-TFP 6.

P084C

BIOACTIVE CARDENOLIDES FROM THE STEMS AND TWINGS OF *NWRIUM OLEANDER*

Liyan Wang,[1] Ming Zhao,[1] Liming Bai,[1,5] Asami Toki,[1] Toshiaki Hasegawa,[2] Midori Kikuchi,[2] Mariko Abe,[2] Jun-ichi Sakai,[1] Ryo Hasegawa,[1] Yuhua Bai,[1,7] Tomokazu Mitsui,[3] Hirotsugu Ogura,[3] Takao Kataoka,[3] Seiko Oka,[4] Hiroko Tsushima,[4] Miwa Kiuchi,[4] Katutoshi Hirose,[5] Akihiro Tomida,[6] Takashi Tsuruo,[6] and Masayoshi Ando[1,7]

[1]Graduate School of Science and Technology and Department of Chemistry and Chemical Engineering, Niigata University, Ikarashi, 2-8050, Niigata, 950-2181, Japan, [2]Mitsubishi Gas Chemical Company, Inc., Niigata Research Laboratory, 182 Shinwari, Tayuhama,Niigata,950-3112,Japan, [3]Center for Biological Resources and Informatics, Tokyo Institute of Technology, 4259 Nagatsuta-cho, Midori-ku, Yokohama 226-8501, Japan, [4]Center for Instrumental Analysis, Hokkaido University, Kita-12, Nishi-6, Kita-ku, Sapporo 060-0812, [5]KNC Laboratories Co. Ltd.3-2-34, Takatukadai, Nishi-ku, Kobe, Hyogo 651-2271, Japan, [6]Cancer Chemotherapy Center, Japanese Foundation for Cancer Research, 3-10-6Ariake,Koto-Ku, Tokyo 135-8500, Japan, and [7]Department of Pharmacy Engineering and Applied Chemistry, College of Chemistry and Chemistry Engineering, Qiqihar University, 30 Wenhuadajie, Qiqihar, Heilongjian Shang, People'sRepublic of China

Four new cardenolide monoglycosides, cardenolides N-1 (**1**), N-2 (**2**), N-3 (**3**), and N-4 (**4**) were isolated from *Nerium oleander*, together with two known cardenolides **5** and **12**, and seven cardeno lide monoglycosides **6**—**11** and **13**. The structures of compounds **1**—**4** were established on the basis of their spectroscopic data. The in vitro anti-inflammatory activity of compounds **1**—**13** was examin ed on the basis of inhibitory activity against the induction of the intercellular adhesion molecule-1 (I CAM-1). Compounds **1**, **5**, **6** and **11**—**13** were active at an IC_{50} value of less than 1 μM. The cytotox icity of compounds **1**—**13** was evaluated against three human cell lines, normal human fibroblast cel ls (WI-38), malignant tumor cells induced from WI-38 (VA-13),and human liver tumor cells (HepG2). Compounds **1**, **4**, **6**, and **11**—**13** were active toward V-13cells and compounds **1**, **11**, and **12** were a ctive toward HepG2 cells at IC_{50} values of less than 1 μM. Compounds **4**, **5**, **10**, and **12** showed selec

tive cell growth inhibitory activity toward VA-13 tumor cells compared with that of parental normal WI-38 cells. The MDR-reversal activity of compounds **1**—**13** was evaluated on the basis of t he amount of calcein accumulated in MDR human ovarian cancer 2780AD cells in the presence of e ach compound. Compounds **4**, **9**, and **10** showed significant effects on calcein accumulation, compo und **4** showing stronger activity than that of verapamil. Structure was showed by Fig.1.

Cell Growth Inhibitory Activities of Cardenolides 1—13 against WI-38, VA-13 and HepG2 Cells.

compound	WI-38	VA-13	HepG2
	IC_{50} (μM)[a]	IC_{50} (μM)[a]	IC_{50} (μM)[a]
1	<0.02	0.80	0.14
2	16.3	85.7	81.4
3	40.9	178	74.1
4	23.0	0.72	140
5	11.8	1.9	18
6	0.07	0.18	1.5
7	0.37	1.3	10.2
8	102	161	151
9	33.1	13.4	76.4
10	9.4	1.6	4.7
11	0.08	0.24	0.82
12	1.7	0.16	0.20
13	0.09	0.17	1.5
Taxol	0.04	0.005	8.1
ADM	0.70	0.40	1.3

[a]IC_{50} represents the mean of duplicate determination.

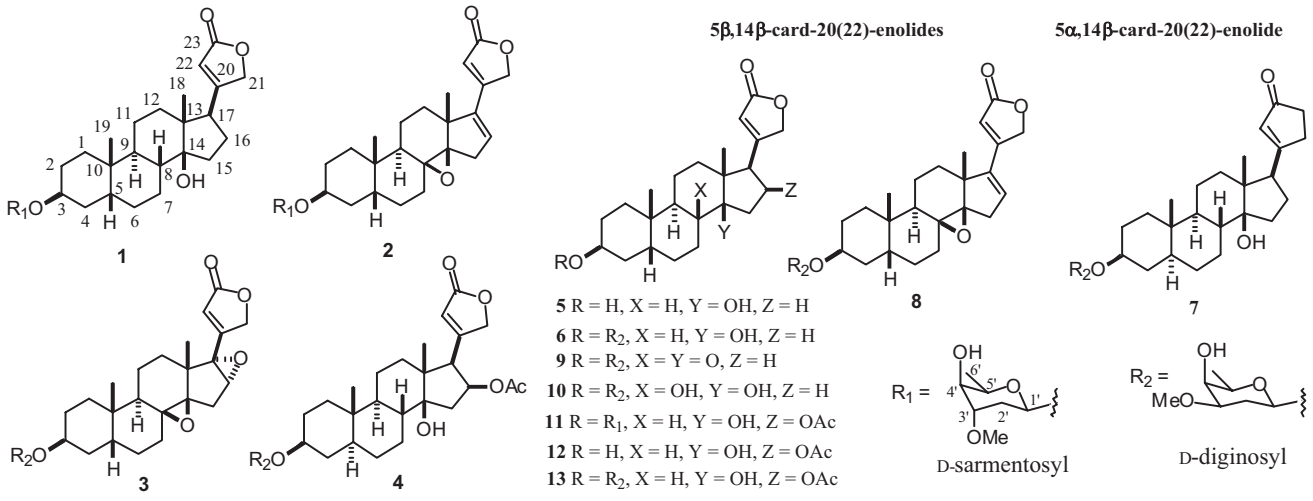

Fig. 1

P085A

Photolithographic Properties of Ultrathin Polymer Langmuir-Blodgett Films Containing Naphthyl Group

Wenjian Xu, Tiesheng Li*, Gouliang Zeng, Suhua Zhang, Wei Shang, Yangjie Wu*

Department of chemistry, Zhengzhou University, Zhengzhou 450052, P. R. China
The Key Lab of Chemical Biology and Organic Chemistry of Henan Province, Zhengzhou 450052, P.R China
The Key Lab of Advanced Nano-information Materials of Zhengzhou, Zhengzhou 450052, P. R. China
**Corresponding author: E-mail: lts34@zzu.edu.cn (T. S. Li), wyj@zzu.edu.cn (Y. J. Wu)*

Introduction

Langmuir-Blodgett (LB) films are expected as a potential candidate of high resolution lithography techniques [1,2], because it can provide an ultrathin film with controlled thickness and well-defined molecular orientation at a molecular size. T. Miyashita. et al. have found that N-alkylacylamide can form an uniform LB film with a highly ordered structure [3.4], yielded a positive-type photopatterning [5.6] and a fine negative pattern by the crosslinking reaction with deep UV and EB irradiation [7]. It was found that the higher sensitivity could be obtained by changing the alkyl side chain to the short-branched type [8]. In addition, the protection reaction of ketal and ester group, which can hydrolyze under acid catalysis, can be used in positive pattern, because the polymer is insoluble in an aqueous developer while the hydrolyzed products are soluble [9,10]. Combining these interesting properties both the film-forming of N-alkylmethacylamide and the chemical amplification of side group using the copolymerization method, the improvement of not only the sensitivity but also the imaging quality can be expected. In this paper, a copolymer of N-dodecylmethacrylamide (DDMA) with ß-naphthyl methacrylate (NPMA) was prepared and its photolithographic properties were also investigated.

Experimental

The copolymer pDDMA-NPMA was prepared by free-radial copolymerization. Molecular weights were determined as $M_n=2.8\times10^4$ and $M_w/M_n=1.84$. Surface pressure (π)-area (A) isotherm and the deposition of monolayers were carried out with a Langmuir-Blodgett system (KSV-5000-3, KSV Instruments, Helsinki, Finland). Optical exposures were performed with EX250 UV light source (Honya-Schott Ltd., Japan).

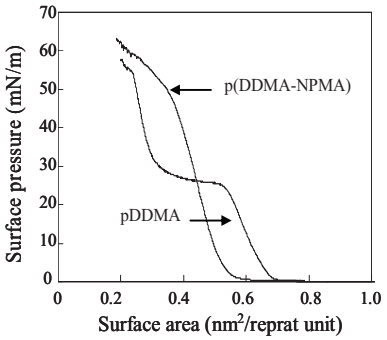

Fig.1 Surface pressure-area isotherms of pDDMA-DNMA and pDDMA on the water surface at 25□ with a compression rate of 10 mm/min.

Results and discussion

The copolymer pDDMA-NPMA and homopolymer pDDMA were spread on water surface from a chloroform solution to measure surface pressure (л)-area (*A*) isotherm of monolayer (Fig.1). The *π- A* isotherm of pDDMA-NPMA shown a steep rise in the surface pressure with a high collapse pressure about 60 mN/m, suggesting the formation of a stable condensed monolayer. The limiting molecular area per repeating unit occupied of the pDDMA-NPMA was estimated to be 0.52 nm^2 from the extrapolation of the liner part of the isotherms to zero surface pressure. The value was smaller than that of monolayer of homopolymer pDDMA. This implied that multilayer or a two-dimensional (2D)

crystal film might form at that time. In order to confirm this deduction, monolayer of the spreading film was transferred on silicon wafer and its AFM image was studied. Numerous fangs and clusters of fangs were observed in the pDDMA-NPMA film, while the surface of pDDMA was very flat. This indicated that strong interactions between the hydrophobic naphthyl groups caused such multilayer or crystal formation of pDDMA-NPMA. The pDDMA-NPMA monolayer could be transferred onto quartz and silicon wafers as a Y-type films. In the UV spectra, the number of layers deposited pDDMA-NPMA LB films as a function of the absorbance at 228 nm apparently increased in a linearity mode at a higher rate up to 11 layers, and then at a lower rate for more layers. This behavior implied that the regular deposition of the copolymer monolayer occurred fewer than 11 layers.

Fig.2 Optical micrograph of pDDMA-DNMA LB films with 11 layers on a silicon plate irradiated with a deep UV light

Naphthyl group is photoactive and can dimerize upon photo-irradiation with UV light. Such kind of photoreaction on the L-B film was investigated through observation of the morphological change of the ultrathin film as a function of irradiation time. Fig.2 showed the optical micrograph of pDDMA-NPMA LB films of 11 layers irradiated with a deep UV light source (248nm) for 5 min through a photomask. We could distinctly see that the exposed areas were much brighter than the masked regions; viz. the thickness of pDDMA-NPMA LB films in the irradiated region which became much thinner than that in no-irradiated region. So, the brightness changes indicated that the photochemical reaction could occur in the LB films and the reaction brought out the photo-decomposition of pDDMA-NPMA. The microscopic photography showed that fine patterns could be drawn at the maximum resolution of 0.75 μm line-and-space, which was the highest resolution of the photomask employed in this study.

Conclusion

Copolymer, pDMMA-NPMA, could aggregate into crystal film on water surface and be transferred on solid substrate to form ultrathin film by Langmuir-Blodgett technique. It was found that the copolymer had high sensitivity to deep UV irradiation. The exposed parts in LB films could be eliminated giving a fine positive tone patterns with a resolution of 0.75 μm without any development process. Just for the high sensitivity to deep UV irradiation, pDMMA/NPMA, which has a structure subjected to decomposition in main chain scission and side chain cleavage, can be used in the dry-development photo-resist system

References

[1] C. H. Zhang, A. M. V, G. D. Darling, Chem. Mater. 7 (1995), pp. 850-855.

[2] T. L. Tan, D. Wong, P. Lee, R. S. Rawat, S. Springham, and A. Patran, Thin Solid Films 504 (2006), pp. 113-116

[3] H. Sugimura, K. H. Lee, H. Sano, and R. Toykawa, Colloid and Surface: A 284-285 (2006), pp. 561-566

[4] T. Miyashita, M. Nakaya, and A. Aoki, Supermolec. Sci. 5 (1998), pp. 363-365

[5] P. B. Sahoo, R. Vyas, M. Wadhwa and S. Verma, Bull, Mater. Sci. 25 (2002), pp. 553-556

[6] J-B. Kim, J.-J. Park, and J.-H. Jang, Polym. 41 (2000), pp. 149-153

[7] D. K. Lee, G. Panlowski, J. Photopolym. Sci. Tec., 15 (2002), pp. 427-34

[8] J. Zhao, K. Abe, H. Akiyama, Z.F. Liu, F. Nakanishi, Langmuir 15 (1999), pp. 2543-2550.

[9] A. Ulman, Chem. Rev. 96 (1996), pp. 1533-1554.

[10] A. Aoki, T. Miyashita, Polym. 42 (2001), pp.7307-7311

P086B

Polymer Langmuir-Blodgett Films Using for Pattern Transformation

Guoliang Zeng, Tiesheng Li*, Wei Shang, Wenjian Xu, Jun Wang, Suhua Zhang, Yangjie Wu*
Department of chemistry, Zhengzhou University, Henan Key Laboratory of Chemistry Biology and Organic Chemistry, Key Lab of Advanced Information Nano-Materials of Zhengzhou, Zhengzhou 450052, PR China
Corresponding authors: lts34@zzu.edu.cn (T.S.Li)

1. Introduction

Lithographic technology is based on projecting an optical image of a device onto a resist in order to record the image for subsequent processing steps [1]. With the development of the integrate circuit chip technology, much attention has been paid to the high resolution photolithography technology. LB films which have ordered structure and controllability of film thickness on the order of molecular sizes have attractive features [2-4]. They can not only overcome the weakness of spin-coat film, in which molecules are distributed randomly, but also be expected to improve the resolution, sensitivity and resistance ability of the resist effectively [5]. Many researches have reported on pattern drawing using LB films in last a few years.

In this paper, we prepared a copolymer p(HDA-BPhMA) which composed of N-hexadecyl-acrylamide (HDA) and 4-tert-butylphenl methacrylate (BPhMA), in which HDA had an excellent ability to form stable monolayer on air/water surface [8]. The process of pattern transfer was studied by atomic force microscopy (AFM).

2. Experimental

Copolymer p(HDA-BPhMA) were prepared by free-radical polymerization of HDA and BPhMA. Copolymer composition and molecular weight were determined by ^{1}H NMR spectra and gel permeation chromatography respectively (mole fraction of BPhMA: 20%; Mn: 1.56×10^4, Mw: 2.80×10^4, Mw/Mn: 1.79). Measurement of surface pressure (π)-surface area (A) isotherms and monolayer deposition were carried out with Langmuir trough (KSV 5000-3) at a compression speed of 10 mm/min at 25℃. Gold film on mica surface was prepared by BTT-IV system.

3. Result and Discussion

The π-A isotherm (Figure 1) of p(HDA-BPhMA) showed sharp rise in surface pressure and high collapse pressure(57mN/m), suggesting that the condensed monolayer was formed at the air/water interface. The monolayer p(HDA-BPhMA) could be transferred onto different solid supports as a Y-type LB films under 28mN/m with a transfer ratio of almost unity.

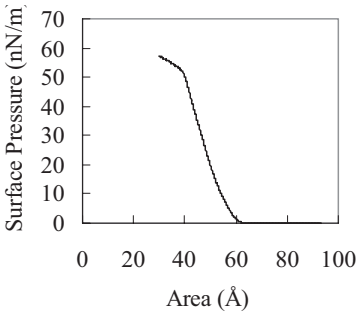

Figure 1. π -A isotherm of pHDA-BPhMA

p(HDA-BPhMA) LB films (40 layers, Y-type) were deposited on mica substrate which coated with gold film firstly, and then, the LB films were irradiated by deep UV lamp (λ=250nm) through a photomask for 40 min and developed with acetone. The regions exposed to UV light were decomposed while the unexposed will not. The fine pattern with high resolution was transferred to LB films. In some area, the resolution of pattern even up to 0.5 μm.

The pattern of LB films was immersed into an etchant solution for 20s. The etchant attacked and

removed the area not covered by LB films, while the protected area unetched. Finally, the gold pattern was obtained after removing residual LB films by chloroform.

From the AFM image of LB films pattern (Figure 2), the average height of the lines with 2 μm linewidth was 59.79 nm, while the height of the lines with 0.75 and 0.5 μm linewidth was 35.38 and 14.21 nm respectively. The height of lines decreased apparently as the width of the lines decreased, which suggesting the unsatisfactory contact between LB films surface and photomask during photopatterning, and diffraction occurred in the narrow slits between mask and LB films. The diffraction affected the pattern transformation apparently especially on lines which had higher resolution. Consequently, the regions of LB films which should have not been irradiated because of coverage of mask also were irradiated slightly by UV light. The LB films in these areas were dissolved partly in development process, and the height decreased apparently. 59.79 nm could be regard as the total height of the LB films with 40 layers. Namely, the average thick- ness of each layer in the LB films was 1.49 nm.

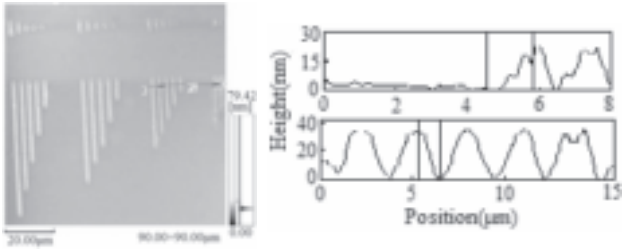

Figure 2 AFM image of LB films pattern and cross-section image

The pattern of gold film was obtained with the resolution of 0.5 μm, but the surface of lines with high resolution was not smooth (Figure 3). Moreover, the average height of lines with resolution of 0.75 μm and 0.5 μm was 60.53 nm and 25.30 nm respectively (average height of gold film is 62.19 nm). These results indicated that the diffraction in photopatterning affected the pattern transformation apparently; the height decreased lines of LB films could not resist the attack of etchant in this condition.

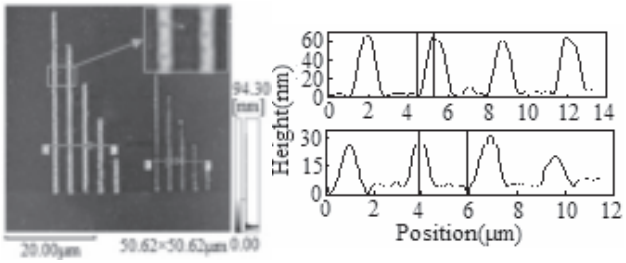

Figure 3 AFM image of gold film pattern and cross-section image

4. Conclusion

The p(HDA-BPhMA) LB films was prepared and applied to photolithography. The metalized pattern with resolution of 0.5 μm was obtained. From the results of AFM, diffraction of UV light was occurred during photopatterning, which affect the pattern transformation apparently.

Acknowledgments

This work is supported by the Nature Science Fund of Henan province (0611020100; 2007150042), the Innovation Found for Outstanding Scholar of Henan Province (0621001100) and the Found for Outstanding Younger Scholar of Henan Province (074100510015)

Reference

1. R. L. Brainard, G. G. Barclay, et al., Microelectronic Engineering 61-62, 707, (2002).
2. T. Miyashita, Y. Ito, Thin Solid Films 260, 217, (1995).
3. Q. Lu, M. H. Liu, Thin Solid Films 425, 248, (2003).
4. Y. Z. Guo, M. Mitsubishi, T. Miyashita, Macromolecules 34, 3548, (2001).
5. Y. Z. Guo, F. Feng, T. Miyashita, Macromolecules 32, 1115, (1999).

P087C

Atomic Force Microscopy studies on Langmuire-Blodgett films of "tailed" porphyrin

Wei Shang[2], Pingping Liu[1],Jun Wang[1], Wenjian Xu[1], Tiesheng Li [1*],Luyuan Mao [2], Suhua Zhang[2], Guoliang Zeng[1] Bing Mu[1], Yangjie Wu[1*]

[1] Department of Chemistry, Zhengzhou University , Zhengzhou 450052, P.R China

[2]Institute of Materials and Engineering, Zhengzhou University,Zhengzhou 450052, P.R China

Abstract: AFM was used to investigate molecular interaction of 5-[2-(6-chloro-glyceryl)] phenyl-10，15，20-tri-p-chlorphenyl copper (Ⅱ) porphyrin (CuTCPP) monolayer, which was formed at 30mN/m and 35mN/m respectively. The result shows that stable and smooth films can be formed for strong π-π interaction among porphyrin macrocycles assisted with the inflection of surface pressure. The aggregation was effected by molecular interaction largely.

Keywords：porphyrin, LB, AFM

Introduction

Langmuir-Blodgett (LB) technique, which is far different from the random molecular arrangements in solution, is a powerful method of making well organized molecular assemblies with precisely controlled thickness on molecular level[1-2]. Metallo-porphyrin thin films prepared by the LB technique have attracted interest for their unique chemical, electrical and optical properties. In this paper, LB films of (CuTCPP) have been studied by AFM to investigate their structures, meanwhile the best configuration model, the mechanics and molecular motion of these monolayers were also studied on molecular level according to different surface pressure.

Experimental Section

CuTCPP was synthesized according to our previous studies[3]. Measurement of surface pressure (π)-area (A) isotherm was carried out with Langmuire trough system (KSV5000-3). Atomic Force Microscopy (AFM) pictures was observed on apparatus (SPM-9500 J3). The monolayer was transferred onto a freshly cleaved mica substrate at 20 (± 0.5 °C) with a compression speed of 5mm/min by the vertical transfer method at a speed of 2 mm/min.

Results and Discussion

A large range surface pressure exists for fabricating LB films seen from Figure 1. Generally, there is substantial attractive π-π interaction between porphyrin macrocycles which is strong enough to cause significant aggregation. The small occupied CuTCPP molecular area about 0.6nm^2 may be due to the spontaneous formation of aggregates after compression, the CuTCPP aggregates were closely packed LB films were fabricated to observe their aggregation and we found that smooth and ordered films could be formed at 30mN/m and 35mN/m..

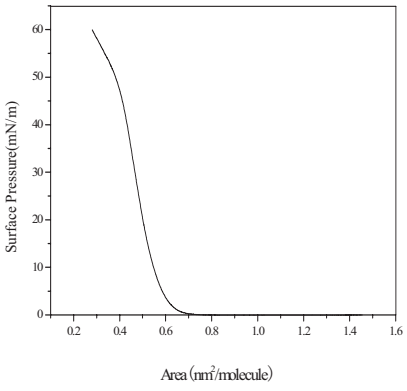

Figure1. The π-A isotherm

The aggregation of LB films was investigated by AFM technique. Compared with the Figure 2 and Figure 3, at the surface pressure of 30mN/m, it can be seen the film was flat and smooth, having directionality and orientation without deficiency; while at a surface pressure of 35mN/m, porphyrin molecule has formed nanoparticles, with each particle embraced about twenty nm^2 neatly. Explained from molecular level, which made the pictures so distinct is the differences of molecular motion. As the surface pressure increased(from 0mN/m to 30mN/m), the distance between porphyrin molecules became shorter, and they move near towards each other, which made the π-π interaction strengthened, when it reached 30mN/m, the pressure

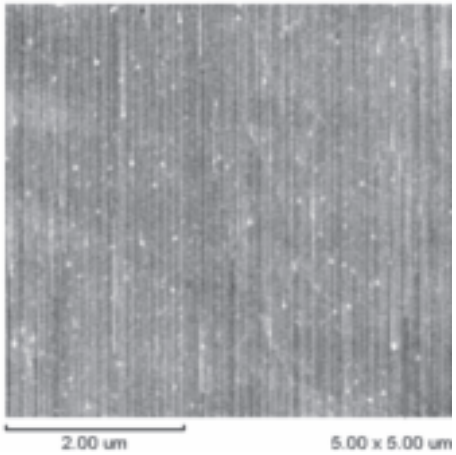

Figure 2. AFM image at 30mN/m

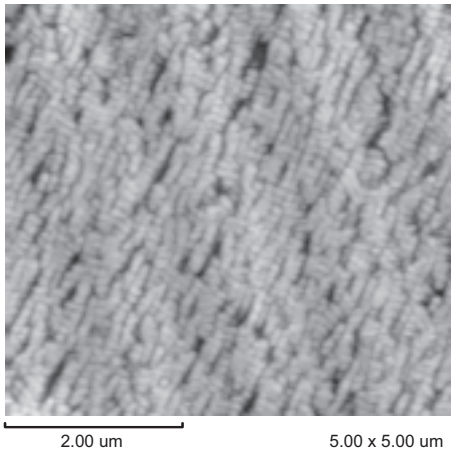

Figure 3. AFM image at 35mN/m

supplied a comfortable force just madding the film resist deformation and form stable monolayer. Porphyrin macrocycles can almost keep their best configuration when they are in free condition. That is the four phenyl perpendicular with porphyrin macrocycle and alkoxy perpendicular with benzene ring. When at 35mN/m,several pirphyrin macrocycles formed “cluster” for the interaction among them increased by higher surface pressure and the whole porphyrin rings became more perpendicular towards the substrate, which made conjugation stronger.

Conclusion

Stable and smooth CuTCPP LB films can be formed at air-water surface.We discussed two AFM images at different surface pressure at 30mN/m and 35mN/m of CuTCPP on molecular level. Results showed that strong π-π interaction among porphyrin macrocycles effects the aggregation of LB films largely.

Acknowledgments

This work is supported by the Nature Science Fund of Henan province (200510459010; 0611020100), the Innovation Found for Outstanding Scholar of Henan Province (0621001100) and the Found for Outstanding Younger Scholar of Henan Province (074100510015)

Reference(s)

[1] M.C. Petty, Langmuir–Blodgett Films. An Introduction, Cambridge University Press,Cambridge, 1996.

[2] Arnold, D. P.; Manno, D.; Micocci, G.; Serra, A.; Tepore, A.; Valli,L. Langmuir, **1997**, 13, 5951.

[3]Tiesheng Li; Yangjie Wu; Zhiian Zhou, Journal of Zhengzhou University of Technology, 1998, 19, 99

P088A

Studies on the characteristics of Langmuir-Blodgett Films of amphiphilic cyclopalladated ferrocenylimines

Bing Mu, Tiesheng Li*, Pingping Liu, Wei Shang, Wenjian Xu, Yangjie Wu*
Department of chemistry, Zhengzhou University, Zhengzhou 450052, P. R. China
The Key Lab of Chemical Biology and Organic Chemistry of Henan Province, Zhengzhou 450052, P.R China
The Key Lab of Advanced Nano-information Materials of Zhengzhou, Zhengzhou 450052, P. R. China
**Corresponding author: E-mail: lts34@zzu.edu.cn (T. S. Li), wyj@zzu.edu.cn (Y. J. Wu)*

Introduction

Cyclopalladated complexes have been widely studied in recent decades.[1] They show important applications for organic or organometallic synthesis, the syntheses of polynuclear organometallic complexes, chiral recognition or discrimination, especially homogeneous catalysis. In previous designs of cyclopalladated catalysts, much emphasis was placed on their activity and selectivity. However, catalyst recovery and recycling are equally important issues. It is obvious that heterogenization of homogeneous catalyst by Langmiur-Blodgett (LB) technique come close to achieving these goals in one system.[2] We thought it was interesting to undertake a broader investigation into Langmuir-Blodgett (LB) films of amphiphilic cyclopalladated ferrocenylimines **1a-d, 2a-d** (Scheme 1). In this presentation, the π-A isothermas of **1a-d, 2a-d** were measured. Then the differences between **1a-d, 2a-d** molecular aggregations in chloroform and LB films were investigated by UV-vis spectra, and the FT-IR spectra of their LB films and of their powder in KBr pellets were studied. In addition, their electrochemical properties in LB films and spin coating films were studied by means of cyclic voltammetric technique. Finally, **3a** was also examined by AFM.

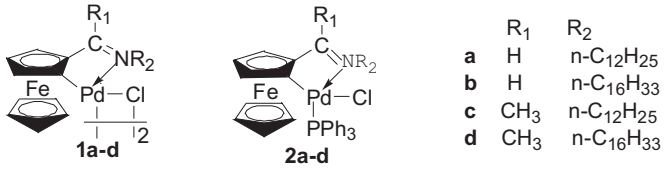

	R_1	R_2
a	H	n-$C_{12}H_{25}$
b	H	n-$C_{16}H_{33}$
c	CH_3	n-$C_{12}H_{25}$
d	CH_3	n-$C_{16}H_{33}$

Scheme 1

Experimental

^{1}H, ^{13}C and ^{31}P {^{1}H} NMR spectra were recorded on a Bruker DPX-400 spectrometer in $CDCl_3$ or DMSO-d_6 with TMS as an internal standard for ^{1}H NMR, ^{13}C NMR and 85% H_3PO_4 as external standard for ^{31}P {1H} NMR. High-resolution mass spectra were measured on a Waters Q-Tof Micro™ spectrometer. Electrochemical experiments were carried out with CHI650A electrochemical analyzer. Infrared spectra were recorded on a Bruker VECTOR22 spectrophotometer. UV measurement was carried out with Lambda 35 UV-vis spectrophotometer. Measurement of surface pressure (π)-surface area (A) isotherms and the deposition of monolayer were carried out with a computer controlled Langmuir trough (KSV 5000-3). The AFM images were obtained with SPM-9500J3 (shimadzu co.) at 20 °C in air.

Results and discussion

Complexes **1a-d, 2a-d** were have been prepared and characterized by ^{1}H NMR, ^{13}C NMR, ^{31}P NMR, IR, HRMS. Figure 1 showed the π- A isotherm of **1a-d, 2a-d** Langmuir films at air/water interface. As could be seen the cyclopalladated ferrocenylimines formed a stable monolayer with a collapse pressure at 40-50 mN / m, and a gradual transition was observed, indicating a slight structure alteration in the molecules. Compared with the absorption peak of ferrocene moiety of **1a-d, 2a-d** in chloroform solution, we found that the peak in LB films deposited from aqueous subphase on a quartz slice shifted toward the shorter wavelength region in the UV-vis spectrum, suggesting that the close molecular packing was H-aggregates. Moreover, UV–vis absorption spectra by successive measurements up to 50 layers of the deposited **1a, 1c-d, 2a-d** LB films, respectively showed that absorption peaks increased linearly with the number of layers deposited. The CH_2 symmetric and asymmetric stretching bands located at 2924 and 2853 cm^{-1} , respectively in IR spectra of **1a**, **1c-d, 2a-d** of the compressed layer on CaF_2 plates. It revealed that the alkyl chains were strongly disordered in LB films, probably because wide available space of ferrocene moiety may enable it to rotate, titlt, interpenetrate with other alkyl chains, producing some gauche conformers in the chain. Therefore, the alkyl chains cannot pack densely to each other. Furthermore, the difference of redox processes in spin coating films by cyclic voltammetric technique should be attributed to the phase separation and formation of aggregates onto ITO, in contrast to the LB films. It is interesting to note that the potential peak separation of the spin coating film is higher than that obtained for the LB films, emphasizing the lack of order of the ferrocenyl complex, unlike the case of the order induced by the LB technique. Finally, Figure 2 showed typical AFM images of one-layer LB films of **2a** deposited on mica substrate suggesting the LB films was uniform, close packing of moleculars.

Conclusion

Complexes **1a-d, 2a-d** were have been prepared and characterized by ^{1}H NMR, ^{13}C NMR, ^{31}P NMR, IR, HRMS. Furthermore, LB films of **1a-d, 2a-d** were studied by π- A isotherm, FT-IR, UV-vis spectra, cyclic voltammetric technique and AFM. These results revealed that the LB films of **1a, 1c-d** and **2a-d** were stable, ordered, uniform, close packing of moleculars.

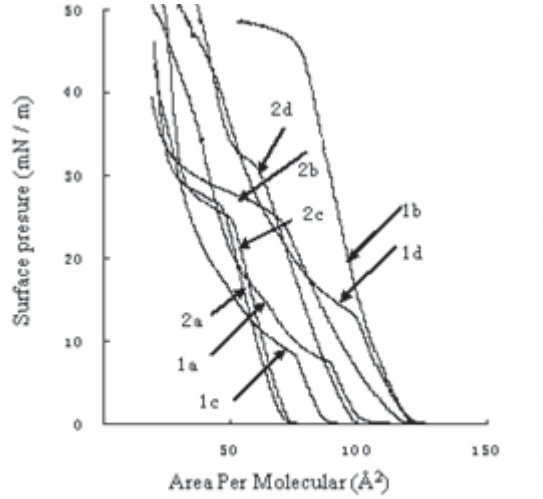

Fig 1. Surface presure – area isotherm of **1a-d**, **2a-d** on a pure water subphase at 20 °C

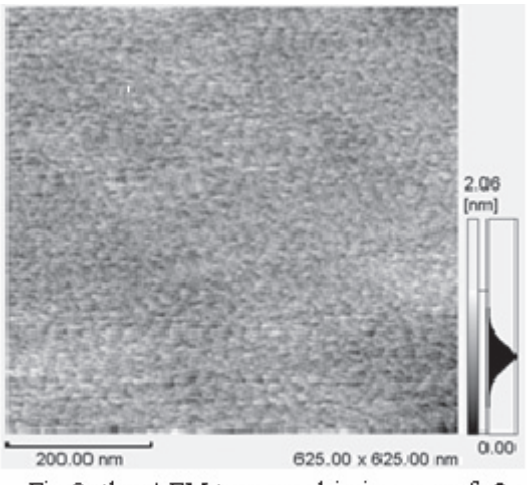

Fig 2. the AFM topographic images of **2a** LB films with 1 layer deposited on the mica

Reference

[1] G. R. Newkome, W. E. Puckett, W. K. Gupta and G. E. Kiefer, *Chem. Rev.* 86**(**1986), 451.

[2] A. K. Kakkar, *Chem. Rev.* 102 (2002**),** 3579.

P089B

Synthesis and Solid-stated Polymerization behavior of Diacetylene Derivative

Lei Zhang[2], Tiesheng Li[1*], Shengli Gao[1] and Yangjie Wu[1*]
[1]*Department of Chemistry, Zhengzhou University, Zhengzhou, 450052, P.R China*
[2]*Institute of Materials and Engineering Zhengzhou University, Zhengzhou 450052.P.R China*
Corresponding author, Tel: +86-371-67766667, Fax: +86-371-67766667,
Email: lts34@zzu.edu.cn

Introduction

Diacetylenes (DAs) have generated a lot of interest during the last few decades due to its peculiar solid state polymerization behavior[1~2] .PDAs exhibit topochemical polymerization and are capable of forming liquid crystals and films as well as single crystal. Polymerization can be initiated by pressure, heat, UV, or γ irradiation [3]. (Scheme 1) The PDA, being a one-dimensional π-conjugated system, shows nonlinear optics (NLO) properties as well as electronic and photonics properties arising due to conjugate system. [4~6]. In this work, we prepared a new diacetylene derivative (2-methyl-8-(9,9-dioctylfluoren)-3,5,7-triyn-2-ol)(MDOFTL) (Scheme 2). The solid-stated polymerization behaviors of MDOFTL were investigated by deep UV light and heating irradiation，finally, fine patterns were obtained by UV irradiation through a mask, following development with petroleum ether/ethyl acetate (10:1,v/v).

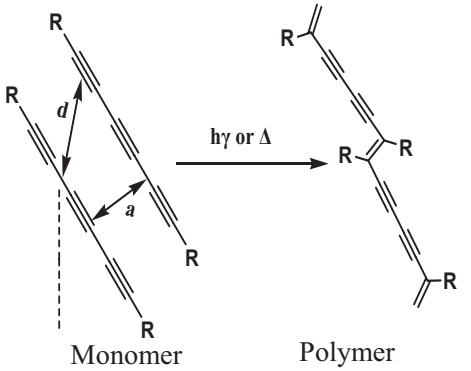

Scheme 1 Topochemical Polymerization of Diacetylene

Experimental

MDOFTL was prepared according to the method used in our Lab [7] and its Solid-stated polymerization was carried out with deep UV light at 250 nm in air. The distance between light source and CaF_2 substrate was fixed about 10 cm. The heating polymerization experiment was carried out at 100℃ in air.

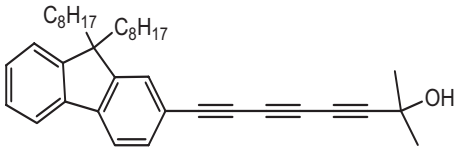

Scheme 1 Structure of 2-methyl-8-(9,9-dioctyl-fluoren)-3,5,7-triyn-2-ol(MDOFTL)

Results and Discussion

When the MDOFTL was irradiated at 250nm UV light, the stretching vibration band of acetylene triple bond which appeared at 2204 cm^{-1}, 2188cm^{-1} decreased, another band which corresponding to conjugated c=c was observed and increased shown in Figure 1. It indicated that polymerization was happened under the experiment condition. It was also proved with negative pattern(Figure3) obtained by MDOFTL spin-coat film irradiated by deep UV for 15 min in air, followed development with petroleum ether /ethyl acetate (10:1,v/v).

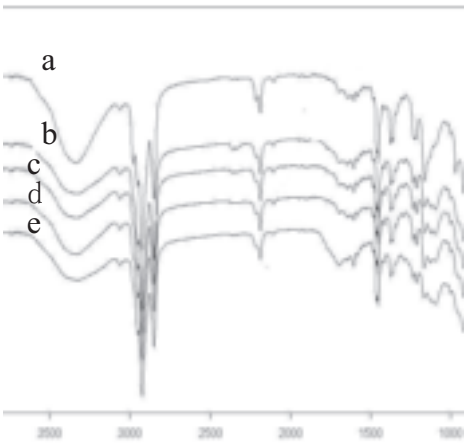

Figure 1 IR spectra of polymer MDOFTL: (a) before Irradiation, (b) irradiated for 1 min, (c) irradiated for 3 min, (d) irradiated for 5min. (e) irradiated for 10 min

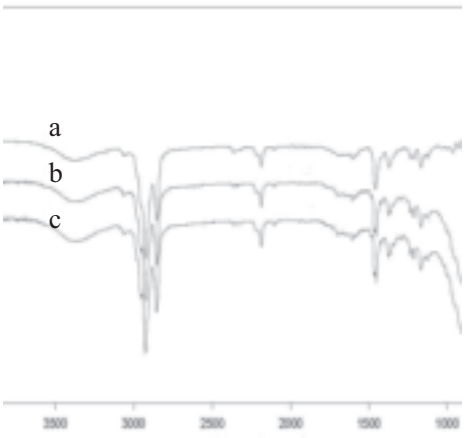

Figure 2 IR spectra of polymer MDOFTL (a) before heated, (b) heated at 100℃ for 10 min, (c) heated at 100℃ for 20 min.

When MDOFTL was heated at 80 ℃, they have no polymerization because of its absorption peaks position did not shifted in its UV spectra. But when it was heated at 100℃, in the IR spectra of monomer MDOFTL (Figure2), the stretching vibration band of acetylene triple bond decreased, and another band which corresponding to conjugated c=c was observed and increased, indicating that the monomers were polymerized when heated to 100℃.

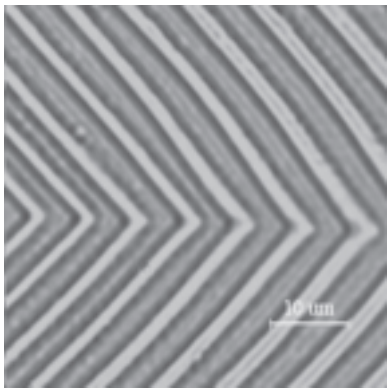

Figure 3 Optical Fine pattern of MDOFTL

Conclusion

We have synthesized a diacetylene derivatives monomer 2-methyl-8-(9,9-dioctylfluoren)-3,5,7- triyn-2-ol (MDOFTL). This monomer was polymerized according to the results of the IR spectra and image when heated at 100℃ or under 250 nm UV light irradiation. The patterning properties may be applied in areas such as sensor where controlling the interfacial properties on a micrometer scale.

Acknowledgments

This work is supported by the Nature Science Fund of Henan province（200510459010）

Reference

[1] Bloor, D, Chance, R .R. EDs. Polydiacetylene; Applied Sciences NO.102 1985
[2] Okada, s, Matsuda, H, Nakanishi,.H , In polymeric Materials Encyclopedia; CRC Press ;1996
[3] Shuji Okada, Hachiro Nakanishi. Polymer materials 1996
[4] Sauteret,C; Hermann,J. P.R , Phys Rev. lett. 1976
[5]Nakanishi.H, Matsuda. H, Polum .Adv. Technol
[6]Ksdali, N. B. Kim, W, Macromolecules 1994
[7]Tiesheng Li, Shuji Okada, Hachiro Nakanishi. Polymer Bulletin, 2003, 51(2)

P090C

Molecular Ordering of 1-TNATA Thin Films and Organic Electroluminescence Device Properties

Dosoon Kang, So Hyun Park, Phuong Thanh Vu, Young-Rae Cho[1] Dae-Won Park, Youngson Choe [*]

[1] *Department of Material Engineering, Pusan National University, Busan 609-735, Korea*

[*] *Department of Chemical Engineering, Pusan National University, Busan 609-735, Korea*

Summary: A molecularly-ordered thin film of vacuum deposited 1-TNATA(4,4′,4″-tris(N-(1-naphthyl)-N phenylamino)triphenylamine) is placed between indium tin oxide (ITO) electrode and a hole transporting layer (HTL) in OLEDs. The molecular ordering of 1-TNATA thin film was obtained by thermal annealing and electromagnetic field and was investigated by Raman spectra. L-V characteristics of multi-layered device showed enhanced luminescence at a given operating voltage in the device.

Introduction

It is known that highly ordered organic thin films are of great importance for OLEDs, organic TFTs and organic solar cells because charge injection and mobility through the layers in the devices are improved. The molecular ordering of organic thin films can be achieved by means of thermal annealing and electromagnetic field induction since many macrocyclic organic materials like metal phthalocyanine possess magnetic behavior.[1,2] In the present study, vacuum-deposited 1-TNATA(4,4′,4″-tris(N-(1-naphthyl)-N-phenylamino)triphenylamine), widely used as a hole injection material in OLEDs, thin films were thermally treated under electromagnetic field to investigate the effect of thermal annealing on the molecular ordering of the device properties.[3,4]

Experimental

1-TNATA thin films were deposited on the pre-patterned ITO-coated glass and the deposition rate was controlled to 30 nm/min to obtain 50 nm thickness of the 1-TNATA thin films. After deposition, thermal treatment of the deposited 1-TNATA films was performed in a cylindrical furnace in which the electromagnetic field(~6mT) was selectively applied as well. Film thickness was measured with a profilometer model Alpha-step 100(KLA-Tencor Co. Ltd.) as well as SEM (HITACHL S-4200). The conductivity of organic films was estimated using four-point probe measurement technique using a source multi-meter (KEITHLEY 2004). Raman spectra analysis was carried out using a Bruker FRA 106/S Fourier Transform Raman Spectrometer. AFM (Nanoscope III-a, Digital Instruments Co. Ltd.) analysis was employed to investigate the topology of the 1-TNATA thin films.

Results and discussion

According to the AFM surface images, after thermal annealing at 110ºC for 1h, it was found that the surface roughness decreased from 10.2 to 7.2nm and the lowered grains on the surface were observed. The Raman spectra of the 1-TNATA thin films are shown in Figure 1. Peak intensities at 1609Cm^{-1} in Figure 1 become higher and sharper with increasing temperature during thermal annealing, which means that the molecules come closer and are ordered in the thin films. The 1609Cm^{-1} band is attributed to a ring stretch. As shown in Figure 2, L-V characteristics of multi-layered device showed enhanced luminescence at a given operating voltage in the device.

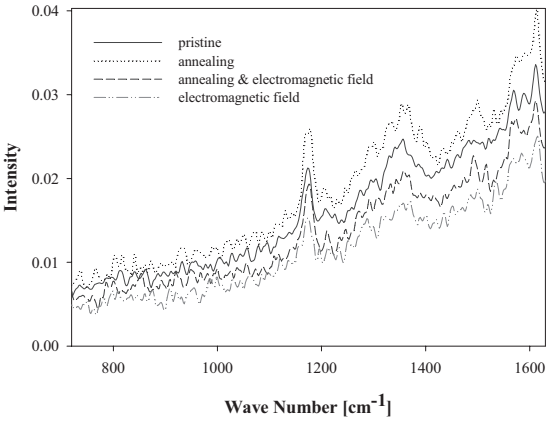

Figure 1. Raman spectra of the 1-TNATA thin film device at various treatments.

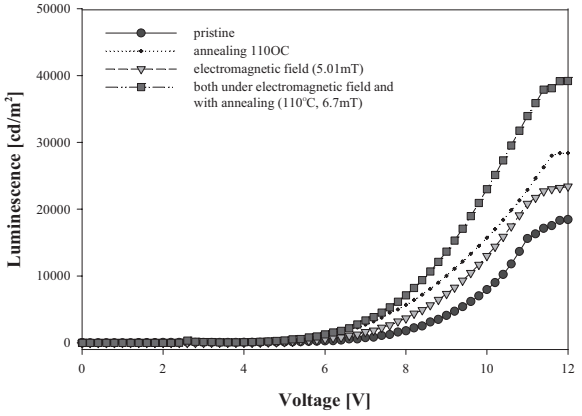

Figure 2. L-V characteristics of molecularly-ordered multi-layered device.

Conclusions

The results of Raman spectra show that the 1-TNATA films are molecularly ordered with increasing temperature during the thermal treatment. The increase of peak intensities in Raman spectra indicates that the 1-TNATA molecules come closer and eventually are molecularly ordered in the films. A molecularly-ordered 1-TNATA thin layer has an important role in improving the devices properties.

References

[1] Z. Bao, A. J. Lovinger, and J. Dodabalapur, Appl. Phys. Lett., **1996**, *69*, 3066.

[2] B. Bialek, I. G. Kim, and J. I. Lee, Thin Solid Films, **2003**, *436*, 107.

[3] M. I. Boamfa, P. C. M. Christianen, J. C. Maan, H. Engelkamp, and R. J. M. Nolte, Physica B, **2001**, *343*, 294.

[4] Z. Ji, Y. Xiang and Y. Ueda, Prog. Org. Coat., 2004, *49*, 180.

P091A

Sensitization Reaction of the Oxime Type Photoacid Generator for Photo-lithography

Tomoaki Tsumita, Shota Suzuki and Shigeru Takahara*

Graduate Course of Advanced Integration Science, Chiba University

Photo-polymer has been always required to make high sensitivity for each light source. In the manufacturing field of the printing plate and the printed wiring board, the construction of the high sensitive photo-initiating system for visible laser is expected as the spread of the laser direct imaging technology. In these fields, the radical polymerization system that uses photo-radical generator is used well. The system is very excellent because of the high sensitivity. However, it has some disadvantages such as that the reaction with oxygen in the atmosphere decreases the sensitivity. Therefore, the oxygen interception film is needed in the system. We proposed here a high sensitive photo-initiating system with photoacid generators in the region of near-ultraviolet light.

For making of the systems that can apply it to micro or submicro-meter fabrication, anthracene derivatives for the dye to sensitize the photoacid generator for 365 nm light were combinated with a t-BOC type polymer and oxime type photoacid generator (Fig. 1, 2). The sensitivity was measured by the step tablet method. The sensitization made the sensitivity ten times as high as that of direct excitation of PAG1. Moreover, they are as high as radical polymerization system's.

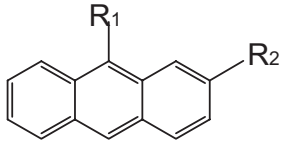

	R_1	R_2
9-methylanthracene	$-CH_3$	-H
9-chloroanthracene	-Cl	-H
9-phenylanthracene	$-C_6H_5$	-H
2-aminoanthracene	-H	$-NH_2$

Fig. 1 Sensitizer

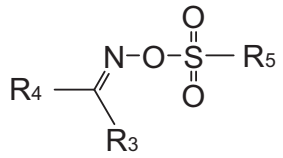

	R_3	R_4	R_5
PAG1	-CN	$-OCH_3$	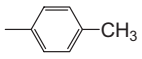
PAG2	$-C_4F_8H$	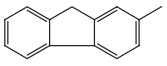	$-C_4F_9$

Fig. 2 Photoacid generator

Quantum yield of acid generation, quenching rate constant and oxidation-reduction potential were measured. The free energy of electron transfer between sensitizing dye and photoacid generator was estimated. It shows the possibility that the electronic transfer happens between them, and that the high yield of acid from anion radical of PAG1 gives the high sensitivity.

Reference

(1) S. Suzuki, X. Allonas, J. P. Fouassier, T. Urano, S. Takahara, T. Yamaoka, *J. Photochem. Photobio. A:Chem.* 181(1) 60-66 (2006)

(2) S. Suzuki, J. Iwaki, T. Urano, S. Takahara, T. Yamaoka, Polym. Adv. Technol. 17(5) 348-353 (2006)

P092B

MULTIPLE ELECTROCHROMIC PERFORMANCE OF AN ALL-SOLID ELECTROCHROMIC DEVICE USING A WO_3 / TRIS(2,2'-BIPYRIDINE)RUTHENIUM(II) / POLYMER HYBRID FILM

Koji Sone, Satomi Iijima, Masayuki Yagi*

Faculty of Education and Human Sciences, and Center for Transdisciplinary Research, Niigata University, 8050 Ikarashi-2, Niigata 950-2181, Japan.

Tungsten trioxide (WO_3) is an electrochromic material and expected to be applied to a large variety of devices such as smart windows, displays and electronic papers due to its reversible color change in a redox reaction between H_xWO_3 (blue) and WO_3 (colorless). $[Ru(bpy)_3]^{2+}$ (bpy = 2,2'-bipyridne) shows a reversible electrochromic response based on a redox of Ru^{II} (orange) / Ru^{III} (colorless). Recently, we reported that a composite film of WO_3, $[Ru(bpy)_3]^{2+}$ and poly(sodium 4-styrenesulfonate) (PSS) (denoted as a Ru-WO_3 film) is prepared by an electrodeposition technique from a colloid solution containing peroxotungstic acid, $[Ru(bpy)_3]^{2+}$ and PSS.[1] A cyclic voltammogram (CV) of the Ru-WO_3 film exhibited a reversible redox of Ru^{II} / Ru^{III} at 1.03 V, in addition to a redox of H_xWO_3 / WO_3 below 0.09 V. The Ru-WO_3 film showed multicolor electrochromic performance. At an applied potential of -0.5 V, the film is green due to absorptions by Ru^{II} and H_xWO_3. On applying 0.4 V, it is yellow due to oxidation of H_xWO_3 to WO_3. On applying 1.5 V, it is colorless due to oxidation of Ru^{II} to Ru^{III}.

An agarose solid electrolyte is known as a tight and elastic solid with a nanostructured network and excess water. It was reported that a diffusion of ions in the agarose solid electrolyte is comparable to that in an aqueous solution.[2] We considered to design an all-solid electrochromic cell of the Ru-WO_3 film using an agarose solid electrolyte. An all-solid cell was fabricated by sandwiching between the Ru-WO_3 film-coated ITO working electrode and an ITO counter electrode. A CV of the all-solid cell as measured in a two electrode system exhibited two anodic peaks at 0.68 V and 1.94 V, as well as a reductive response below -1.60 V. These anodic and cathodic responses were assigned by an in situ visible absorption spectral change recorded at the same time as the CV. The all-solid cell exhibited multiple electrochromic performance based on WO_3 and $[Ru(bpy)_3]^{2+}$. The response time of electrochromic performance (within a few seconds) was faster than those (10 ~ 200 s) of all-solid electrochromic cells reported previously. The present all-solid cell resulted in the higher-contrast electrochromic performance than that using aqueous electrolyte solution. The detailed electrochromic performance of the all-solid cells will be discussed including alternating-current impedance spectroscopic data.

References

1) M. Yagi, K. Sone, M. Yamada, S. Umemiya, *Chem. Eur. J.* **2005**, *11*, 767-775.

2) H. Ueno, M. Kaneko, *J. Electroanal. Chem.* **2004**, *568*, 87-92.

P093C

DIFFERENT EFFECTS DUE TO SHAPE CONFIGURATION IN THREE-LAYER ELECTROACTIVE POLYMERS.

Josue F. Guzman L.[1], Jorge A. Cortes R.[2], Sergio Gallegos C.[3], Lucio Florez C.[4], Manuel Martinez M.[5]

[1], [2], [3], [4]Centro de Innovacion en Diseño y Tecnologia, Instituto Tecnologico y de Estudios Superiores de Monterrey (ITESM) Campus Monterrey. Ave. Eugenio Garza Sada 2501 Sur, Col. Tecnologico, 64849, Monterrey, N.L., Mexico; [5]ITESM Campus Saltillo, Saltillo, Coah., Mexico; E-mail: a00775922@itesm.mx[1], jcortes@items.mx[2], sergio.gallegos@itesm.mx[3], lflorez@itesm.mx[4], manuel.mmartinez@itesm.mx[5]

Phone: +(5281)83282000 ext. 5356[1], 5116[2], 5410[3], 4681[4]; +(52844) 4118036 ext.2036[5]

Abstract. The recently growing field in the research of electroactive polymers has lead to look for practical applications of these materials as mechanical actuators. This is the case of three-layer electroactive polymers such as Ionic Polymer-Metal Composites (IPMC). The traditional cantilever arrangement, typically seen, may help achieve some of these applications. However, it is also true that, though common electroactive materials have been built as thin sheets or strips, their 2D configuration may be take in advantage by means of cutting the material into different configurations over its surface. The present paper describes the work of constructing, processing, and evaluating an electroactive polymer sheet sample in two different configurations. The purpose of this is to analyze differences in the behavior of the IPMC, when electrically stimulated, in order to use the information to pursue different applications due to the configuration of the material. The methodology begins with a square sample of IPMC, which is constructed by oxidation-reduction reactions. The sheet consists in a three-layered arrangement using Nafion® as the base polymer, and Platinum as the conducting layers. Lithium ions are use in order to achieve motion. The resulting sheet is stimulated with an electrical signal and its behavior is observed as a first evaluation. The sheet is then processed by cutting and shaping as a flat circular arrangement and its behavior is observed and compared to the previous configuration to complete the evaluation. The results of doing so are shown as differences in the behavior of both configurations; which are confirmed to be different even after having used the same polymer sample. The primarily noticeable differences in both configurations are the displacements and the deformed shapes.

P094A

VISIBLE LIGHT INDUCED PHOTOCURRENT GENERATION BY PERYLENE DERIVATIVES ADSORBED ON METAL OXIDE SEMICONDUCTOR FILMS IN AN AQUEOUS SOLUTION

Takeo Takahashi, Satoru Sasagawa, Syou Maruyama, Masayuki Yagi*

Faculty of Education and Human Sciences, and Center for Transdisciplinary Research, Niigata University, 8050 Ikarashi-2, Niigata 950-2181, Japan.

Recent social problems on energies and environments request a new system for providing an environment-friendly and safe energy source instead of fossil fuel. Artificial photosynthetic devices are expected to be promising energy-providing systems that are socially acceptable in future. It is important for constructing them to develop photoanodes capable of catalyzing water oxidation under visible light irradiation as well as photocathodes capable of catalyzing proton reduction. Metal oxide semiconductor films have been applied to dye-sensitized solar cells which show high incident photon to current conversion efficiency. Perylene derivatives have high molar extinction coefficients in the visible light region and are thermodynamically capable of oxidizing water by visible light. In this study, we prepared metal oxide semiconductor films adsorbing perylene derivatives as photoanodic electrodes, and examined photoelectrochemical properties of these electrodes to show it gives high energy conversion efficiency.

N-octyl-3,4:9,10-perylenetetracarboxylic monoimide (C_8-PTCMI) was synthesized according to the literatures.[1, 2] A cyclic voltammogram of the ITO / SnO_2 / C_8-PTCMI electrode in a 0.1 M KNO_3 aqueous solution (pH = 7.0) exhibited a small photoanodic current (i_p) (25 μA cm^{-2} at 0.7 V vs. Ag / AgCl) under visible light ($\lambda > 400$nm) irradiation. When the present electrode was irradiated by visible light in the electrolyte solution containing ethylenediamine tetraacetic acid disodium salt (EDTA) as a sacrificial donor, a significant i_p (5.3 mA cm^{-2} at 0.7 V) was generated above 0 V in contrast to almost no current under dark conditions in the range of 0 ~ 0.7 V. The i_p at 0.7 V increased linearly with concentration of EDTA (C_E / M) and thereafter saturated above C_E = 0.1 M. The linear relationship between i_p and C_E below C_E = 0.1 M shows that i_p is based on photo-oxidation of EDTA. The saturation of i_p above C_E = 0.1 M could be attributed to the fact that the reaction rate of oxidation of EDTA by oxidized C_8-PTCMI is sufficiently fast under the conditions employed. The i_p at 0.7 V increased linearly with light intensity (mW cm^{-2}) below 100 mW cm^{-2} in the presence of 0.1 M EDTA. The photoaction spectrum of photo-current efficiency revealed that i_p is based on the photoexcitation of C_8-PTCMI.

References

1) Y. Nagao, T. Misono, *Bull. Chem. Soc. Jpn*., **1981**, *54*, 1191-1194.

2) S. Wang, Y. Li, C. Du, Z. Shi, S. Xiao, D. Zhu, E. Gao, S. Cai, *Synth. Met.*, **2002**, *128*, 299-304.

P095B

CATALYTIC ACTIVITY FOR WATER OXIDATION OF DIPYRIDYL PYRAZOLE-BRIDGED DINUCLEAR RUTHENIUM COMPLEX IN A HETEROGENEOUS SYSTEM

Shouhei Tajima, Masayuki Yagi*

Faculty of Education and Human Sciences, and Center for Transdisciplinary Research, Niigata University, 8050 Ikarashi-2, Niigata 950-2181, Japan.

Development of synthetic catalysts for water oxidation to evolve O_2 (eq 1) has been attracting much attention not only for understanding the water oxidation mechanism at oxygen-evolving complex (OEC) in photosynthesis, but for constructing an artificial photosynthetic device which is expected to be renewable energy resource in future.

$$2H_2O \rightarrow O_2 + 4H^+ + 4e^- \qquad (1)$$

The activities of molecule-based catalysts immobilized in various heterogeneous matrixes such as clay compounds, inorganic particles, and polymer membranes have been extensively investigated in order to apply them to photochemical and electrochemical systems. In our earlier work, a trinuclear ruthenium complex, $[(NH_3)_5Ru\text{-}O\text{-}Ru(NH_3)_4\text{-}O\text{-}Ru(NH_3)_5]^{6+}$ which is capable of four-electron water oxidation by one catalyst molecule underwent bimolecular decomposition to deactivate at high concentrations in a homogeneous aqueous solution. However, the bimolecular decomposition was remarkably suppressed by incorporating the catalyst into a Nafion membrane.[1] This result shows that heterogeneous systems might be useful for constructing an artificial photosynthetic device. Llobet's group reported that a dinuclear ruthenium complex, $[Ru_2^{II}(dpp)(trpy)_2(H_2O)_2]^{3+}$ (dpp = 3,6-di(2-pyridyl)pyrazole, trpy = 2,2':6',2"-terpyridine) (**1**) acts as a catalyst for water oxidation to evolve O_2 in a homogeneous aqueous solution.[2] In this study, we examined the catalytic activity of **1** for water oxidation in a heterogeneous Nafion membrane using a Ce^{IV} oxidant. The kinetics and mechanism for O_2 production from water will be discussed compared with a homogeneous system.

References

[1] M. Yagi, S. Tokita, K. Nagoshi, I. Ogino, M. Kaneko, *J. Chem. Soc., Faraday Trans.*, **1996**, *92*, 2457-2461.

[2] C. Sens, I. Romero, M. Rodríguez, A. Llobet, T. Parella, J. Benet-Buchholz, *J. Am. Chem. Soc.*, **2004**, *126*, 7798-7799.

P096C

SUBSTITUENT EFFECTS ON CATALYTIC ACTIVITY FOR WATER OXIDATION BY DI-μ-OXO MANGANESE COMPLEX SUPPORTED BY CLAY COMPOUNDS

Hirosato Yamazaki, Masayuki Yagi*

Faculty of Education and Human Sciences and Center for Transdisciplinary Research, Niigata University, 8050 Ikarashi-2, Niigata 950-2181, Japan.

Water oxidation to evolve O_2 (eq 1) is an important and fundamental chemical reaction in photosynthesis. This reaction is catalyzed by a unique manganese enzyme referred to as oxygen evolving complex (OEC), whose active site is comprised of an oxo-bridged tetramanganese cluster. Though synthetic manganese-oxo complexes have guided thoughts on the chemical and electronic structures of the OEC, most of the structural models have not catalyzed water oxidation to evolve O_2 in a homogeneous aqueous solution so far.

$$2H_2O \rightarrow O_2 + 4H^+ + 4e^- \qquad (1)$$

Limburg et al. reported O_2 evolution from water by the reaction of $[Mn_2^{III/IV}(\mu\text{-}O)_2(terpy)_2(OH_2)_2]^{3+}$ (terpy = 2,2':6',2''-terpyridine) (**1**) with NaClO or $KHSO_5$.[1,2] However, the mechanism of O_2 formation is completely unclear, including even disproportionation of $2ClO^- \rightarrow O_2 + 2Cl^-$. We reported that the reaction of **1** with a Ce^{IV} oxidant leads to the decomposition of **1** to permanganate ions without O_2 evolution in an aqueous solution, but O_2 evolution from water is achieved by hybridization of **1** and clay compounds.[3-5] In this study, we synthesized complex **1** derivatives with either an electron-donating or withdrawing groups, $[Mn_2^{III/IV}(\mu\text{-}O)_2(4'\text{-}R\text{-}terpy)_2(OH_2)_2]^{3+}$ (R = Methoxy(**2**), Pyridyl(**3**), Phenyl(**4**), Chrolo(**5**)), and investigated substituent effects on the catalytic activity of di-μ-oxo manganese complexes in clay hybrids for water oxidation. The reactions of each complex with a Ce^{IV} oxidant yielded O_2 evolution in the mica hybrid. However, the maximum turnover number (TN) of **2**, **3** or **4** / mica hybrid was over 15, whereas TN of **5** was less than 1. This result reveals that **2**, **3** or **4** works as a catalyst for water oxidation in mica.

The time courses of the amount of O_2 evolved in the reaction of the complex / mica hybrids with a large excess Ce^{IV} oxidant were measured by a Clark-type oxygen electrode. The initial O_2 evolution rate (v_{O2} / mol s^{-1}) was calculated from the initial slope of the time course. The v_{O2} increased with increasing the amount (n_{ads} / mol) of complexes adsorbed on mica for each complex / mica hybrid. It was analyzed by the kinetic model (eq 2) assuming on combination between first- and second-order O_2 evolutions with respect to the adsorbed complexes,

$$v_{O2} = k_1 n_{ads} + k_2 n_{ads}^2 \quad (2)$$

where k_1 / s^{-1} and k_2 / mol^{-1} s^{-1} are first-order and second-order rate constants for O_2 evolution, respectively. For comparison of the turnover frequency of adsorbed complexes on mica, v_{O2} was normalized by n_{ads} to define the apparent turnover frequency, $(k_{O2})_{app}$ / s^{-1}, as eq 3.

$$(k_{O2})_{app} = v_{O2} / n_{ads} = k_1 + k_2 n_{ads} \quad (3)$$

The plots of $(k_{O2})_{app}$ versus n_{ads} gave the straight lines with significant slopes passing through the origin for **2**, **3** or **4** / mica hybrid. The significant slope (corresponding to k_2 in eq 3) suggests that O_2 is predominantly evolved by a bimolecular reaction of adsorbed complexes on mica. It is most likely that adsorbed complexes works cooperatively for the catalysis. The k_2 was significantly different among **2**, **3** or **4** / mica hybrids, showing that it is affected by the substituent group on terpy ligands. For the **5** / mica hybrid, however, the plot of $(k_{O2})_{app}$ versus n_{ads} gave the straight line with almost no slope, suggesting that O_2 is predominantly evolved by a unimolecular reaction. We will discuss the effect of the substituent group of terpy ligands on the catalysis.

References

[1] Limburg, J.; Vrettos, J. S.; Liable-Sands, L. M.; Rheingold, A. L.; Crabtree, R. H.; Brudvig, G. W. *Science* **1999**, *283*, 1524-1527.

[2] Limburg, J.; Vrettos, J. S.; Chen, H. Y.; de Paula, J. C.; Crabtree, R. H.; Brudvig, G. W. *J. Am. Chem. Soc.* **2001**, *123*, 423-430.

[3] Yagi, M.; Narita, K. *J. Am. Chem. Soc.* **2004**, *126*, 8084-8085.

[4] Narita, K.; Kuwabara, T.; Sone, K.; Shimizu, K.; Yagi, M. *J. Phys. Chem. B* **2006**, *110*, 23107-23114.

[5] Yagi, M.; Narita, K.; Maruyama, S.; Sone, K.; Kuwabara, T.; Shimizu, K. *Biochim. Biophys. Acta, Bioenerg.*, in press.

P097A

WATER OXIDATION CATALYSIS BY $[Ru(TERPY)LOH_2]^{2+}$ (L = BIDENTATE LIGAND) COMPLEXES ADSORBED IN LAYER COMPOUNDS

Manabu Komi, Masayuki Yagi*

Faculty of Education and Human Sciences, and Center for Transdisciplinary Research, Niigata University, 8050 Ikarashi-2, Niigata 950-2181, Japan.

Hybridization of a functional molecule and a heterogeneous matrix such as polymer membranes, ion-exchange resins, and intercalation compounds has attracted much attention because development of a new function different from homogeneous systems and its application to electronic and photoelectronic devices are expected. In the previous report, we found that the reaction of $[Mn_2^{III/IV}(\mu\text{-}O)_2(terpy)_2(OH_2)]^{3+}$ (terpy = 2,2':6',2"-terpyridine) with a Ce^{IV} oxidant leads to decomposition of the complex to MnO_4^- without O_2 evolution in an aqueous solution but catalytically produces O_2 from water when the complex is adsorbed on clay compounds.[1)] This result shows that catalytic activity for water oxidation is induced by hybridizing the complex with clay compounds. Meyer's group reported that a mononuclear ruthenium complex, $[Ru(terpy)(bpy)OH_2]^{2+}$ (bpy = 2,2'-bipyridine) (**1**) works as a catalyst based on $Ru^{II/IV}$ oxidation states for oxidation of organic compounds such as alcohols, aldehydes, and unsaturated hydrocarbons in a homogeneous aqueous solution.[2)] However, **1** has not been used for water oxidation. We have studied the catalytic activity for water oxidation by **1** to evolve O_2 using a Ce^{IV} oxidant both in a heterogeneous clay compound and a homogeneous aqueous solution (Scheme 1). In the presentation, we will discuss the kinetics and mechanism for O_2 evolution from water by **1** and derivatives of **1**.

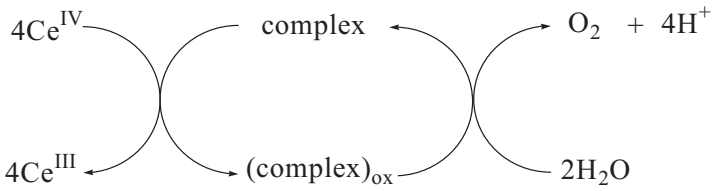

Scheme 1. Chemical water oxidation using a Ce^{IV} oxidant.

References

1) M. Yagi, K. Narita, *J. Am. Chem. Soc*. **2004**, *126*, 8084-8085.

2) B. A. Moyer, T. J. Meyer, *J. Am. Chem. Soc*. **1980**, *102*, 2310-2312.

P098B

ARTIFICIAL MODEL OF PHOTOSYNTHETIC PS II: PHOTOCHEMICAL PRODUCTION OF O_2 FROM WATER BY A DI-μ-OXO MANGANESE COMPLEX IN A HETEROGENEOUS SYSTEM

Satoshi Yamada, Mayuu Toda, Masayuki Yagi*

Faculty of Education and Human Sciences, and Center for Transdisciplinary Research, Niigata University, 8050 Ikarashi-2, Niigata 950-2181, Japan.

Water oxidation to evolve O_2 (eq 1) in photosynthesis is one of the most important and fundamental processes in nature. This reaction is catalyzed by a unique manganese enzyme referred to as oxygen evolving complex (OEC).

$$2H_2O \xrightarrow{\text{OEC}} O_2 + 4H^+ + 4e^- \qquad (1)$$

Although it is known that the active site of OEC is comprised of an oxo-bridged tetramanganese cluster, the mechanism of water oxidation by OEC is still a question under debate. O_2 evolution by synthetic manganese complexes as an OEC model is important for mechanistic understanding of water oxidation catalyzed at OEC. Many manganese-oxo complexes have given thoughts on the structure of OEC. However, catalytic O_2 evolution from water by manganese-oxo complexes had not been reported to be demonstrated clearly. Recently, we reported that the reaction of $[(OH_2)(terpy)Mn^{III}(\mu\text{-}O)_2Mn^{IV}(terpy)(OH_2)]^{3+}$ (terpy = 2,2':6',2"-terpyridine) (**1**) with a Ce^{IV} oxidant leads to decomposition of **1** to permanganate ions without O_2 evolution in an aqueous solution, but catalytically producing O_2 from water when **1** is adsorbed on clay compounds.[1-3] In photosynthetic PS II, photoinduced electron transfer from P680 to pheophytin generates a $P680^{\cdot+}$ radical cation, to which electrons are transferred from OEC *via* a tyrosine residue. On accumulation of four equivalents of oxidizing ability at OEC, water is oxidized to evolve O_2. $[Ru(bpy)_3]^{2+}$ (bpy = 2,2'-bipyridine) is one of the available visible-light-sensitizers, and photoinduced electron transfer from $[Ru(bpy)_3]^{2+}$ to an electron accepter is known to generate Ru(III) which has strong oxidizing power. An artificial PS II model might be possible to be designed using **1** and $[Ru(bpy)_3]^{2+}$ adsorbed on clay as OEC and P680 models, respectively. We found that O_2 is photochemically produced in the artificial PS II. The evidence and mechanism for photoinduced O_2 evolution will be presented.

References

(1) M. Yagi, K. Narita, *J. Am. Chem. Soc.*, **2004**, *126*, 8084-8085.

(2) K. Narita, T. Kuwabara, K. Sone, K. Shimizu, M. Yagi, *J. Phys. Chem. B*, **2006**, *110*, 23107-23114.

(3) M. Yagi, K. Narita, S. Maruyama, K. Sone, T. Kuwabara, K. Shimizu, Biochim. Biophys. Acta Bioenerg. in press.

P099C

INVERTED BULK-HETEROJUNCTION ORGANIC SOLAR CELLS USING A SOL-GEL-DERIVED TITANIUM OXIDE THIN FILM AS AN ELECTRON INJECTION ELECTRODE INSERTED INTO ITO/ORGANIC SOLID LAYER INTERFACE

Takayuki KUWABARA[1], Yasunori SIGEYAMA[2], Takahiro YAMAGUCHI[2], Kohshin TAKAHASHI[2]*,

Faculty of Engineering[1], and Graduate School of Natural Science & Technology[2], Kanazawa University, Kakuma-machi, Kanazawa, Ishikawa, 920-1192 JAPAN.

An Al metal has been used frequently as the top electrode for organic solar cells due to its low work function. However, the surface of Al is easily oxidized to insulator Al_2O_3 in the air. We are developing organic solar cells using a non-corrosive ITO/TiO_x electrode prepared by a sol-gel technique instead of the low functional Al electrode. Herein, we present the performance and the durability of ITO/TiO_x/ poly(3-hexylthiophene) (P3HT):[6,6]-phenyl C61-butyric acid methyl ester(PCBM)/poly(3,4-ethylene dioxylene thiophene) (PEDOT):poly(4-styrene sulfonic acid)(PSS)/Au bulk-heterojunction organic solar cells.

In order to prepare a TiO_x thin film acting as the electron injection layer, a precursor solution was spin-coated on ITO being accompanied by hydrolysis in an ambient atmosphere and by heat treatment. Thereafter, a mixed chlorobenzene solution of P3HT and PCBM was spin-coated onto the ITO/TiO_x substrate, further a PEDOT:PSS aqueous solution was spin-coated onto its substrate. Finally, an Au metal as the top electrode was vacuum-deposited on the PEDOT:PSS solid film. The device was heated at 150°C. The photocurrent-voltage (I-V) curves of the solar cell were measured under the irradiation of a simulated solar light (AM1.5) with 100 mW cm^{-2} intensity. The effective area of the solar cell was restricted to 1.0 cm^2.

Figure 1 shows the I-V curves of the ITO/TiO_x/P3HT: PCBM/PEDOT:PSS/Au type solar cell with the elapse time under the irradiation. The improvement of the cell performance was observed with increasing the irradiation time. This suggests that the

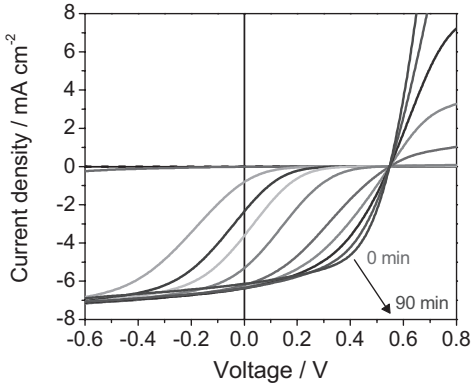

Figure 1 Photo I-V curve change of the cell with the elapse time during 90 min from starting the irradiation of the solar simulated light AM1.5 with 100 mW cm^{-2} intensity.

photo-produced electrons in the organic solid film firstly fill in electron traps in the TiOx layer disturbing the electron transport, resulting in relatively smooth charge separation with irradiating the solar simulated light. After all, the power conversion efficiency (η) of 1.9 % was obtained after irradiating for 90 min. Further the photovoltaic properties were stored under continuous light irradiation for 10 h and its excellent durability was demonstrated.

This work was supported by the Incorporated Administrative Agency New Energy and Industrial Technology Development Organization (NEDO) under Ministry of Economy, Trade and Industry (METI).

P100A

INVERTED BULK-HETEROJUNCTION ORGANIC SOLAR CELLS USING AN ELECTRODEPOSITED ZINC OXIDE THIN FILM AS AN ELECTRON INJECTION ELECTRODE

Yoshitaka KAWAHARA[1], Takayuki KUWABARA[2], Takahiro YAMAGUCHI[1], Kohshin TAKAHASHI[1]*

Graduate School of Natural Science & Technology[1] and Faculty of Engineering[2], Kanazawa University, Kakuma-machi, Kanazawa, Ishikawa, 920-1192 JAPAN.

In normal organic thin film solar cells, low work function metals are used as an anode. However, the low work function metals are easily oxidized in an ambient atmosphere containing O_2 and H_2O, producing metal oxides as an insulator. Therefore, using air-stable and transparent n-type semiconductors as the anode may promise the improvement of the device durability. In our research, we fabricated an ITO/ZnO/poly(3-hexylthiophene) (P3HT):[6,6]-phenyl C61-butyric acid methyl ester(PCBM)/poly(3,4-ethylene dioxylene thiophene) (PEDOT):poly(4-styrene sulfonic acid)(PSS)/Au inverted bulk-heterojunction type solar cells by using an electrodeposited ZnO thin film as the anode and evaluated the photoelectric conversion properties of the device and the durability.

The ZnO thin film was prepared onto an ITO substrate by cathodic electrodeposition method from an aqueous solution containing $Zn(NO_3)_2$ under the potentiostatic condition at -1.3 V (vs. Ag / AgCl).[1),2)] Second, a mixed chlorobenzene solution of P3HT and PCBM was spin-coated onto the ITO/ZnO substrate. And then, a PEDOT:PSS aqueous solution was spin-coated to the substrate. Finally, an Au metal as the top electrode was vacuum-deposited on the PEDOT:PSS solid film. The device was annealed at 150°C. Figure 1 shows the schematic structure of this device. The photocurrent-voltage (I-V) curve of the solar cell was measured under the illumination of a simulated solar light (AM1.5) with 100 mW cm^{-2} intensity. The effective area of the solar cell was restricted to 1.0 cm^2.

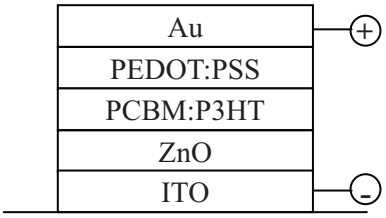

Figure 1 Schematic structure of the device.

A surface SEM image of the electrodeposited ZnO electrode is shown in Figure 2. The SEM image showed that the

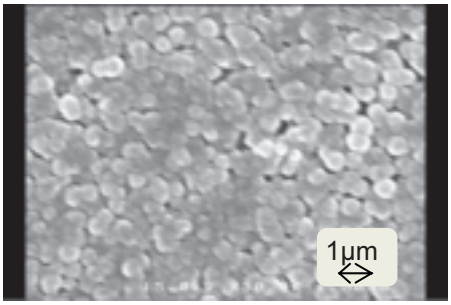

Figure 2 A surface SEM image of electrodeposited ZnO film on ITO.

surface was densely covered with ZnO particles of ca. 500 nm. The bold line in Figure 3 shows the initial I-V curve for ITO/ZnO/P3HT:PCBM/PEDOT:PSS/Au inverted bulk-heterojunction type solar cell inserting the thin ZnO layer between the ITO electrode and the P3HT:PCBM blend film. The energy conversion efficiency (η) achieved up to 1.9 %. However, the short-circuit photocurrent (J_{sc}) decreased with the elapse of the illumination time as shown in Figure 3. Figure 4 shows the change of the cells performance under light irradiation during 10 h. The open-circuit voltage (V_{oc}) and the fill factor (FF) almost held the initial values even after irradiating during 10 h, whereas the J_{sc} and the η decreased down to 79 and 82 %, respectively. The reason that the η value decreased with the decrease of the J_{sc} will be discussed in this presentation.

This work was supported by the Incorporated Administrative Agency New Energy and Industrial Technology Development Organization (NEDO) under Ministry of Economy, Trade and Industry (METI).

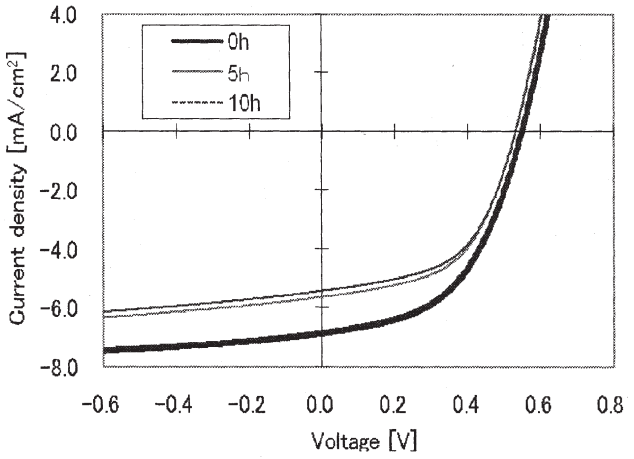

Figure 3 I-V curves of ITO/ZnO/P3HT:PCBM/PEDOT:PSS/Au type solar cells after light illumination. Illumination time; 0h(—), 5h(– –), and 10h(···).

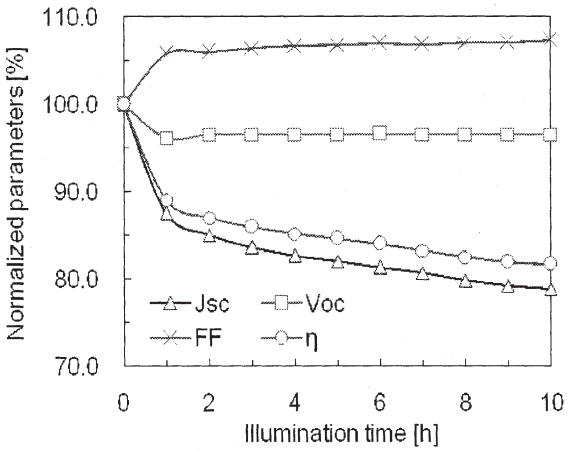

Figure 4 Change of the normalized device performances against the elapse time by irradiating AM 1.5 solar simulated light of 100 mW/cm^2 intensity.

Reference

1) M. Izaki, T. Omi, Appl. Phys. Lett., 68, **1996**, 2439-2440

2) S. Peulon, D.l Lincot, Adv. Mater., **1996**, 8, 166-169

P101B

INVERTED BULK-HETEROJUNCTION ORGANIC SOLAR CELLS USING AN ELECTRODEPOSITED TITANIUM OXIDE THIN FILM

Hirokazu SUGIYAMA[1], Takayuki KUWABARA[2], Takahiro YAMAGUCHI[1], Kohshin TAKAHASHI[1]*

Graduate School of Natural Science & Technology[1] and Faculty of Engineering[2], Kanazawa University, Kakuma-machi, Kanazawa, Ishikawa, 920-1192 JAPAN.

Low work function metals such as Al are extensively employed as the top electrode of organic solar cells. However, the Al is easily converted to insulator Al_2O_3 in the air. We are developing an inverted cell that an organic active layer consisting of poly(3-hexylthiophene) (P3HT):[6,6]-phenyl C61-butyric acid methyl ester(PCBM) was sandwiched between non-corrosive Au top electrode and F-doped SnO_2 (FTO)/TiO_2 bottom electrode. Herein, we present the cell performance and the durability of FTO/TiO_2/P3HT:PCBM/poly(3,4-ethylene dioxylene thiophene) (PEDOT):poly(4-styrene sulfonic acid)(PSS)/Au bulk-heterojunction organic solar cells.

The as-deposited TiO_2 film was prepared on FTO by an electro-deposition method at -1.8 V vs. Ag/AgCl in a solution containing $TiOSO_4$, H_2O_2, and KNO_3.[1)] Conversion of the as-deposited TiO_2 to the crystalline TiO_2 was achieved by heat treatment. Thereafter, a mixed chlorobenzene solution of P3HT and PCBM was spin-coated onto the FTO/TiO_2 substrate. Further, a PEDOT:PSS aqueous solution was spin-coated onto the substrate. Finally, the Au metal as the top electrode was vacuum-deposited on the PEDOT:PSS solid film. The devices were annealed at 150°C. Figure 1 shows the schematic structure of the solar cell. The photocurrent-voltage (I-V) curves were measured under the irradiation of a simulated solar light (AM1.5) with 100 mW cm^{-2} intensity. The effective area of the solar cell was restricted to 1.0 cm^2.

Figure 1 Schematic structure of the inverted type cell.

Surface SEM images of bare FTO and as-deposited TiO_2 on FTO are shown in Figures 2a and 2b, respectively. The SEM image of the electro-

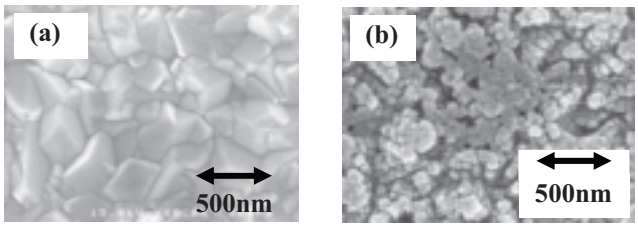

Figure 2 Surface SEM images of bare FTO (a), as-deposited TiO_2 film on FTO (b).

deposited film showed that the surface was densely covered with TiO_2 particles of ca. 30 ~ 100 nm. For the FTO/TiO_2/P3HT:PCBM/ PEDOT:PSS/Au sandwich-type organic photovoltaic cells, reproducible power conversion efficiencies (η) over 2 % were obtained by irradiating the solar simulated light. Figure 3 shows the change of photovoltaic properties during 10 h under light irradiation.

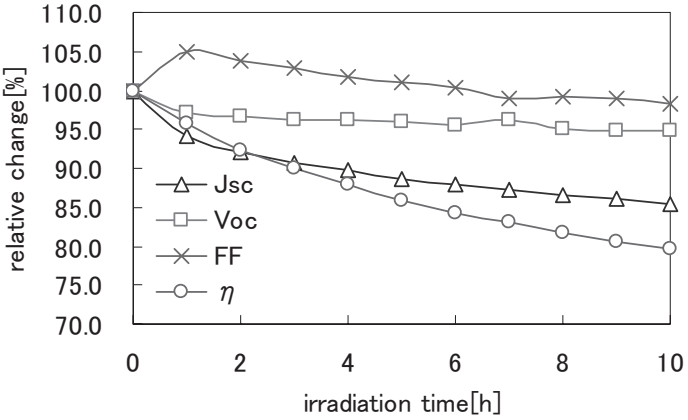

Figure 3 Change of photovoltaic properties against the elapse time under irradiation of the solar simulated light.

The open-circuit voltage (V_{oc}) and the fill factor (FF) almost held the initial values during 10 h, whereas the short-circuit photocurrent (J_{sc}) and the η decreased down to 90 % and 80 %, respectively.

This work was supported by the Incorporated Administrative Agency New Energy and Industrial Technology Development Organization (NEDO) under Ministry of Economy, Trade and Industry (METI).

Reference

1) S. Karuppuchamy et.al., *Appl. Surf. Sci.*, **2006**, *253*, 2924-2929.

P102C

INVERTED BULK-HETEROJUNCTION ORGANIC SOLAR CELLS USING A SELF-ASSEMBLED ZINC SULFIED THIN FILM AS AN ELECTRON INJECTION ELECTRODE INSERTED INTO ITO/ORGANIC SOLID LAYER INTERFACE

Masayuki NAKAMOTO[1], Takayuki KUWABARA[2], Takahiro YAMAGUCHI[1], Kohshin TAKAHASHI[1]*

Graduate School of Natural Science & Technology[1] and Faculty of Engineering[2], Kanazawa University, Kakuma-machi, Kanazawa, Ishikawa, 920-1192 JAPAN.

Soft chemical deposition method of compound semiconductors from solutions has been actively studied, and the thin films have attracted much attention as a promising electron injection layer in the organic photovoltaic solar cells. Zinc sulfide (ZnS) is an excellent n-type semiconductor and can deposit densely on substrates by the soft chemical deposition method. In our research, we prepared a self-adsorbed ZnS film by using a chemical bus deposition (CBD) method, and fabricated an ITO/ZnS/poly(3-hexylthiophene) (P3HT):[6,6]-phenyl C61-butyric acid methyl ester(PCBM)/poly(3,4-ethylene dioxylene thiophene) (PEDOT):poly(4-styrene sulfonic acid)(PSS)/Au inverted bulk-heterojunction type solar cells inserting the ZnS thin film as an anode.

An aqueous solution containing $Zn(OAc)_2$ was mixed with a thioacetamide (TAA) aqueous solution in a glass reaction vessel being used as the film deposition bus. The ZnS thin film was self-adsorbed on an ITO electrode by using the CBD method.[1)] Second, a mixed chlorobenzene solution of P3HT and PCBM was spin-coated onto the ITO/ZnS electrode. Further a PEDOT:PSS aqueous solution was spin-coated to the substrate. Finally, an Au metal as the top electrode was vacuum-deposited onto the PEDOT:PSS solid film. The devices were annealed at 150 °C. The schematic structure of the device is shown in Figure 1. The Photocurrent-voltage (I-V) curves of the solar cell were measured under the irradiation of a simulated solar light (AM1.5) with 100 mW cm^{-2} intensity. The effective area of the solar cell was restricted to 1.0 cm^2.

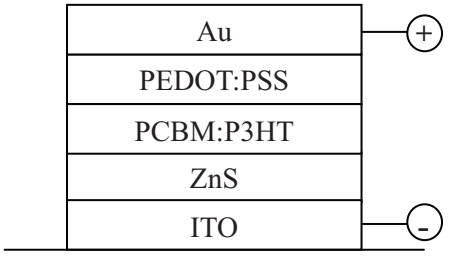

Figure 1 Schematic structure of the device.

The deposition characteristics of ZnS particles on the ITO electrode were controlled by the bus temperature and the $Zn(OAc)_2$ concentration in the solution. Figure 2 shows a surface SEM image of ZnS thin film when the film was deposited in the reaction bath with 0.05 M $Zn(OAc)_2$ and 0.05 M TAA at 60 °C. The

SEM image of the ZnS film showed that the surface was densely covered with ZnS particles of ca. 70 to 100 nm. Figure 3 shows I-V curves for the devices with and without the ZnS layer as the electron injection layer being inserted into the ITO/P3HT:PCBM blend film interface. The energy conversion efficiency (η) of the device with the ZnS layer achieved up to 1.04 %, and it was ca. 10 times larger than that without ZnS. This suggests that the ZnS layer is potentially capable of serving as the electron injection layer of OPV cells resulting in an improvement of the rectification. We will discuss about optimization condition of the ZnS layer in this presentation.

This work was supported by the Incorporated Administrative Agency New Energy and Industrial Technology Development Organization (NEDO) under Ministry of Economy, Trade and Industry (METI).

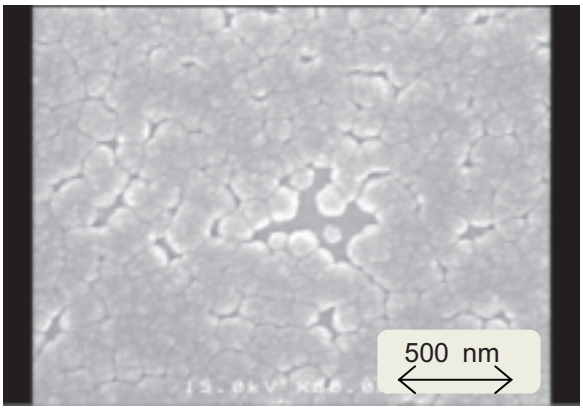

Figure 2 A surface SEM image of electro-deposited ZnS film on an ITO electrode.

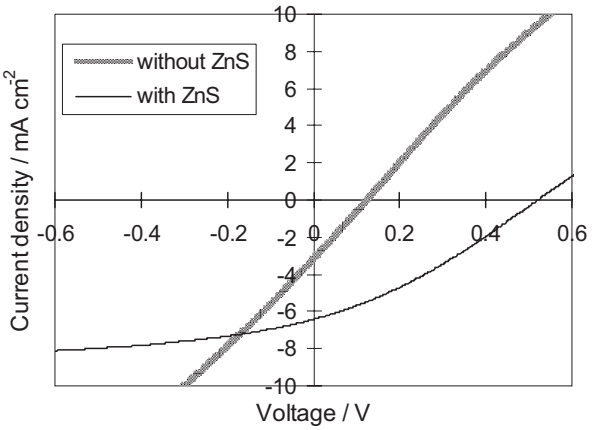

Figure 3 I-V curves of solar cells with and without ZnS layer under irradiation of AM1.5 solar simulated light with 100 mW/cm^2 intensity.

Table 1 Device performances of the solar cell with and without ZnS layer.

	J_{sc} / mA cm^{-2}	V_{oc} / V	FF	η / %
with ZnS	6.43	0.52	0.31	1.04
without ZnS	3.15	0.12	0.25	0.10

Reference

1) K. Yamaguchi et.al., *J. Phys. Chem.* B, **2003**, *107*, 387-397.

P103A

ANODIC OXIDATION OF METHANOL ON HYDROPHOBIC NICKEL ELECTRODE

Masaki IGARASHI, Yasushi ONO

Niigata University, Department of Graduate School of Science & Technology / Center for Education and Research on Environmental Technology, Materials Engineering, and Nanochemistry

1. Introduction

Sacrificial anodic reaction in the noble metal plating with a low applied voltage would reduce energy consumption. Nickel oxide electrode has high catalytic activity for oxidation of organic compounds in basic aqueous solution, so that electro-oxidation of organic compounds on this electrode has potential for the sacrificial reaction. Most organic compounds are, however, so hydrophobic that water oxidation as a side reaction would take place. In this work, hydrophobic fine particles, such as polytetrafluoroethylene (PTFE) were fixed by the composite-plating to improve affinity between organic compound and electrode surface and to electrolyze organic compound with high-efficiency. We investigated methanol oxidation on this hydrophobic electrode.

2. Experimental

Composite-plating solution was prepared by dispersing 0-100 g dm^{-3} of PTFE fine particles (0.2 μm) into sulfamate nickel plating bath. Composite-plating carried out at 5 A dm^{-2} of current density at 318 K till 60×10^{2} C dm^{-2} of charge passed. Voltammetry was carried out in H-shaped cell added with 0.1 mol dm^{-3} of NaOH aqueous solution saturated with N_2 containing 0-7.8×10^{-2} mol dm^{-3} methanol. Potential refered to Ag|AgCl electrode was anodically scanned with 5 mV s^{-1} of scan rate. Working electrodes were composite-plated nickels, and platinum was employed as counter electrode.

Zinc plating (8 g dm^{-3} of ZnO, 80 g dm^{-3} of NaOH, and 0-7.8×10^{-2} mol dm^{-3} methanol) was conducted at 0.7 A dm^{-2} of current density with 42.2×10^{2} C dm^{-2} of charge passed and at 323 K.

3. Results and discussion

Voltammograms on various composite-plated nickels in 0.1 mol dm^{-3} NaOH aqueous electrolyte were shown in Fig. 1, and those in 0.1 mol dm^{-3} of NaOH electrolyte containing 7.8×10^{-2} mol dm^{-3} of methanol in Fig. 2. In Fig. 1, anodic current of oxygen evolution was observed above 0.7 V. Higher current density was observed on hydrophobic electrode than hydrophilic electrode, while lower current was observed on highly hydrophobic electrode than hydrophilic electrode. This is because PTFE particles took up evolved O_2 molecules, so that active sites on electrode remained. But in the case of highly hydrophobic electrode, O_2 accumulated on the particels to form bubbles shielded electrode surface. On the other hand, in Fig. 2, current was steeply increased and larger current was observed on hydrophobic electrode than on hydrophilic electrode. Methanol molecules were effectively collected on PTFE surface and electrolyses proceeded efficiently.

To compare charge passed on various electrode, electrolyses were carried out at constant-potential of 0.8 V for one hour. Results were that 42.45 C passed on hydrophilic electrode, and 53.87 C passed on hydrophobic electrode.

Anodic oxidation of methanol as sacrificial reaction for zinc plating was investigated. Fig. 3 showes the time-course of applied voltage. Results were that 0.0235 Wh expended on hydrophilic electrode in 0 mol dm^{-3} methanol, and 0.213 Wh expended on hydrophobic electrode in 7.8×10^{-2} mol dm^{-3} methanol. About 10 % energy gain was observed in methanol oxidation on hydrophobic electrode referred to water oxidation on hydrophilic electrode. About 10% gain was due to fraction of 2

V of water oxidation voltage and 1.8 V of methanol oxidation voltage.

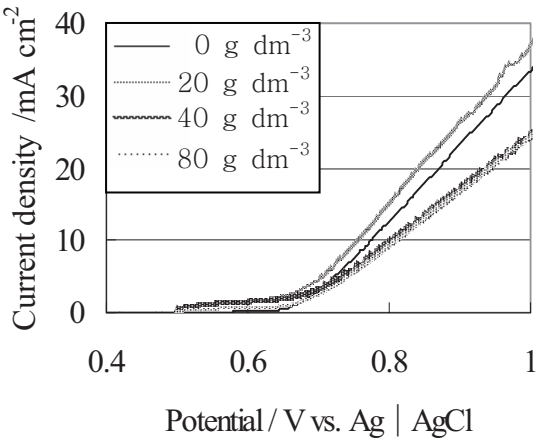

Fig. 1 Linear sweep voltammograms on Ni and Ni/PTFE plate electrodes in N_2 - saturated 0.1 mol dm^{-3} NaOH aqueous solution.

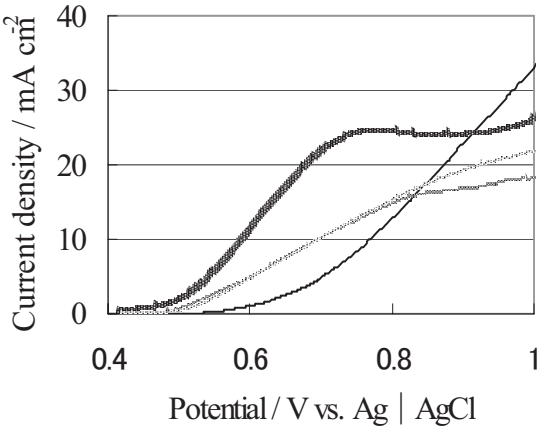

Fig. 2 Linear sweep voltammograms on Ni and Ni/PTFE plate electrodes in N_2 - saturated 0.1 mol dm^{-3} NaOH + 7.8×10^{-2} mol dm^{-3} methanol aqueous solution.

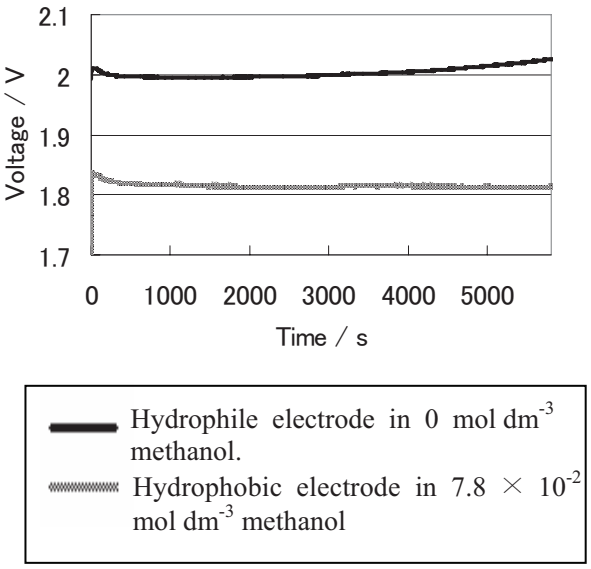

Fig. 3 Variation of voltage with time in zinc plating.

P104B

PREPARATION OF ELECTROCONDUCTIVE POLYMER FILM BY DIP COATING METHOD AND ITS CHARACTERIZATION

Atsushi TAMURA, Yasushi ONO*

Niigata University , Depertment of guraduate school of science & technology / Center for Education and Research on Environmental Technology , Materials Engineering , and Nano-chemistry

1. Introduction

Controlling microscopic structure of electroconductive polymer is essential for organic device such as organic EL, semiconductor, and solar cell. Any safe and convenient method for structure control, however, has not been established. Recently, close-packed orientation of fine particles was reported. It was mentioned that evaporation of suspension conducted fall of meniscus to sweep down a substrate and coat it with particles. This withdrawal coating may also be achieved with dip-coating method (DC method), and hence structure control of conductive polymer would be possible with the dip-coating method. A substrate was vertically pulled up from water phase to organic electrolyte thin layer containing monomer formed on the water phase while the substrate was anodically polarized to polymerize the monomer.

In this research, ethyl acetate was employed as an organic phase solvent. Because of low dielectric constant of ethyl acetate, we aimed to confirm first the characteristic of the conductive film prepared in ethyl acetate, relative to that in a common organic solvent such as acetonitrile.

2. Experimental

0.5 mol dm^{-3} of pyrrole as monomer and 0.1 mol dm^{-3} 1-butyl-3-methylimidzolium hexafluorophosphate (bmim [PF_6]) as supporting electrolyte were added to the ethyl acetate (AcOEt) or acetonitrile (AN). Polymerization was carried out at constant current density of 4.0 mA dm^{-2} and 1.0~17 C dm^{-2} of charge passed at 25°C. In the DC method, substrate (ITO transparent electrode) was immersed into water saturated with AcOEt, and then 3 mm in thick of AcOEt electrolyte was poured onto the water phase. The substrate was pulled up by the speed of from 9 to 156 μm s^{-1} while from 1.0 to 17 C dm^{-2} of electricity was passed with 4.0 mA dm^{-2} of current density.

4 terminal method was employed to measure conductance of polypyrrole films. Polypyrrole film surface was also observed by scanning electron microscope (SEM).

3. Results and discussion

The polymerized film of pyrrole was successfully prepared in AcOEt electrolyte. Conductivity of polypyrrole films were 18 S cm^{-1} for AcOEt electrolyte and 28 S cm^{-1} for AN electrolyte, respectively. Thus, the organic solvent of low dielectric constant could be employed as

electrolytic solvent with soluble ionic liquid, bmim [PF_6], and give almost equivalent conductivity.

Fig.1 showed SEM images of surface structure of the polypyrrole films. It was observed from Fig. 1(a) that polypyrrole prepared by common method was smooth and homogeneous. On the other hand, Fig.1 (b), the film prepared with DC method, we could see the surface structure of locally crystalline polypyrrole. This structure change resulted from restriction of propagation direction in which electro-oxidation of pyrrole was carried out in thin electrolytic solution and the substrate was withdrawn vertically upward.

Fig.2 showed the ratio of film conductivity of vertical direction to that of horizontal direction. Apparently DC method gave higher conductivity ratio than common method. These results suggested anisotropic orientation of polypyrrole caused of DC method.

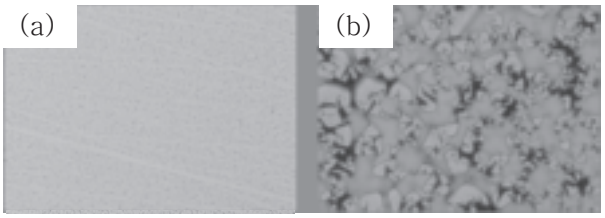

Fig.1 SEM images of polypyrrole films in electric quantity 0.09 C (a) common method (b) dip-coating method.

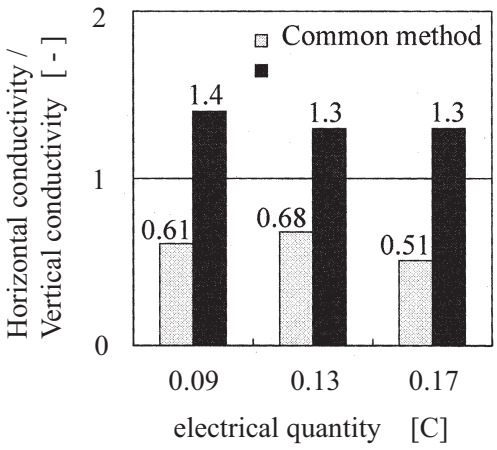

Fig.2 Ratio between horizontal conducti vity and vertical conductivity.

P105C

Electropolymerization of Pyrrole in Ionic Liquid Diluted by The Organic Solvent

Daichi MORI, Yasushi ONO

Niigata University, Department of Graduate School of Science and Technology, Center for Education and Research on Environmental Technology, Materials Engineering, and Nanochemistry

1. Introduction

The electrosynthetic reaction of the conducting polymers in ionic liquid as a reaction media has already been reported. However, the ionic liquid is used as neat because of its functional character. So the function as the salt of the ionic liquid has not been evaluated in many researches. Moreover, when considering for many phenomena, high viscosity of ionic liquid has been taken account for too much. If other characteristics of the ionic liquid were paid attention to, and furthermore the ionic liquid were allowed to be diluted by solvent, much more additional function would be achieved. Therefore, we regarded the ionic liquid as a supporting electrolyte and the electropolymerization of pyrrole was carried out in the ionic liquid diluted by organic solvent, the ethyl acetate. Conductivity of polymer films was also evaluated.

2. Experimental

Polymerization electrolyte was prepared by diluting 1- butyl-3-methylimidazolium hexafluoro-phosphate as the ionic liquid with the ethyl acetate, and then adding 0.3 mol dm^{-3} of pyrrole. Indium tin oxide electrode (0.1×0.1 dm^2), platinum electrode (0.1×0.1 dm^2), and silver-silver chloride electrode were employed as working electrode, counter electrode, and reference electrode, respectively. Galvanostatic electro-polymerization was carried out at 100 mA dm^{-2} of current density for 5 minutes.

Surface of polymer film was observed by scanning electron microscope (SEM). The film thickness was measured with the micrometer and the electric conductivity by four terminal method.

3. Results and Discussions

The conductive polymer film was obtained in the ionic liquid diluted with the ethyl acetate that is a non-polar solvent. The relation between the polymer film thickness and/or electric conductivity of electrolyte and concentration of the ionic liquid was shown in Fig. 1. The relation between the electric conductivity of the polymer film and concentration of the ionic liquid was also shown in Fig. 2.

The electric conductivity of electrolyte show the same increase and decrease tendency as the polymer film thickness as illustrated in Fig. 1. In the case of high concentration of the ionic liquid, it seemed that dense packing of the polymer film was obtained

because of the decrease in the electric conductivity by decrease in the ionic mobility due to the high viscosity.

On the other hand, low concentration of ionic liquid gave the thin polymer film. It is thought that because of extension of the potential gradient according to a low electric conductivity of electrolyte, the electrode reaction might take place in the bulk. Therefore, polymer and oligomer did not adhered to the electrode, and hence the polymer film thickness thinned.

However, the electric conductivity of the polymer film has been comparable in the order of one digit as illustrated in Fig. 2. Preparation of polymer films with constant current might make all reaction velocities the same. Additionally, the ultra small amount of moisture contained in the ionic liquid seemed to cause the decrease in the electric conductivity of the polymer film. Water would also trigger polymerization at 2nd and/or 3rd position of the pyrrole and the bond between polymer and hydrogen. Therefore, decrease in the electric conductivity of the polymer film occurred with high concentration of the ionic liquid. On the other hand, the decrease in the doping level due to the low concentration of the ionic liquid conducts the decrease in the electric conductivity of the polymer film. These two factors may mutually counterbalance, and the electric conductivity of the polymer film has indicated a constant value against the change in the concentration of the ionic liquid.

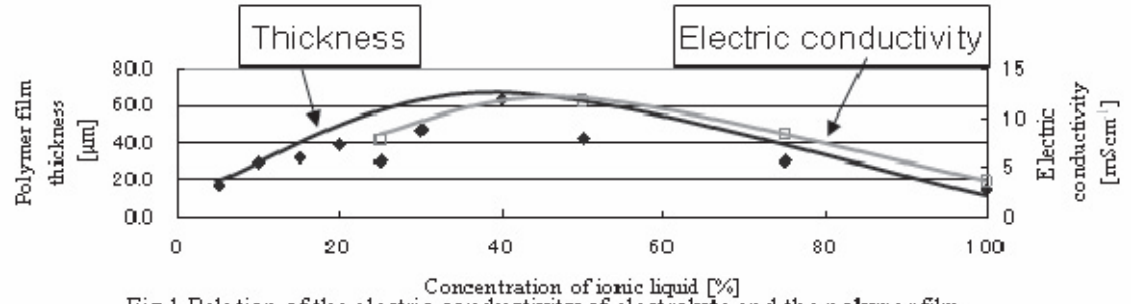

Fig.1 Relation of the electric conductivity of electrolyte and the polymer film thickness

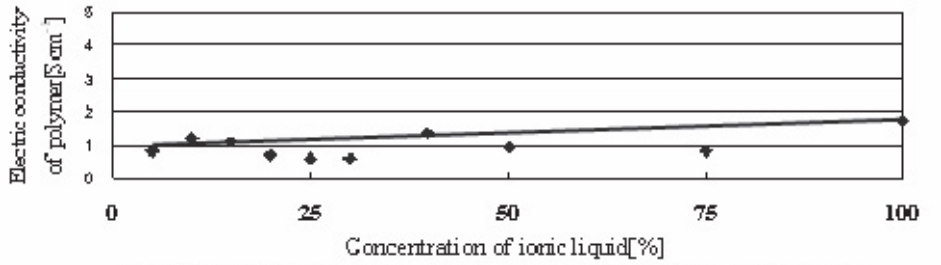

Fig. 2 Relation of the electric conductivity of the polymer film

P106A

INDIRET ELECTROORGANIC REACTION WITH OXYGEN REDUCTION ON HYDROPHOBIC SILVER GRANULES CATHODE

Tomohiro SHIOTA, Yasushi ONO

Niigata University, Department of Graduate School of Science & Technology / Center for Education and Research on Environmental Technology, Materials Engineering, and Nanochemistry

1. Introduction

It is very significant to establish the easy process of hazardous organics electrolytic decomposition. In general, the high potential is required to direct electrolysis organics. So the indirect electrolysis with mediators can be thought of as a useful way. Considering an environmental load, it is desirable to adopt the indirect electrolysis by reactive oxygen species produced by oxygen reduction. General electrode materials have, however, a low affinity for oxygen, so their current efficiencies are very low. We fixed hydrophobic particles to the surface of electrode by composite plating and made hydrophobic silver granules to construct bed electrode. In this work, silver was employed as electrode matrix metal, and polytetrafluoroethylene (PTFE) as hydrophobic particles.

2. Experimental

PTFE fine particles (0.2 μm) were dispersed into thiocyanate silver plating bath and composite plating was carried out onto Ni plates or Cu granules, and the hydrophobic silver electrodes were made. Composite plated plates were used for the measure of linear sweep voltammetry. Composite plated granules were used for the constant-potential electrolysis. These measurements and electrolysis were carried out in 0.1mol dm^{-3} NaOH aqueous solution under the oxygen atmosphere at 298K. Composite plated granules were also used for the electrolysis in 0.1 mol dm^{-3} NaOH aqueous solution containing 0.07 mmol dm^{-3} of amaranth under the oxygen atmosphere.

3. Results and Discussion

Fig. 1 shows linear sweep voltammograms for the reduction of O_2 on hydrophobic silver granules in 0.1mol dm^{-3} NaOH under the oxygen atmosphere. As hydrophobicity of electrodes increase, the reduction current becomes higher. At -0.7 V vs. Ag | AgCl , it is considered that reactive oxygen species (hydrogen peroxide) were generated by two electron reduction of oxygen. At -1.1 V , it is considered that water was generated by four electron reduction of oxygen. The constant-potential electrolysis was carried out for one hour at -0.7 V on hydrophobic silver granules electrode with O_2 bubbling (Fig. 2). As hydrophobicity of electrodes increased, the amount of charge passed increased. Thus it seemed

that more reactive oxygen species generated by improving the hydrophobicity. Hydrophobic silver granules electrode that was prepared in the composite plating bath containing 100 g dm^{-3} of PTFE gave the maximum charge passed. Similarly constant-potential electrolysis was carried out in amaranth solution on hydrophobic silver granules electrode and hydrophilic silver granules electrode respectively (Table 1). The hydrophobic silver granules electrode showed the about four times the decomposition rate of amaranth compared to that of the hydrophilic silver granules electrode. The highly effective electrolysis was seemed to be conducted by higher concentration of reactive oxygen species generated in the vicinity of the hydrophobic silver granules electrode and also by concentrated amaranth on the hydrophobic interaction.

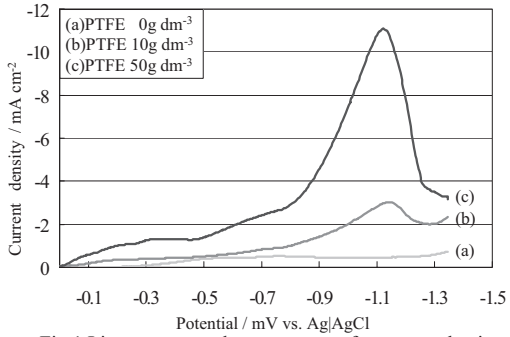

Fig.1 Linear sweep voltammograms of oxygen reduction on composite-plated sheet electrodes.

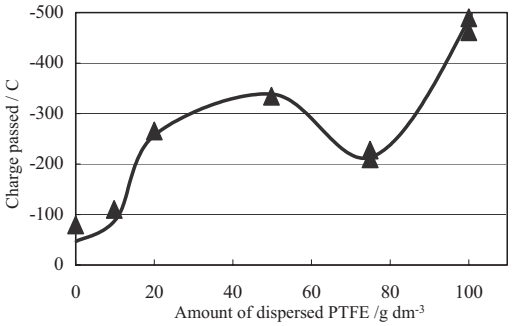

Fig.2 Dependence of charge passed on amount of dispersed PTFE.

Table 1 Result of electrolytic decomposition of amaranth on hydrophilic and hydrophobic electrodes.

	Electrode	
	Hydrophilic	Hydrophobic
Decomposition ratio / %	6	24

P107B

APPLICATION OF LAYERED TANTALUM OXIDES NANOSHEET TO PHOTOCATALYTIC REACTION

Yoshiyuki Mori[1], Hidetoshi Kibe[1], Kazuyoshi Uematsu[2], Kenji Toda[1]*, Mineo Sato[2]

[1] *Graduate School of Science and Technology, Niigata University*
[2] *Department of Chemistry and Chemical Engineering, Niigata University*
Center for Education and Research on Environmental Technology, Materials Engineering, and Nanochemistry

The development of photocatalysts for the overall splitting of water has been a key issue in the field of hydrogen energy, which is currently attracting great interest. Nanosheet has two dimensional strong anisotropy and large surface area. This study is photocatalytic activity of nanosheet for water splitting without restacking.

$NaRbNdTaO_5$[1)] was synthesized by a conventional solid state reaction. The $NaRbNdTaO_5$ powder (0.5 g) suspended in 200 ml of pure water was stirred with a magnetic stirrer at room temperature. Usually a layered materials were treated with a tetrabutylammonium hydroxide (TBAOH) solution to promote delamination. On the other hand, layered compound $NaRbNdTaO_5$ was exfoliated in pure water without any intercalation. The colloidal solution was filtered using a membrane filter (pore size, 450 nm) to remove a coarse grains. The residue and filtrate were characterized using XRD, UV-Vis, SEM, TEM, electron diffraction. Photocatalytic reaction was carried out in an air-free closed gas circulation system with an inner irradiation type reaction cell made of quartz under Ar atmosphere by a high pressure Hg lamp (400 W). Gas chromatography determined the amount of the evolved gas.

Filtrate was composed of colloid solution. It was confirmed by tyndall phenomenon with irradiating a 635 nm laser. Colloidal solution was composed of nanosheets as shown in Fig. 1. Colloidal solution evoluted H_2 by water splitting under UV irradiation as shown in Fig. 2. The amount of evolved gas increased with the progress of reaction time without deactivation. Colloidal solution had optical absorption edge (240 nm). Bandgap of nanosheet was bigger than bulk's. This is quantum size effect. Therefore, there were nanosheets in colloidal solution. The nanosheets showed photocatalytic activity without restacking in spite of extremely small amount. It was reported that photocatalytic activity of restacked nanosheets[2)]. On the other hand, this study was photocatalytic activity of nanosheets without restacking.

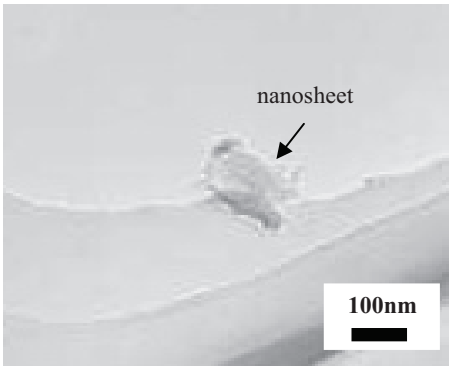

Fig. 1 TEM micrograph of $NaRbNdTaO_5$ nanosheet.

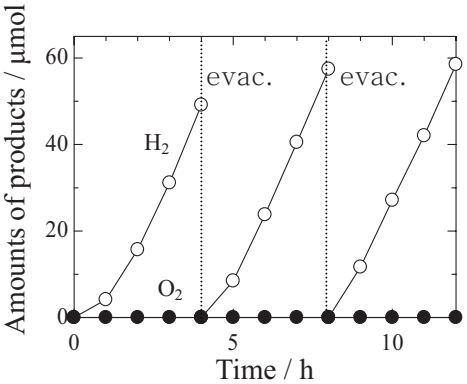

Fig. 2 Photocatalytic water splitting of $NaRbNdTaO_5$ colloid solution.

Reference
1) R. J. Cavazos, R. E. Schaak, Mater. Res. Bull, 39 (2004) 1209-1214.
2) K. Domen, Y. Ebina, S. Ikeda, A. Tanaka, J. N. Kondo, K. Maruya, Catalysis Today, 28 (1996) 167-174.
Acknowledgements
This work was supported by SORST.

P108C

MELT SYNTHESIS AND MORPHOLOGY CONTROL OF PHOSPHOR MATERIALS

*Kenji Toda[1,2,3)], Masafumi Hosoume[1)], Kazuyoshi Uematsu[4)], Mineo Sato[2,3,4)], Tadashi Ishigaki[5)] and Masahiro Yoshimura[5)]

[1)]*Graduate School of Science and Technology, Niigata University, 8050 Ikarashi 2-nocho, Niigata 950-2181, Japan*

[2)]*Center for Education and Research on Environmental Technology, Materials Engineering, and Nanochemistry, Niigata University*

[3)]*Center for Transdisciplinary Research, Niigata University*

[4)]*Department of Chemistry and Chemical Engineering, Niigata University*

[5)]*Materials and Structures Laboratory, Tokyo Institute of Technology*

In general, the luminescence efficiency of phosphor material decreases with the decrease of particle size. Fine particle phosphors have large surface area with many defects than that of bulk phosphor. Therefore, well-crystalline bulk phosphor with several microns diameter has been usually used in many applications such as displays and lamps.

The synthesis of well-crystalline multi-component phosphor material is not easy by conventional solid-state reaction techniques because the reaction rates among oxides are slow by solid-state diffusion as to form homogeneous compounds or solid solutions. The melt reactions are very fast and homogeneous due to liquid mixing and fast diffusion in the liquid phase in contrasting to conventional solid-state reactions. These melt synthesis techniques are, therefore, suitable for synthesizing multi-components compounds and solid solutions where homogenous cation mixing is essentially required.

In order to synthesize multi-component phosphor materials $Y_3Al_5O_{12}:Ce^{3+}$ [1] and $SrAl_2O_4:Eu^{2+}$, Dy^{3+} [2], we have applied a novel "melt synthesis technique" rather than conventional solid state reaction techniques. In the melt synthesis, the mixture of oxides or their precursors is melted in a short period of time (1-60s) by a strong light radiation in arc imaging furnace. A spherical molten sample where multiple cations were mixed homogeneously was directly solidified on a Cu hearth. Both phosphors display bright light emission by excitation of visible light.

[1] G. Blasse and A. Bril, *Appl. Phys. Lett.*, **11**, 53 (1967).

[2] T. Matsuzawa et al., *J. Electrochem. Soc.*, **143**, 2670 (1996).

P109A

REMOVAL OF FLUORINE FROM WASTE WATER BY ETTRINGITE

Kenji Sato,[1] Hiroko Morinaga,[2] Toshiaki Tokumitsu,[1] Kazuyoshi Uematsu,[2] Kenji Toda,[1, 3] and Mineo Sato[2, 3]

[1] *Graduate School of Science and Technology, Niigata University*
[2] *Department of Chemistry and Chemical Engineering,*
[3] *Center for Education and Research on Environmental Technology, Materials Engineering, and Nanochemistry*

Law for the standard of "Fluorine and the compounds" become severe newly in June 2001, and it was promulgated. When a human drinks water with a large amount of fluorines for a long term, fluorine breaks the bone structure, and sometimes leads to the difficulty in walking. Additionally, acute toxicity fluorines cause vomiting, stomachache, and nausea. Fluorine in natural water originates in geological features, though recent pollutions were increased by the plant effluent of a power plant and electronic industry. For example, the 10000 tons / year fluorine has been used in the manufacturing process at the semiconductor factory in only Japan as an etching chemical of the silicon wafer in the form of HF and NH_4F. The removing method of the fluoride ion includes the calcium addition method, the activated alumina method, and the bone charcoal method, etc. The calcium addition method is industrially used. However, even if the calcium salt is added in a high concentration, the constant concentration of the fluoride ion remain for this method because of high solubility of the calcium fluoride (0.0016 g/100 g 18°C). Although the calcium addition method and other methods have been the effective fluoride removing method, fluorine removing has become difficult in the past methods.

In this study, we report $3CaO\text{-}Al_2O_3\text{-}3CaSO_4\text{-}32H_2O$ (ettringite) as a new absorbent for the fluorine.The fluorine concentration of the water treated with the ettrin gite wasachieved to be less than 8 mg/l. The fluorine rem oval mechanism isdifferent with the pH of the water. Whe n the pH of the fluorine solutionis adjusted to alkalinity, t he ettringite can remove the fluorine component without s ludge. Ettringite is one of the cement hydrates with a com position of $3CaO{\cdot}Al_2O_3{\cdot}3CaSO_4{\cdot}32H_2O$. Ettringite have 3 2 molecules of hydration water. The composition formula of Ettringite is $[Ca_6Al_2(OH)_{12}{\cdot}24H_2O]\,(SO_4)_3{\cdot}2H_2O$.

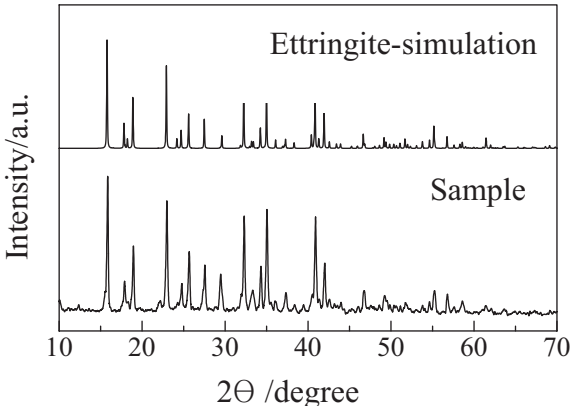

Fig.1. X-ray diffraction patterns of ettringite

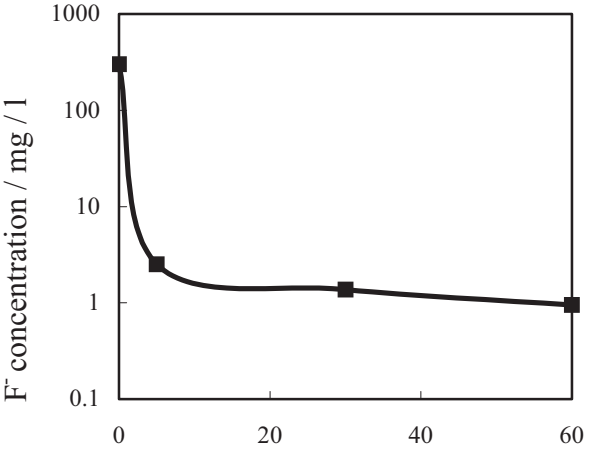

Fig.2. Variation of F^- concentration with time

P110B

PREPARATION OF $KNbO_3$ THIN FILM AT ROOM TEMPERATURE

Toshinari Takahashi[1] , Kazuyoshi Uematsu[2] , Kenji Toda[1,3*] , Mineo Sato[2,3]

[1] Graduate School of Science and Technology, Niigata University
[2] Department of Chemistry and Chemical Engineering
[3] Center for Education and Research on environmental Technology, Materials Engineering, and Nanochemistry

$KNbO_3$ (KN) is one of a candidate of lead-free piezoelectrics, since the single crystal shows a large electromechanical cupling and nonlinear optical coefficient. However the syntering of KN is a difficult a high-temperature process because of the massive vaporization of K during sintering process. In this study, we present a new process for the synthesis of KN thin film using the layered perovskite precursor, K_2NbO_3F (KNF) single crystal. KN thin film was prepared by selective dissolution of a KNF single crystal in saturated vapor at room temperature. KN thin film obtained by the new process show strong c-axis orientation.

The layered perovskite precursor, K_2NbO_3F single crystal was grown by flux method. High-purity KF(2N5), K_2CO_3(3N5) and Nb_2O_5(3N5) powders were weighed out in the ratio $KF/K_2CO_3/Nb_2O_5$ = 0.6 : 0.4 : 0.175, mixed in aceton. The dried mixture was heated at 800℃ for 1h. The precursor, K_2NbO_3F single crystal, was cooled to 600℃ at rate of 4℃/h. Procedures to construct KN thin film are as follows. A quartz substrate was washed with a nitric acid solution. The $KNbO_3$ thin film was prepared by selective dissolution of a K_2NbO_3F single crystal in saturated vapor at room temperature. Reaction time was about 24h. The $KNbO_3$ thin film formed on quartz substrate was characterized using X-ray diffraction (XRD) and the Second Harmonic Generation (SHG) experiment.

Fig.1 shows the XRD patterns of KNF single crystal and KN thin film. The XRD data showed intense diffraction peak for (002), (006) and (008) in the KNF single crystal. On the other hand, it confirmed diffraction peak of (001), (002) and (200) in the KN thin film. This observation suggests that KNF single crystal and KN thin film are c-axis orientation. Fig.2 shows the SHG intensity of KN thin film. KN thin film showed the intense SHG which comparable to y-cut α -quartz as a reference sample.

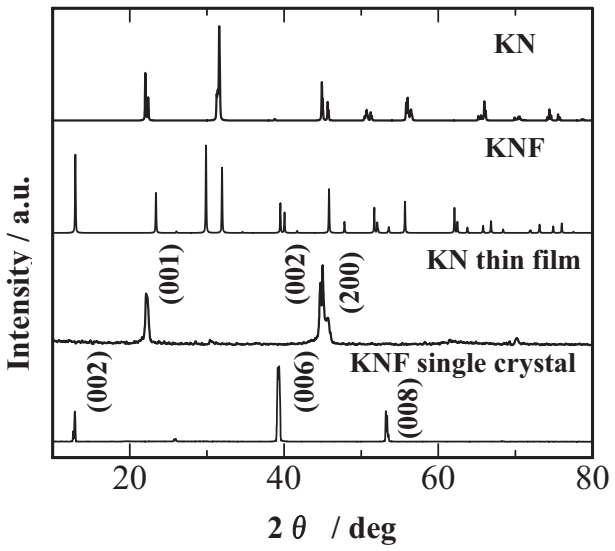

Fig. 1 XRD patterns of KN thin film and KNF single crystal

.

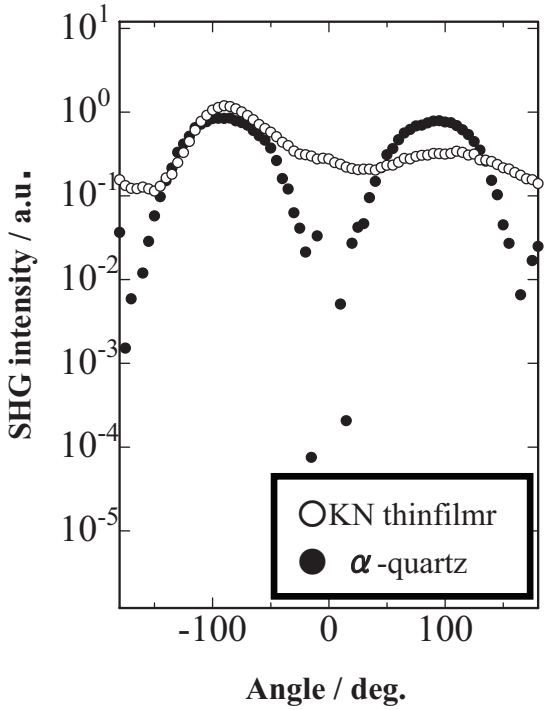

Fig. 2 SHG intensity of (a) KN thin film (b) y-cut α -quartz single crystal.

P111C

DEVEPOPMENT OF NOVEL PHOSPHOR FOR A WHITE LED

Yoshitaka Kawakami[1], Akira Komeno[1], Kazuyoshi Uematsu[2], Kenji Toda[1,3]*, Mineo Sato[2,3]

[1] *Graduate School of Science and Technology, Niigata University*
[2] *Department of Chemistry and Chemical Engineering, Niigata University*
[3] *Center for Education and Research on Environmental Technology, Materials Engineering, and Nanochemistry*

White LED is the one of the possible candidates for new lighting system in the near future. The most dominant white LED use a 450 – 470 nm blue-emitting LED that excites a yellow-emitting $Y_3Al_5O_{12}:Ce^{3+}$ (YAG:Ce^{3+}) phosphor dispersed in the epoxy resin on a blue LED chip. This method is presently the most efficient technique. However, the light color is not true white. Therefore, the importance of blue-excitable phosphor is increasing.

Alkaline earth silicates have excellent luminescence properties as hosts of phosphors with various crystal structures and high stability. In this study, we studied luminescent properties of $Ba_9Sc_2Si_6O_{24}:Eu^{2+}$ as novel alkaline earth silicate phosphor for white LED. In this phosphor, the blue light can be strongly absorbed by the allowed f-d transition of Eu^{2+}. The emission at about 510 nm depends on the environment of the emission ion site in the host lattice. Strong crystal fields with the covalent bond and distorted coordination affect the excited state because the energy level of the $4f^65d$ has a wide distribution of the electron cloud. Since the splitting of $4f^65d$ energy level becomes wider with the increase of the crystal field strength, the difference between the ground state ^8S level and lower $4f^65d$ component becomes smaller. Therefore, the luminescence wavelength shifts to long wavelength side. The samples exhibit high intensity green emission under near–UV and blue excitation.

A stoichiometric mixture was fired in an alumina boat at 1773 K for 6 h in weak reductive atmosphere of 5 % H_2-95 % Ar gas. The crystal structure of $Ba_9Sc_2Si_6O_{24}$ is given in figure 1. The structure closely resembles the structure of NASICON in their linkage of [SiO_4] tetrahedral and [ScO_6] octahedral. There are three different Ba sites. The coordinations of the Ba^{2+} are slightly irregular nine-, ten- and twelve-folds. Figure 2 shows the excitation and emission spectra of $(Ba_{1-x}Eu_x)_9Sc_2Si_6O_{24}$ at room temperature. The phosphor can be efficiently excited by visible lights (350 - 450 nm), yielding an intense green emission around 510 nm. The emission intensity is comparable to that of the commercial YAG:Ce^{3+} phosphor. At 100 ºC, the decrease in emission intensity is a 25 percent.

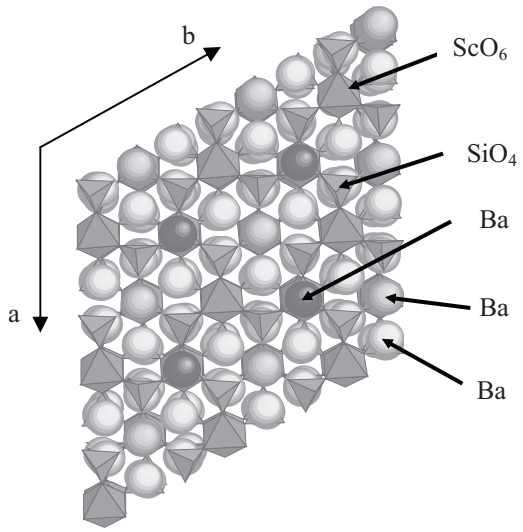

Fig.1 Crystal structure of $Ba_9Sc_2Si_6O_{24}$.

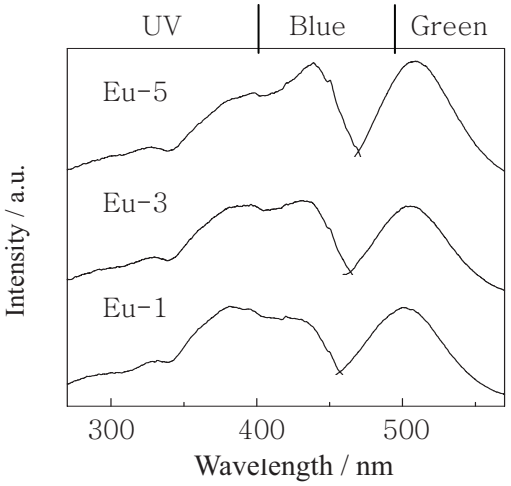

Fig.2 Excitation and emission spectra of $(Ba,Eu)_9Sc_2Si_6O_{24}$.

P112A

NEW PHOTOCATALYST OF METAL OXIDES WITH d^{10} CONFIGULATION

Hironori Ishikawa[1], Kazuyoshi Uematsu[2], Kenji Toda[1,3], Mineo Sato[2,3]

[1] *Graduate School of Science and Technology, Niigata University*
[2] *Department of Chemistry and Chemical Engineering, Niigata University*
[3] *Center for Education and Research on Environmental Technology, Materials Engineering, and Nanochemistry*

In view of the importance of hydrogen as a clean energy source, photocatalytic water decomposition over semiconductor materials is one of the most creative scientific concerns. Although a number of visible-light-driven photocatalysts have been proposed as potential candidates for overall splitting, a satisfactory material has tet to be devised.Many tantalates such as $NaTaO_3$: La[1)] were known to show high photocatalytic activity under UV irradiation. However, tantalates have a wide bandgap and cannot absorb sunlight efficiently.

Recently, P-block metal ions with d^{10} configulation such as Ga^{3+}, In^{3+}, Sn^{4+} and Sb^{5+} became a core element to be photocatalytic activity in pure water[2)].

In this study, $La_2BaIn_2O_7$, which has layered perovskite structure, has a photocatalytic activity in pure water under UV light irradiation. $La_2BaIn_2O_7$ showed photocatalytic activity for water splitting without co-catalyst.

The crystal structure of $La_2BaIn_2O_7$ was determined by the X-ray diffraction pattern. This result showed to synthesis single phase. $La_2BaIn_2O_7$ showed a photocatalytic activity for water decomposition initial rate of H_2 evolution under UV irradiation in Fig. 3. This is the first successful example of layered perovskite with d^{10} configulation such as In^{3+}.

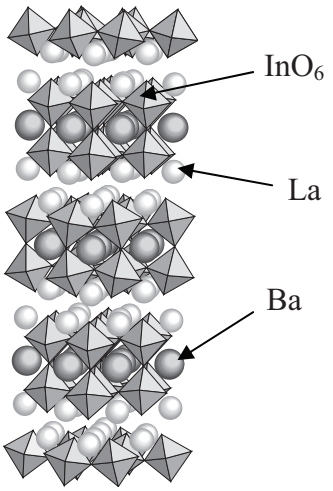

Fig. 1 Crystal structure of $La_2BaIn_2O_7$.

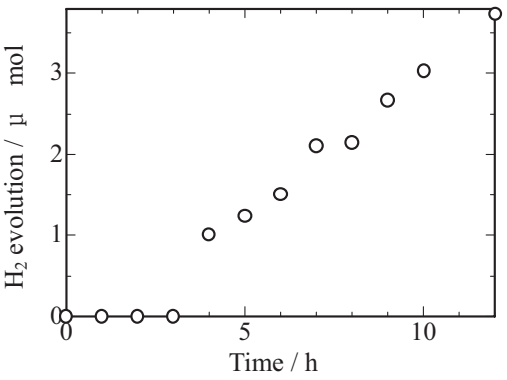

Fig. 2 Photocatalytic activity of $La_2BaIn_2O_7$.

References

1) H. Kato, A. Kudo, *Catalysis Today.*, 78, 561-569 (2003)
2) J. Sato, H. Kobayashi, H. Nishiyama and Y. Inoue,. *J. Phys. Chem, B,* 108, 4369-4375 (2004)
3) M. Caldes , C. Michel. T. Rouillon, M. Hervieu and B. Raveau,. *J. Materials. Chem,* 12*,* 473-476 (2002)

Acknowledgements

This work was supported by SORST.

P113B

LOW TEMPERATURE GROWTH OF POTASSIUM NIOBATE SINGLE CRYSTAL

Iida Akihiro[1], Uematsu Kazuyoshi[2], Toda Kenji[1,3], Sato Mineo[2,3]

[1] *Graduate School of Science and Technology, Niigata University*
[2] *Department of Chemistry and Chemical Engineering, Niigata University*
[3] *Center for Education and Research on environmental Technology, Materials Engneering, and Nanotechnology*

Lead zirconate titanate (PZT) ceramics have been widely applied as a piezoelectric material. However, RoHS directive restricts the use of hazardous substances in themanufacture of electrical and electronic equipment. After July 2006, electrical and electronic equipment containing the harmful chemicals cannot be introduced to the European market. Although the PZT was not the object of the present restrictions, the use of lead based piezoelectric materials will be prohibited in the near future. Perovskite $KNbO_3$ is possible candidate for many lead-free piezoelectric devices due to its large electromechanical coupling coefficients and high Curie temperature. However, high temperature and large-scale equipments are required for growth of $KNbO_3$ single crystal. In this study, we present a new process for low temperature growth of $KNbO_3$ single crystal using template precursor, K_2NbO_3F.

The starting material was a mixture of KF, K_2CO_3 and Nb_2O_5. A mixture molar ratio was $K_2CO_3/Nb_2O_5/KF$ = 1/1/18. Excess KF acts as a flux. The mixture were placed on a platinum plate and heated up to 790-900°C range. Then, samples were cooled to 600 °C at 4 °C/min. Excess KF was washed by de-ionized water.

Plate like single crystals of $KNbO_3$ were grown from a layered perovskite precursor, K_2NbO_3F, at 890 °C. The K_2NbO_3F single crystals with plate like morphology were synthesized at 790 °C as a template precursor. At over 800 °C, K and F components are eliminated from the precursor K_2NbO_3F and plate like $KNbO_3$ single crystals were formed.

We expect this new template synthesis process using a layered perovskite precursor can be extended to the growth of other single crystals.

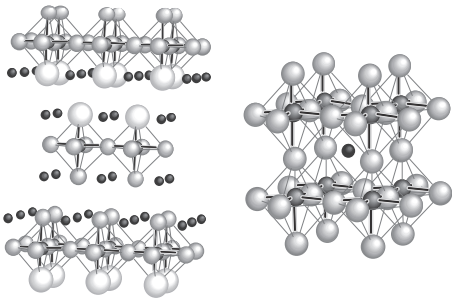

Fig. Crystal structures of K_2NbO_3F(left) and $KNbO_3$(right).

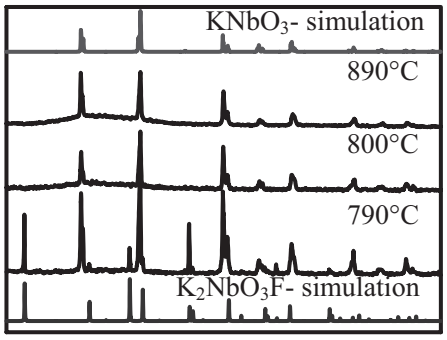

Fig. XRD patterns of various samples.

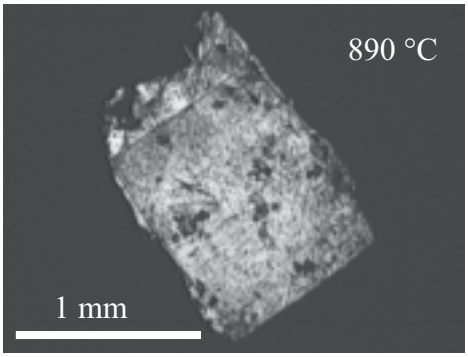

Fig. Photograph of $KNbO_3$ crystal.

P114C

PHOTOCATALYTIC ACTIVITY OF BISMUTH LAYERED PEROVSKITE TREATED WITH ACID

Yousuke Narumi [1] , Kenji Toda [1,*] , Kazuyoshi Uematsu [2] , Mineo Sato [2]

[1] *Graduate School of Science and Technology, Niigata University*
[2] *Department of Chemistry and Chemical Engineering, Niigata University*

The decomposition of water into H_2 and O_2 using semiconductor photocatalysts has been intensively investigated for solar energy conversion and storage.

Double layered tantalate of $SrBi_2Ta_2O_9$ (SBT), a member of the Aurivillius phase had $(Bi_2O_2)^{2+}$ sheets [1)]. SBT was known to show ferroelectric property and selective dissolution of bismuth oxide interlayer [2)]. Doping of rare earth ions (R^{3+}) for A-site improved the polarization property of SBT. Considering charge neutrality, the substitution of R^{3+} for Sr^{2+} site lead to a change of band structure of perovskite-blocks.

In this study, we synthesized $Sr_{0.7}La_{0.2}\square_{0.1}Bi_2Ta_2O_9$ (SBTL , $\square$ = vacancy), and measured their photocatalytic activity for water decomposition under UV light irradiation after acid treatment.

SBTL powder were synthesized by a conventional solid state reaction. SBTL powder were treated with 3 M HCl for 3 days. The products were characterized by powder X-ray diffraction, UV-Vis spectrometer, SEM, fluorescent X-ray analysis and ICP.

Fig. 2 shows the powder XRD patterns of SBTL calcined at 1373 K and the acid treated SBTL.

The pattern of the acid treated product is quite different from SBTL. The results of ICP indicated no detection of Ta and dissolution of Bi in a solution. The selective dissolution of the bismuth oxide interlayer was performed successfully. SBTL treated with acid showed the high photocatalytic activity under UV light irradiation (H_2 evolution (213μ mol / h) , O_2 evolution (82μ mol / h)) as shown in Fig. 3.

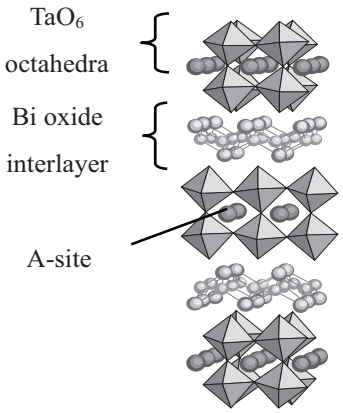

Fig.1 Crystal structure of SBTL.

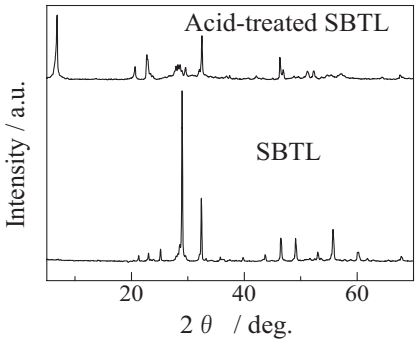

Fig.2 Powder XRD patterns of samples.

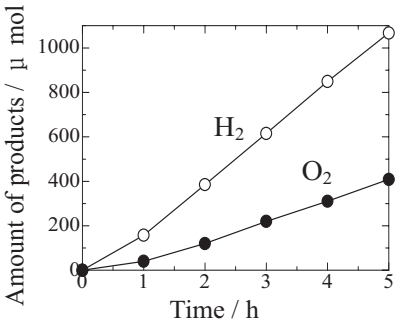

Fig.3 Photocatalytic activity of sample.

References

1) B. Aurivillius, *Ark. Kemi,* **2**, 519 (1950)

2) Y. Sugahara, et. al. .*Chem. Phys. Lett.,* **393**, 12-16 (2004)

Acknowledgements

This work was supported by SORST.

P115A

SYNTHESIS OF NOVEL MOLYBDATE PHOSPHOR

Satomi Seki[1], Yutaka Ito[1], Uematsu Kazuyoshi[2,3], Toda Kenji[1,3], Sato Mineo[2,3]

[1] *Graduate School of Science and Technology, Niigata University*
[2] *Department of Chemistry and Chemical Engineering,*
[3] *Center for Education and Research on Environmental Technology, Materials Engineering, and Nanochemistry*

Light of conventional white LED which is concise of used most now is yellow photoluminescence of a cerium-doped yttrium aluminum garnet (YAG) phosphor and blue emission of a blue LED[1)]. However, this light color is not true white. As the other methods of white LED, pumping of red, green and blue phosphors with a near UV LED have great potential for true white solid-state lighting. Unfortunately, an efficiency of currently applied red phosphor $Y_2O_2S:Eu^{3+}$ is much lower than other green $SrAl_2O_4:Eu^{2+}$ and blue $BaMgAl_{10}O_{17}:Eu^{2+}$[2)]. Therefore, the true white LED requires new phosphors that absorb in the near UV light and emit in the red region. We report the synthesis and luminescence properties of new red molybdate phosphor, $Ba_2Gd_3Li_3Mo_8O_{32}:Eu^{3+}$ for near UV LED based white LEDs.

Polycrystalline phosphor samples were synthesized using a conventional solid-state reaction. A stoichiometric starting material, which $BaCO_3$, Gd_2O_3, Li_2CO_3, MoO_3 and Eu_2O_3, mixture was fired in Pt crucible at 1173 K for 1h in air. Products were characterized by powder X-ray diffraction and photoluminescence.

The XRD patterns of $Ba_2Gd_3Li_3Mo_8O_{32}:Eu^{3+}$ phosp hors is shown Figure 1. The excitation and emission sp ectra of $Ba_2(Gd_{0.7}Eu_{0.3})_3Li_3Mo_8O_{32}$ and $Y_2O_2S:Eu^{3+}$ ph osphor are shown Figure 2. The observed emission int ensity of $Ba_2(Gd_{0.7}Eu_{0.3})_3Li_3Mo_8O_{32}$ is about 5 times h igher than that of a commercial $Y_2O_2S:Eu^{3+}$ phosphor.

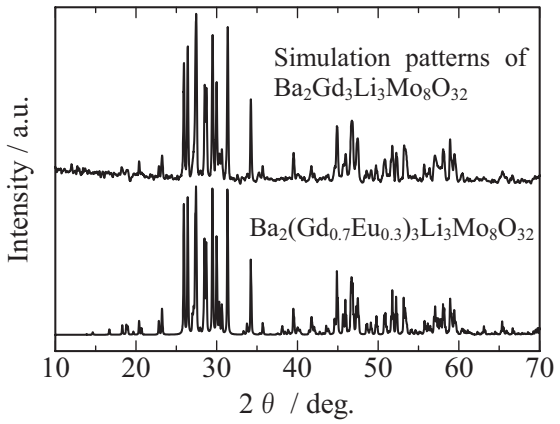

Fig.1 X-ray diffraction patterns of $Ba_2(Gd_{0.7}Eu_{0.3})_3Li_3Mo_8O_{32}$.

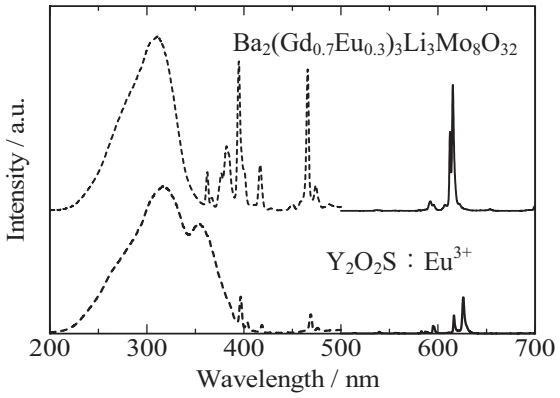

Fig.2 Excitation and emission spectra of $Ba_2(Gd_{0.7}Eu_{0.3})_3Li_3Mo_8O_{32}$ and $Y_2O_2S:Eu^{3+}$.

Reference
1)Y. Q. Li, A. C. A. Delsing, G. de With, and H. T. Hintzen, Chem. Mater., pp 3242-3248, vol.17 (2005).
2)S. Shionoya and W. M. Yen, Phosphor Handbook, CRC Press, New York (1998).

P116B

LOW TEMPERATURE SYNTHESIS OF TiO_2

Sae Nakajima[1], Yoshiomi Yamanaka[1], Kazuyoshi Uematsu[2], Kenji Toda[1,3*], Mineo Sato[2,3]

[1]*Graduate School of Science and Technology, Niigata University*

[2]*Department of Chemistry and Chemical Engineering, Niigata University*

[3]*Center for Education and Research on Environmental Technology, Materials Engineering, and Nanochemistry*

TiO_2 is usually produced from ilmenite or rutile ores as a raw material using either a sulfate or chloride process. The chloride process will eventually become a preferred process. However, this process produces hazardous by-products such as Cl_2 and HCl. Therefore, cost-saving and safety processes are required for the synthesis of the crystalline titania. In previous research, we reported a new solution-based process for the production of titania fine particle. A layered perovskite compound, $NaYTiO_4$ was dissolved into an aqueous HNO_3 solution to give crystalline rutile titania particles at 90℃ [1]. In this study, we report a manufacturing method using rutile or ilmenite ores as a titanium source.

Powder $NaYTiO_4$ samples were prepared by a conventional solid-state reaction [2]. The starting materials were a mixture of sodium carbonate, yttrium oxide and rutile ore (95.4%TiO_2). For ilmenite ore, the starting materials were a mixture of sodium carbonate and ilmenite ore (52.7 %TiO_2). The mixtures were heated for 1 h at 900-1000℃. The layered titanate powder (0.1 g) were gradually dissolved in the 10 M HNO_3 solution (10 ml) at room temperature. After the evaporation (90℃) of the solution, the precipitate was washed with distilled water and air dried. The completion of the reaction and the phase purity of the samples were confirmed by powder X-ray diffraction (XRD). Morphology of titania powder was observed using SEM.

The natural rutile ore could be used in preparing the high purity layered precursor, $NaYTiO_4$. It couldn't synthesize from natural ilmenite ore. However, pure titania was synthesized by the dissolution of the other precursor from ilmenite ore when the ratio of the mixture was Ti : Na = 1 : 3. Rutile titania was produced from rutile or ilmenite ores in nitric acid process.

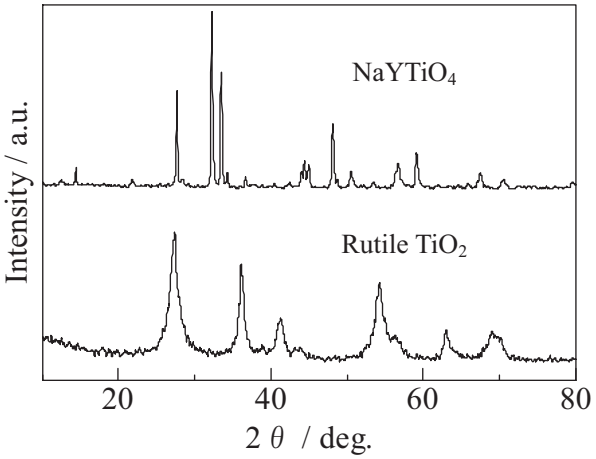

Fig.1 XRD patterns of samples from rutile ore.

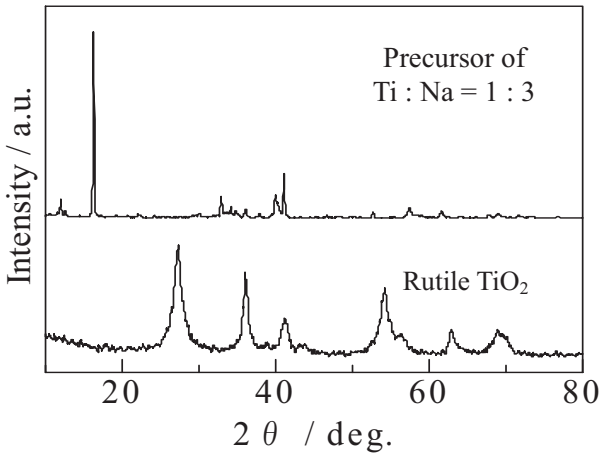

Fig.2 XRD patterns of samples from ilmenite ore.

Reference

1. K. Toda, M. Kawakami, K. Uematsu, and M. Sato, Trans. Mater. Res. Soc., Japan, 28 [2], (2003) 313-316
2. K. Toda, Y. Kameo, M. Ohta, and M. Sato, J. Alloys Compd., 218, (1995)228-232

P117C

DOUBLE-WALLED TUBULER REACTOR WITH MOLTEN SALT THERMAL STRAGE FOR SOLAR REFORMING OF METHANE

Shin-ichi Inuta[1], Daisuke Nakano[1], Yoshinori Hara[2] Nobuyuki Gokon[1], Tatsuya Kodama[2,*]
[1] *Graduate School of Science and Technology, Niigata University*
Center for Education and Research on Environmental Technology, Materials Engineering, and Nanochemistry
[2] *Department of Chemistry and Chemical Engineering, Niigata University*

Solar reforming of natural gas (methane) has been investigated as solar high-temperature thermochemical processes for conversion of high-temperature solar heat to chemical fuels. An essential problem in solar reforming of methane is to cause deactivation of catalyst due to a fluctuating incident solar radiation. In order to solve this problem, we recently proposed a tubular reformer system using a novel type of "double-walled" reactor tubes with molten-salt thermal storage[1]. This molten salt thermal storage has an advantage for solar reforming: molten salt has a high heat capacity and a large latent heat at high-temperatures. Thus, the rapid temperature change of the reactor tubes can be circumvented under fluctuating insolation.

The authors have investigated some solar tubular reformers for converting high-temperature solar heat into hydrogen. In the present work, we have improved the design of the recent tubular reactor to enhance the heat transfer from the molten-salt thermal storage to the internal catalyst tube (Fig.1). The prototype reactor is demonstrated on the heat-discharge and reforming performance during cooling mode of the tubular reformer in a laboratory scale.

In order to test the reforming performance during cooling mode of the reactor, molten-salt (Na_2CO_3) was loaded in the outer annulus of the double-walled reactor tube while the Ru-based catalyst particles were loaded in the inner tube of that. After the reactor tube was heated in a cylindrical electric furnace up to 920ºC, CH_4/CO_2 mixture was introduced to the catalyst-loaded inner tube of the reactor at a flow rate of 2-5Ndm^{3}min^{-1} at atmospheric pressure. After reaching 920ºC, the reactor was cooled by natural convection.

Fig.2 shows the time variations of the methane conversion and catalyst bed temperature during cooling mode of the reforming performance test using the Na_2CO_3 thermal storage. As a result, a plateau region of cooling curve in a vicinity of m.p. (858 ºC) appeared on the reforming test using the Na_2CO_3 thermal storage in comparison to blank test without Na_2CO_3 molten salt. This result indicates that the heat discharge from the Na_2CO_3 thermal storage into catalyst bed circumvented the rapid temperature change of the catalyst bed. The chemical conversion during cooling mode of the reactor tube was highly kept. This novel reactor tube will be used in solar tubular reformers to realize more stable operation of the reforming reaction under fluctuating insolation during a cloud passage.

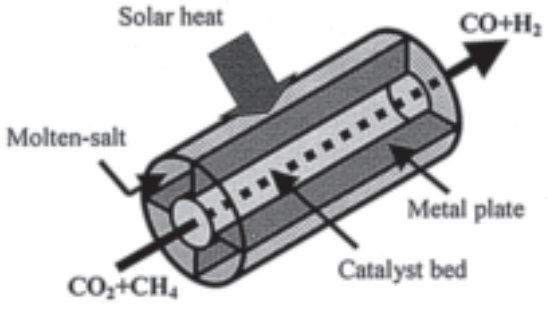

Fig.1 Concept of "double-walled" reactor tubes with molten-salt thermal storage.

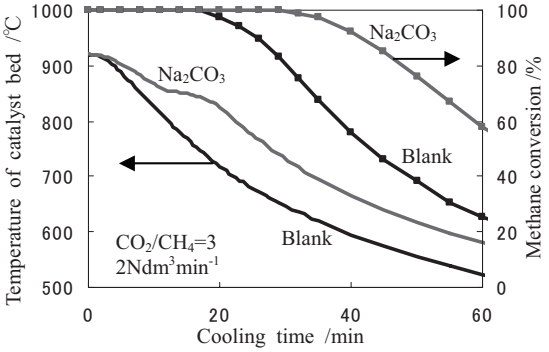

Fig.2 Time variations of the methane conversion and catalyst bed temperature.

[1]Kodama, T. et al, 2006, "Double-Walled Reactor Tube with Molten Salt Thermal Storage for Solar Tubular Reformers," Journal of Solar Energy Engineering, **128**(2), pp.134-138.

P118A

THERMOCHEMICAL TWO-STEP WATER-SPLITTING CYCLE BY ZrO_2-SUPPORTED Fe_3O_4 FOR SOLAR HYDROGEN PRODUCTION

Hiroko Murayama, Shingo Takahashi, Nobuyuki Gokon, Tatsuya Kodama[a,*]
Graduate School of Science and Technology, Niigata University
Center for Education and Research on Environmental Technology, Materials Engineering, and Nanochemistry
[a]*Department of Chemistry & Chemical Engineering, Niigata University*

Thermochemical two-step water splitting cycle with a metal-oxide redox pair has been investigated to produce hydrogen from water at high-temperature solar heat. In some two-step water splitting cycles, iron oxide redox pair is a simple and non-corrosive process, which was originally proposed using a Fe_3O_4(magneite)/FeO(wustite) redox pair by Nakamura. One of the major problems in this cycle is rapid deactivation of the iron oxide particles for the cyclic reaction. This is due to the high-temperature melting and sintering of iron oxide particles of wustite. We successfully demonstrated a repeatable two-step water splitting cycle at 1400-1000ºC by Fe_3O_4 supported on monoclinic ZrO_2 (*m*-ZrO_2)[1]. Reaction mechanism of the thermochemical water splitting using ZrO_2-supported Fe_3O_4 has been proposed by X-ray diffraction patterns: the redox reaction occurs on *m*-ZrO_2 as follows;

$$Fe_3O_4/m\text{-}ZrO_2 = 3FeO/m\text{-}ZrO_2 + 1/2O_2 \quad \text{(Thermal-reduction step at 1400℃)}$$

$$3FeO/m\text{-}ZrO_2 + H_2O = Fe_3O_4/m\text{-}ZrO_2 + H_2 \quad \text{(Water-decomposition step at 1000℃)}$$

However, the ZrO_2 support has phase transitions with respect to temperature as follows:

$$\text{monoclinic} \overset{1170ºC}{\Leftrightarrow} \text{tetragonal} \overset{2360ºC}{\Leftrightarrow} \text{cubic}$$

There is a possibility that the *m*-ZrO_2 support is transformed to tetragonal ZrO_2 (*t*-ZrO_2) during thermal reduction step. In the present study, two-step water splitting cyclic reaction was examined for *m*-ZrO_2-supported Fe_3O_4 by liqid-N_2 quenching method: after thermally reducing *m*-ZrO_2-supported Fe_3O_4 at 1400-1600ºC, the solid sample was rapidly quenched in liqid-N_2 bath as shown in Fig. 1. The reaction mechanism at high-temperature was examined by a quantitative analysis of oxygen and hydrogen gases released, ICP chemical analysis and XRD analysis for solid materials formed. Fig. 2 shows the relationship between the amount of hydrogen evolved from the thermally-reduced sample in subsequent water–decomposition step and thermal reduction temperature. As a result, the amount of hydrogen evolved increased with increasing thermal-reduction temperature and conversion of Fe_3O_4 reached over 50% at 1600ºC. The conversion of Fe_3O_4 to wustite phase on *m*-ZrO_2 was estimated from the amount of hydrogen produced by assuming that the wustite phase formed in the thermal-reduction step was completely reoxidized to Fe_3O_4 in the subsequent water-decomposition step. In addition, an oxygen/ hydrogen ratio was calculated through 1st-5th runs of the repeated water splitting cycle. The ratio was approximately 2.0 through five runs. This result indicates that the repeated water splitting cycle proceeded stoichometrically. From the results of XRD analysis and chemical analysis, major Zirconia had monoclinic structure while a part of *m*-ZrO_2 was transformed into *t*-ZrO_2; iron ions of Fe_3O_4 contributed to the water splitting cycle, and the cycle proceeded on the surface of *m*-ZrO_2 without entering the iron ions into Zirconia crystal lattice.

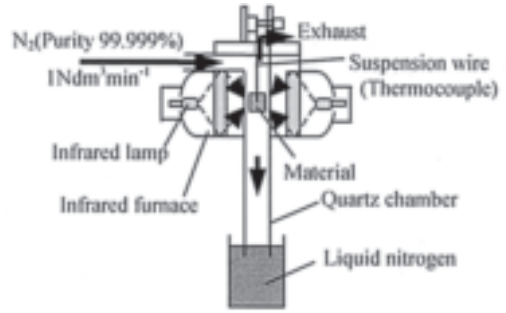

Fig.1 Experimental set-up for thermal reduction by liqid-N_2 quenching method

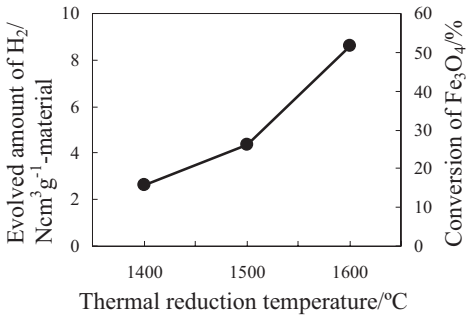

Fig.2 Variations of evolved amount of H_2 per weight of material and conversion of Fe_3O_4

Reference:

[1] Kodama, T., Kondoh, Y., Kiyama, A., Shimizu, K-I., *Proceeding of International Solar Energy Conference (ISEC) 2003* (Hawaii, 2003), M.D.Thornbloom, and S.A.Jones, eds., ASME, New York, ISEC2003-44037(CD publications)

P119B

REMOVAL OF MANGANESE IN WASTEWATER ACCOMPANIED BY THE PRECIPITATION OF FINE FERRITE PARTICLES

Kenji Miyamura,[1] Yoji Tagchi,[2] and Isao Kimura[1,3,*]

[1] *Graduate School of Science and Technology, Niigata University*

[2] *Faculty of Engineering, Niigata University*

[3] *Center for Education and Research on Environmental Technology, Materials Engineering, and Nanochemistry, Niigata University*

1. Introduction

Manganese exists abundantly on the earth and is used in various fields such as raw materials of alloys and dry batteries. Manganese is an essential element to the human body, but excessive intake may cause the Parkinson's disease. Fine ferrite particles can include some metals when they are precipitated. A ferritization method, which utilizes this principle, is one of the methods to treat the wastewater containing heavy metal ions. It has some advantages that most of heavy metals are removed by one processing, the solid-liquid separation by using magnet is possible, and so on. In this study, it was attempted to remove manganese with a high removal ratio and produce the stable ferrite by ferritization.

2. Experimental

2.1 Production of manganese ferrite

Manganese solutions were prepared from $MnCl_2$ (II), Mn_2O_3 (III), MnO_2 (IV), and $KMnO_4$ (VII) at 1000 ppm as mock wastewater samples. $FeSO_4$ (II)·$5H_2O$ was added and stirred at 298 K to 338 K. The pH was controlled with NaOH at 8 to 11, and then air was blown at a rate of 1 L/min to start ferritization. After separating particles produced, the concentration of residual manganese in the solution was measured by inductively coupled plasma (ICP) emission spectrometry. Manganese removal ratio was defined as the ratio of the concentration of manganese removed to the initial concentration.

2.2 Dissolution experiment

The ferrite, produced at 338 K and pH = 9, of 1.0 g was put in 100 mL of hydrochloric acid at 2 mol/L, and the manganese concentration was measured at given intervals.

2.3 Adsorption experiment

The ferrite, produced without manganese at 338 K and pH = 9, of 1.0 g was added in the

manganese solutions of 200 mL at 1000 ppm under stirring. The manganese concentration in the solution was measured at given intervals.

3. Results and discussion

The manganese removal ratio at 338 K and pH = 9 was 99.9 % for 20 min and 99.99 % for 60 min. It was not affected by pH under 9. Re-dissolution to a small extent was observed at pH over 10.

The dissolution of the ferrite produced from seven-valent manganese was so fast that it was dissolved in 4 h. On the other hand, the ferrite produced from two-valent manganese was less dissolvable as to take 8 h to dissolve completely. The dissolution rate was accelerated after 3 h. It was confirmed that the ferrite generated from two-valent manganese was stable for acid, and manganese existed from this internal.

Two-valent manganese adsorbed for 300 min was 23 mg, and seven-valent manganese was 16 mg. It is considered that a lot of manganese was taken into the ferrite because two-valent manganese is adsorbed easily than seven-valent manganese.

4. Conclusion

It was confirmed that manganese in wastewater can be removed enough by ferritization. For wastewater containing highly valent manganese, preliminary reduction may be effective. The ferrite produced from two-valent manganese have the structure that manganese exists more in the center of a particle. This method is expected to apply to the preparation of gradient magnetic materials.

P120C

Release and control of alkaline earth metal ions from methylcellulose hydrogel

Masashi Nakagawa[1] and Isao Kimura[1,2,3,*]

[1] *Graduate School of Science and Technology, Niigata University*

[2] *Center for Education and Research on Environmental Technology, Materials Engineering, and Nanochemistry, Niigata University*

[3] *Food Science Center, Niigata University*

1. Introduction

Methylcellulose (MC) is a water-soluble polymer. MC aqueous solution shows the thermal gelling property to be gelated by heating and reversibly liquefied by cooling. This property has been applied in the food industry for retaining the shape during processing at high temperatures. If this property is usable to immobilize metallic ions in the gel, it is expected that a procedure for preparing new inorganic materials with controlling the morphology can be developed. In this study, the immobilization of alkaline earth metal ions in the MC gel was attempted. The analysis of the release characteristics and the control of each alkaline earth metal ion from the MC gel to water were carried out.

2. Experimental

2.1 Gelation and liquefaction temperatures

MC solution with or without containing 1mol/kg $Ca(NO_3)_2$ were put in a test tube and heated from 40℃ to measure the gelation temperature. The liquefaction temperature was measured by cooling the consequent gel from 60℃.

2.2 Release and control of alkaline earth metal ions

The MC solutions of 2, 4, or 6wt% containing each alkaline earth nitrate of 0.2, 0.5, or 1 mol/kg were gelated at 60 to 80℃, and distilled water having been kept at the gelation temperature was put on the gels produced. After given intervals, a small amount of the water was drawn, and the concentrations of metallic ions with time were measured by inductively coupled plasma (ICP) emission spectrometry. Sodium alginate of 0.01, 0.02, or 0.05wt% was added to control the release characteristic.

3. Results and discussion

3.1 Gelation and liquefaction temperatures

The change in the gelation and liquefaction temperatures with MC concentration is shown in Fig. 1. The gelation temperature was gradually decreased with increasing MC concentration. The liquefaction

temperature shows a similar tendency.

3.2 Release and control of alkaline earth metal ions

The Ca^{2+} release rate was not affected by the gelation temperature and MC concentration. The effect of $Ca(NO_3)_2$ concentration on the Ca^{2+} release rate is shown in Fig. 2. The release rate was linearly decreased with time. This result indicates that the driving force of Ca^{2+} transfer is a concentration gradient between the inside and the outside of the MC gel. The nitrates of the other alkaline earth metals showed the same behavior.

The change in the Ca^{2+} release rate with sodium alginate concentration is shown in Fig. 3. It was confirmed that the addition of sodium alginate is effective in decreasing the Ca^{2+} release rate. This effect may be due to calcium alginate produced in the MC gel.

4. Conclusions

The dissolution of nitrates did not affect the release characteristics of alkaline earth metal ions from the MC gel. The release rate can be decreased by the addition of sodium alginate.

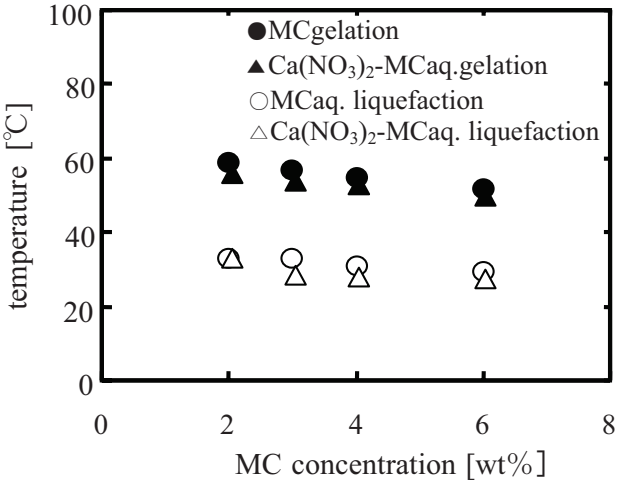

Fig.1 Gelation and liquefaction characteristics.

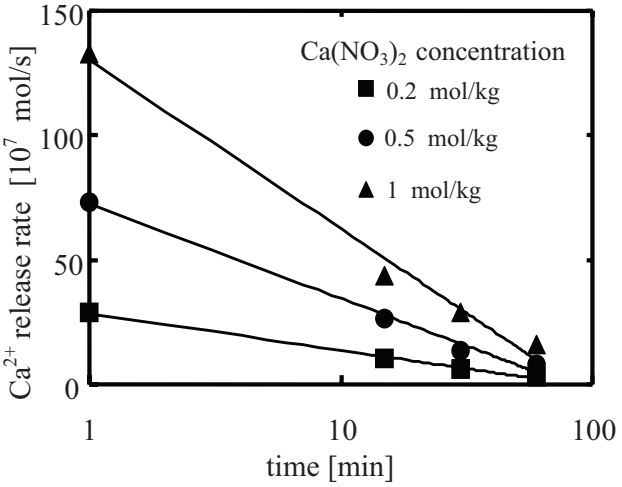

Fig.2 Relation between Ca^{2+} release rate and $Ca(NO_3)_2$ concentration.

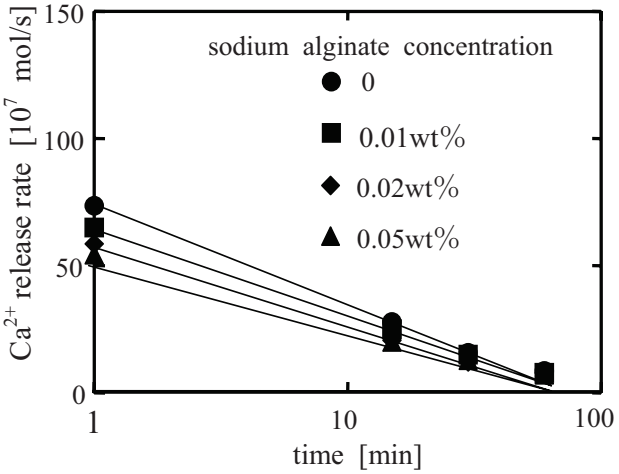

Fig.3 Relation between Ca^{2+} release rate and the addition of sodium alginate.

P121A

EFFECTS OF OIL PHASE MEDIA ON THE PREPARATION OF HYDROXYAPATITE MICROSPHERES IN A MULTIPLE DISPERSION

Tatsuro Honma[1] and Isao Kimura[1,2,*]

[1] *Graduate School of Science and Technology, Niigata University*

[2] *Center for Education and Research on Environmental Technology, Materials Engineering, and Nanochemistry, Niigata University*

1. Introduction

Interfacial reaction in a W/O/W multiple emulsion is a method to prepare inorganic microspheres. In this system, microspheres are produced by the reaction of one ionic species in the inner aqueous phase with another ionic species, which diffuses in the oil phase to the W/O interface. We have been investigating the preparation of hydroxyapatite (HAp) microspheres by this method. In this paper, several oil phase media were used and the effects of them on the characteristics of HAp particle produced were discussed.

2. Experimental

Cyclohexane, benzene, hexane, cyclohexene, and toluene were used as oil phase media. An inner aqueous phase was 0.3 mol/kg K_2HPO_4 solution, of which pH was adjusted at 12.0 with KOH. Span80 as dispersion stabilizer for an inner aqueous phase was dissolved in one of oil phase media to prepare an oil phase. An outer aqueous phase was 0.5 mol/kg $Ca(NO_3)_2$ solution, in which Tween20 was dissolved as suspension stabilizer for the oil phase.

The inner aqueous phase and the oil phase were mixed and emulsified for 5 min at 12000 rpm to produce a W/O emulsion. This emulsion was poured into the outer aqueous phase and stirred at 323 K and 300 rpm to prepare a W/O/W emulsion. After keeping the stirring for 3 h, the solid product was washed, freeze-dried, and calcined at 773 K for 1 h.

The crystalline phases of the solid product was identified by X-ray diffraction of CuKα radiation. The morphology of the product was characterized with a scanning electron microscope (SEM). Part of the product was dissolved in nitric acid, and the Ca and P concentrations were measured by inductively coupled plasma (ICP) emission spectrometry to evaluate the Ca/P ratio.

3. Results and discussion

Microspheres of about 1 μm in diameter were obtained by using cyclohexane, hexane, or cyclohexene as oil phase medium. On the other hand, the products have aggregated in irregular shape when benzene or toluene were used. From these results, it can be concluded that for preparing microspheres aliphatic hydrocarbons are more suitable than aromatic hydrocarbons.

X-ray diffraction patterns of the products were shown in Fig. 1. All specimens are recognized as single phase HAp. Therefore, it is suggested that the type of oil phase medium does not influence the reaction for producing HAp.

The Ca/P ratio of HAp prepared was shown in Table 1. The value ranges from 1.44 to 1.50, while the theoretical value of HAp is 1.67. Cyclohexane is thought to be the most adequate as oil phase medium.

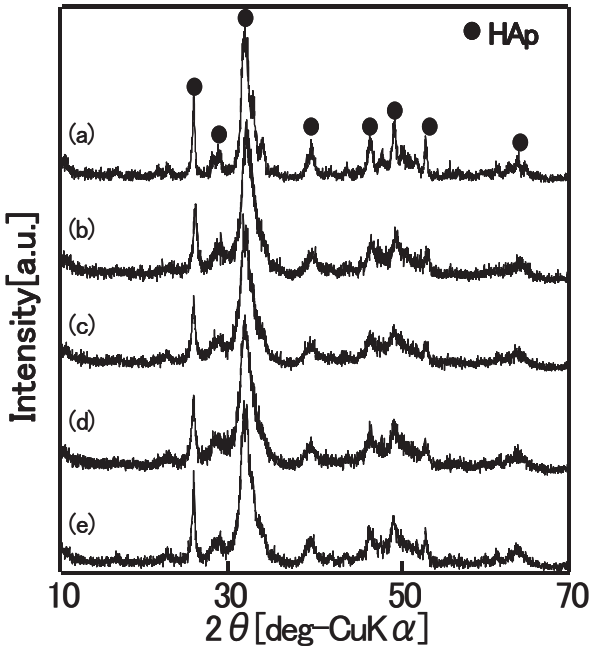

Fig.1. X-ray diffraction patterns of HAp prepared with cyclohexane (a), benzene (b), hexane (c), cyclohexene (d), and toluene (e).

Table 1. Ca/P ratio of HAp prepared with each oil phase medium

Oil phase medium	Ca/P ratio
Cyclohexane	1.50
Hexane	1.46
Cyclohexene	1.44
Benzene	1.46
Toluene	1.46

Acknowledgments

Part of this study was financially supported by a Grant-in-Aid for Scientific Research (C) No. 18560666, Japan Society for the Promotion of Science and a Grant for Promotion of Niigata University Research Projects, 2006.

P122B

Comparison of O_2/N_2 and N_2O/N_2 plasma etching of polymer

Y.W. Joo, J. K. Kim, Y. H. Park, G. S. Cho, H. J. Song and J. W. Lee*

(School of nano Engineering, Inje University, 621-749, 607, Obang-dong, Gimhae, Gyeongnam, Korea(ROK)

**e-mail : jwlee@inje.ac.kr*

Understanding of plasma etching of polymer is becoming more important. Polycarbonate is an attractive material as a substrate for bio, optical and MEMS devices due to its low cost, high transparency and light weight. However, there has been little data for dry etching of the material. We studied O_2/N_2 and N_2O/N_2 plasma etching of polycarbonate, acrylic and polyethylene telephthalate (PET) using a reactive ion etcher. In this time, we will mainly focus on etch results of polycarbonate. We used UV lithography for dry photoresist on polycarbonate. Important experimental parameters during RIE etching included RIE chuck power (25 -200W) and composition of N_2O and O_2 in the gases (total 20sccm). We analyzed polycarbonate after etching with a surface profilometry, scanning electron microscopy (SEM) and atomic force microscope (AFM). And we also used optical emission spectroscopy for basic understanding of discharge intensity during plasma etching. The results showed that polycarbonate could be etched in $12N_2O/8N_2$ plasma in range of 0.05 – 0.32 um when RF power was varied from 25W to 150W. It also etched in $4O_2/16N_2$ plasma in range of 0.12 – 0.29 um when RF power was varied 75W to 200W in the experiment. We compared experimental results of polycarbonate etched in O_2/N_2 and N_2O/N_2 plasmas. In conclusion, O_2/N_2 plasma provided higher etch rate of polycarbonate that N_2O/N_2 in the similar etching conditions.

P123C

A mechanism of ablation of metals by sub-femto second laser pulses

Guan Sik Cho*, Eun Mi Ko, Myung Hoon Kang, Jewon Lee

Department of Nano Systems Engineering and Institute for Nano Manufacturing, Inje University at Gimhae, Gyeongnam, South Korea

Cristina G. Serbanescu, and Ying Yin Tsui

Department of Electrical and Computer Engineering, University of Alberta at Edmonton, Alberta, Canada

Theoretically a possible ablation mechanism is discussed that works within a femtosecond of a p-polarized laser irradiation on a metal surface. This is caused by a net positive normal laser force on surface ions due to screening out of a half of a period of electric field oscillation by surface electrons, only the positive normal period surviving. In relation to the self field of surface ions, there is a threshold intensity required for the incident laser to exert a pulling force on surface ions.

According to Gamaly et al.[1], ablation models to date relies upon heating of electrons by laser energy. Once electrons are heated, for ions heating the laser pulse should be long enough for the electrons to have time to collide with ions within the laser pulse duration. Thus with short laser pulses lasting for less than a picosecond only electrons are heated and explode out of the metal and drag ions out by Coulomb force. However, when the laser pulse width goes well over a picosecond ions are heated also and moves hydrodynamically out of the metal. Of course the energy of a laser pulse should exceed a threshold to sufficiently overcome work functions et cet.

In this paper we consider a model where electrons do not have to be heated. Rather than a random thermal motion of electrons, a directed oscillatory motion causes a force on ions out of the metal surface. To get electrons oscillate normal to the surface the laser polarization should have a normal component. Then at the surface of the metal the electric field is a sum of the laser field (incident plus reflected) and the space charge field (oscillating electrons plus fixed ions). For a practical metal the phase change in reflection from the surface is not 180 degrees. Rather the phase change dramatically decreases to zero as the incident angle approaches 90 degrees. Furthermore the reflectance rises steeply to 100 % with the incident angle. Thus electrons quiver under the cooperating incident and reflected laser electric field. Here during a half cycle of the laser electric field electrons are drawn out of the surface and the fields by both electrons and ions are in the same positive normal direction and thus tend to cancel the laser electric field. However, during the other half cycle where electrons are pushed into the metal, electrons and ions produce the field in the opposite directions to each other, only to cancel field of each

other. Thus the laser field is not influenced by the space charges formed by electrons and ions. In short, the screening effect of electrons work only during a half of a laser cycle. During the other half cycle where laser field is directed in the positive normal direction, the surface ions can feel a force out of the metal surface.

After all, our model does not need any time for heating of particles. This may operate during the very beginning of a laser pulse without any concern for the pulse width. And with such a short laser pulse as a sub-femto pulse there can be no time to heat particles sufficiently to explode, and one can consider our model as a mechanism of ablation. This can be expected for a p-polarized laser pulse with a grazing incidence upon a metal surface. And the incident intensity should exceed a certain threshold for the positive normal electric field to surpass the self field of surface ions.

Reference

[1] E. G. Gamaly, A. V. Rode, and B. Luther-Davies, "Ablation of solids by femtosecond lasers: Ablation mechanism and ablation thresholds for metals and dielectrics", Physics of Plasmas vol. 9, no. 3, pp. 949-957 (2002).

P124A

ULTRASOUND EFFECT ON HYDROGEN BONDING FORMATION APPEARED IN ALUMINA-POLYACRYLIC ACID SLURRY

Ngo Le Ngoc, Kobayashi Takaomi*

Department of Chemistry,Nagaoka University of Technology, Kamitomioka 1603-1, Nagaoka 940-2188 , Japan

Introduction

Ultrasound (US) technology has been applied widely and more popularly in many fields of research and industrial production. In mechanical fabrication, cleansing industry, health, etc, US has been known to promote both physical and chemical processes. In chemical processing, US influences chemical reactivity in order to enhance formation of radical species through the cavitation effect. As a result, reaction rate and yield were on enhancements. In polymer chemistry the major advantage was of performing sonochemical synthesis of polymer and additional way was of molecular weight control of polymer by US exposure.

In the present research, we carried out studying influence of US on hydrogen bond between Alumina (Al_2O_3) and Polyacrylic acid (PAA) by meaning viscosity of the slurry solution. Influence of the US was studied on using PAA and Al_2O_3 slurry solution. US emitting three kinds of frequency 28, 45 and 100kHz (200 W/cm^2) was used to influence on the slurry viscosity. We found that the hydrogen bonding networks between Al_2O_3 and PAA led to be weaking under the US exposure. The slurry used contained both Al_2O_3 and PAA in 100ml water was composed with weight ratio of 10:3, 20:3, and 30:3 respectively. After the US was exposed, the viscosity was measured by B type viscosity meter. The data indicated that US broken hydrogen bonds between PAA and Alumina, depending on the slurry pH. Evidence presented that US influenced hydrogen bonding of Alumina and PAA.

Experiment

The slurry solutions contained both Al_2O_3 and PAA (molecular weight 250000) in 100ml water adjust pH of the solution was performed at pH 3. In the slurry solution, viscosity was measured using B type viscosity meter with 6 and 60 rpm rotation after exposure of different frequency (28, 45 and100kHz) of US with 200W/cm^2.

Result and Discussion

Figure 1 shows result viscosity of slurry solution containing Al_2O_3/PAA with different weight ratio of 30:3, 20:3 and 10:3 respectively. When the weight of Al_2O_3 in the slurry increased but that of PAA was fixed, the slurry viscosity was increased. This proved that in the slurry solution of the Al_2O_3 and PAA having hydrogen bond networks were proportional to the content of Al_2O_3 to increase viscosity. Namely, the viscosity increased with increase of Al_2O_3 by hydrogen bonding networks. After the US was exposed for 5 min, the slurry viscosity was similarly measured. When the US frequency was 28kHz, the viscosity was significantly decreased. The tendency was higher than that

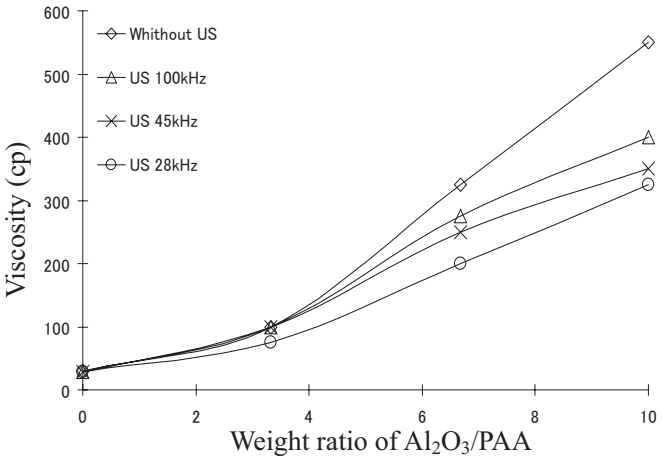

Fig1. Viscosity of Al_2O_3/PAA slurry containing different weight ratio by obtaining without and with US at US power 200W/cm^2, rotating speed 6rpm

of 45kHz and 100kHz. Therefore, this meant that the hydrogen bond networks in the slurry was easy to be broken by the US stress.

Figure 2 shows the result of the time course of viscosity of the solution. The time for the irradiated US frequency was at 28kHz, as the concentration of the slurry solution Al_2O_3/PAA = 30:3 and rotating speed of the viscosity meter was 60rpm. The US was changed as values of power were 175, 200, 250 and 300W/cm^2. When the US was irradiated, the viscosity was apparently decreased, for example to be 75cp for 300W/cm^2. When the hydrogen bond between Al_2O_3 and PAA in the solution was broken, the viscosity of the solution be came to be less. When the US was turned off, the viscosity increased gradually and returns to the primary value within 55 seconds. Then, US was exposed again as the second measurement, causing same result with that of the first time. The third cycles were also similarly repeated. On the other hand, from Figure 2 we could see that the reduced viscosity was changed with different the US intensity. When the US intensity increased the effect of US also increased.

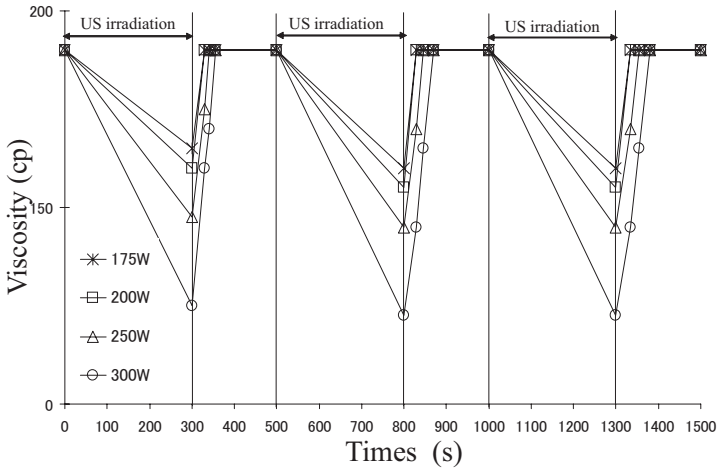

Fig2. Viscosity of Al_2O_3-PAA slurry containing 30/3 weight ratio. The US exposed was at 28kHz with different US intensity of 175, 200, 250 and 300(W)

Figure 3 shows the influence of US to hydrogen bond networks of PAA and Al_2O_3 .Hydrogen bonds between PAA and Al_2O_3 tended to be broken by US exposure. When the US was turned off, hydrogen bonds were re-formed in the slurry, in which the viscosity increased.

Therefore, the control of the increase and decrease in viscosity of the slurry solution could be adjusted using US exposure.

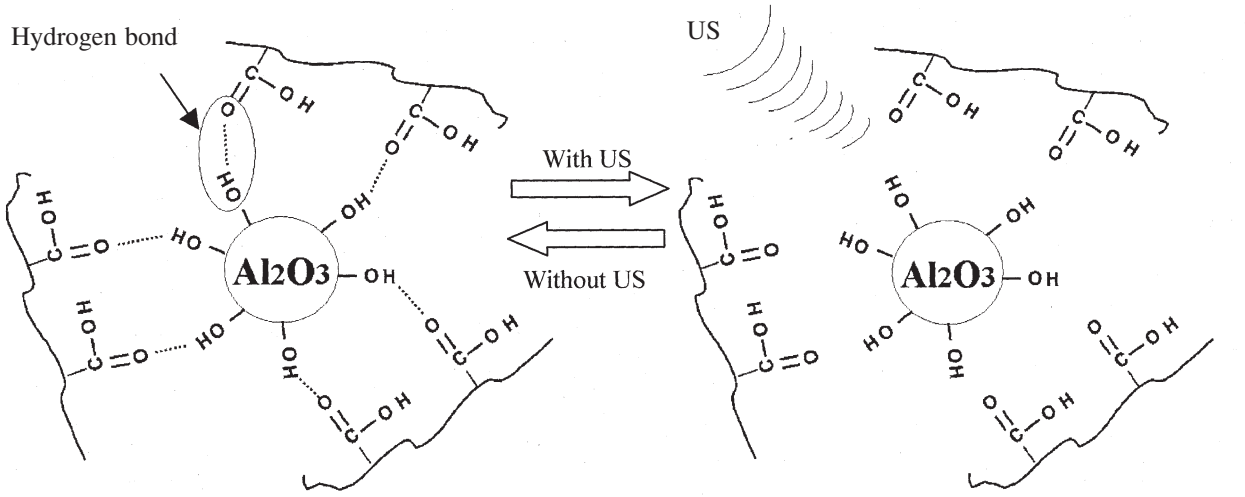

Fig.3 Influence of US upon hydrogen bond networks between Al_2O_3 and PAA

References

【1】 D.Huo and T.Kobayashi, *Chem. Lett.* , 35(7), 776(2006).

P125B

EFFECT OF REFLECTED ULTRASOUNDS HAVING DIFFERENT FREQUENCY ON PREPARATION OF NANO-SIZED SOL-GEL TiO_2 POWDERS

Kyaing Kyaing Latt, Takaomi Kobayashi*

Department of Chemistry, Nagaoka University of Technology, 1603-1 Kamitomioka, Nagaoka, Japan. 940-2188

Introduction

We prepared anatase-TiO_2 powders by sol-gel polymer process of titanium tetra-isopropoxide (TTIP) under ultrasound (US) irradiation with different frequency of 28, 45 and 100 kHz. US effect in frequency led to reduce the particles size of resultant TiO_2, thereby increasing the reactive surface area. Based on our previous study[1)], it was noted that efficiency of transmitted US was improved by reflection technique; placing stainless steel reflection plate (RP) in the vicinity of reaction vessel. In the present work, the US sol-gel polymer process was carried out in the absence and presence of RP and studied about different frequency effect on formation of resultant TiO_2 powders. To examine the photodegradation activity of US-TiO_2 and US-RP-TiO_2 powders, Rhodamine 640 (Rh-640) dye was used. Also, we determined the standing wave of US intensity and sonoluminescence occurred in sonic bath by different US frequency and reflection technique to evaluate the US media.

Experimental

As precursor of titania, 12.5 mM of TTIP was hydrolyzed in 100 ml of 10% ethanol-water solution under stirring. The hydrolysis processes were carried under US and reflected US irradiation in different frequencies for 1 h at room temperature. After hydrolysis, centrifugation, separation and drying for 8 h at 100˚C were followed. Then, sample powders were grinded and calcined at 300, 400, 500, 600 and 700˚C. The calcination temperature played as a role to transform the crystalline structure of TiO_2 powders from anatase to rutile phase. The specific surface area and diffraction particle size measurements of resultant US-TiO_2 and US-RP-TiO_2 powders were observed. To investigate the properties of US-TiO_2 and US-RP-TiO_2 powders, photodegradation of 10 μM Rh-640 was examined in the presence of resultant powder under UV light irradiation (1.5 mW). As a blank test, photodegradation of Rh-640 without TiO_2 powder under UV irradiation was also performed. At every 5 min interval of photodegradation experiment, UV absorbance of the Rh-640 was detected at 576 nm and calculated the concentration changes. The standing waves of emitted US intensity in different frequency were measured by using immersion transducer probe that was connected to pulse receiver. Sonoluminescence

occurred in sonic bath filled with 0.23 mM luminol solution was visualized by taking photos in dark room.

Results and discussion

Comparing the results of US and US-RP TiO_2 powders, it was demonstrated that frequency effect influenced on particle size of TiO_2 powder. Especially in 28 kHz US, average particle size measured by laser scattering technique (LST) was about 0.11 μm and the large surface area enhanced the photo-decomposition reaction rate of Rh-640. Also, it could be seen that the reflected US effected to be small size in all different frequencies. By using LST, the smallest TiO_2 particles having 0.09 μm were obtained under 28 kHz frequency US-RP process. There was tendency that the reflection effect was distinctly marked in cases of 28 and 45 kHz frequency. In order to confirm the particle size, we measured TEM images for the powders. The pictures of resultant TiO_2 powders in 28 frequency US with and without RP are shown in Fig. 1. Comparing with non-US-TiO_2 powders was to clarify the particle size changes by reflection technique as shown in the resultant data of TEM. It was estimated that the particle sizes of US-TiO_2 and US-RP-TiO_2 powders were about 7 and 5 nm, respectively. Non-US TiO_2 powders were around 10-20 nm. Herein, the resulting particles sizes measured by TEM were smaller than those observed with LST measurement. For LST data of the TiO_2 particles distribution, it was reasonable to be aggregated in water and became larger. For the characterization of resultant TiO_2 powder, XRD measurement was observed and the pattern showed that the peak intensities of anatase increased in the range of calcined temperature from 300 to 600˚C and transformed to rutile phase at 700˚C. From the results of photodegradation experiments, it was noted that anatase phased TiO_2 powder had higher photodegradation properties than rutile. Also, the photodegradation activity was improved with increasing surface area of dispersed US-TiO_2. Moreover, low calcination temperature and low frequency US for TiO_2 preparation were more affected for photodegradation of Rh-640.

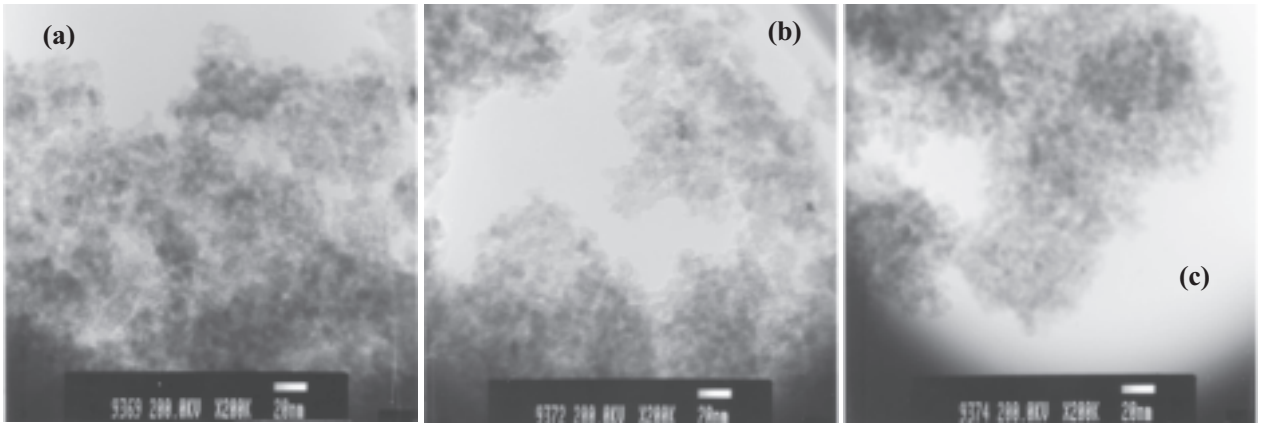

Figure 1. TEM pictures of (a) non-US (b) 28-US-TiO_2, and (c) 28-US-RP-TiO_2 powders calcined at 300ºC.

Reference

[1] K.K. Latt, T. Kobayashi, *Ultrasonics Sonochemistry,* 13 (2006) 321-328

[2] J.C. Yu, J. Yu, L. Zhang, W, Ho, *J. Photochem. Photobio. A: Chem.,* 148 (2002) 263-271

協賛企業および団体一覧

バリアン テクノロジーズ ジャパン リミテッド

オフィス株式会社

株式会社アヅマテクノス

株式会社新潟科学

株式会社ヒウラ

株式会社タケショー

(株)カネコ商会新潟営業所

鐘通化学薬品株式会社

轟産業株式会社

株式会社鈴商

有限会社名古屋三立製作所

株式会社小林印刷所

日本分光株式会社

（財）内田エネルギー科学振興財団

（財）インテリジェント・コスモス学術振興財団

新潟市

協賛企業および団体の皆様に心より感謝申し上げます。

Cary Since 1947
FTS Since 1969

二つの信頼と歴史のブランド

Varian Molecular Spectroscopy Products

Inspiring Excellence

FastImageIR™

バリアン 顕微赤外分光イメージングシステム

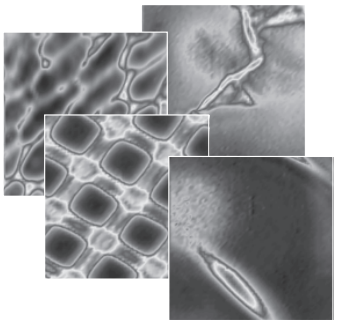

バリアンの誇る技術の結晶による顕微赤外分光イメージングシステム Varian FastImageIR は、赤外顕微鏡に対する考えを一新します。特に、特許技術である顕微ATRイメージング法は、回折限界に迫る5ミクロン以下の微小物測定を高精度で実現。今まで得られなかった新たな情報をもたらします。1969年世界に先駆けてFT-IRを上市以来、最先端技術の開発に挑戦し続けるバリアンが、赤外分光の歴史にまた一つ大きな功績を残します。

Varian FastImageIR FT-IR Imaging Microscope

Cary® series

バリアン 紫外-可視-近赤外 分光光度計

世界初の自記分光光度計として1947年に発表された Cary シリーズ分光光度計は、50年以上の長きにわたり“ 世界標準機”と呼ばれるまでに高い評価を頂いております。高度に最適化された高性能モノクロメータやフェーズロック波長走査技術を始め、バリアン独自の革新的な技術の積み重ねにより、常に安定した精度の高いデータを提供します。比類なき低迷光、高感度、波長再現性、高速性は、何れも世界最高性能を誇り、一般分析から各種工業材料の評価まで、様々な分野でその能力を発揮しています。

Varian Cary 5000 UV-Vis-NIR Spectrophotometer

VARIAN

バリアン テクノロジーズ ジャパン リミテッド 科学機器本部 分子分光グループ

東 京 〒108-0023 東京都港区芝浦4-16-36 住友芝浦ビル8F Tel.03-5232-1322 Fax.03-5232-1263

大 阪 〒532-0011 大阪市淀川区西中島7-5-25 新大阪ドイビル Tel.06-6305-6552 Fax.06-6305-6556

URL: http://www.varianjapan.com or http://www.varianinc.com E-Mail: jp.ftir.sales@varianinc.com

GC・LC・MS・AA・ICP・UV-Vis-NIR・FT-IR・Raman・Fluorescence・Dissolution・NMR・MRI・Consumables・Data Systems

Varian 400-MR

Varian NMR Systems

Inspiring Excellence

400MHz NMR 測定装置が新登場 !!

- 卓越したコストパフォーマンス
- 業界初の日本語ソフトウェア搭載
- 溶液専用のハイパフォーマンスルーチン機

新製品

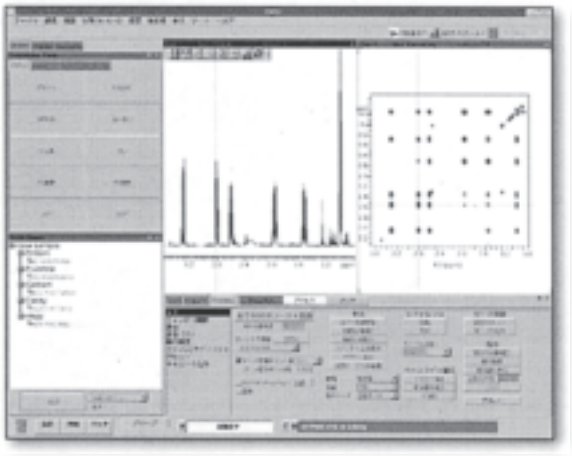

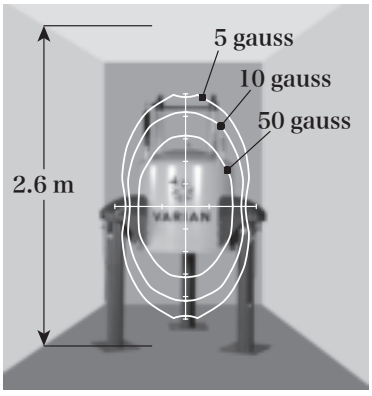

- 最小の漏洩磁場
  （5ガウスライン＝水平：0.55 m／垂直：1.0 m）
- 設置フリー（最低必要天井高：2.6 m）
- 低ランニングコスト
  （液体ヘリウム消費量：95 L／270 日）
- Varian NMR System の優れた特長を継承
  （ダイレクトドライブ RF システム、ダイレクトデジタルレシーバーなど）
- 操作性に優れたコンパクトな設計
- 構造解析や定量分析などに有用な情報を迅速に取得可能
- 創薬、バイオテクノロジー、化学、教育等広範囲の応用分野に対応

VARIAN

バリアン テクノロジーズ ジャパン リミテッド　科学機器本部　NMRグループ

東 京　〒108-0023　東京都港区芝浦4-16-36 住友芝浦ビル8F　Tel.03-5232-1236　Fax.03-5232-1263
大 阪　〒532-0011　大阪市淀川区西中島7-5-25 新大阪ドイビル　Tel.06-6305-6552　Fax.06-6305-6556
URL: http://www.varianjapan.com　http://www.varianinc.com　E-Mail: nmr.sales@varianinc.com

GC・LC・MS・AA・ICP・UV-Vis-NIR・FT-IR・Raman・Fluorescence・Dissolution・NMR・MRI・Consumables・Data Systems

Organized by

The Society of Polymer Science, Japan, Hokuriku Branch

Center for Education and Research on Environmental Technology, Materials Engineering, and Nanochemistry, Niigata University

Center for Transdisciplinary Research, Niigata University

The Advanced Nano Membrane of Niigata

Japan Advanced Institute of Science and Technology